



**DEVELOPMENT OF SILVER NANOPARTICLES-LOADED
ALGINATE BEADS EMBEDDED IN GELATIN SCAFFOLDS
FOR WOUND DRESSING APPLICATIONS**

PORNTIPA PANKONGADISAK

**MASTER OF SCIENCE
IN
MATERIALS SCIENCE**

**SCHOOL OF SCIENCE
MAE FAH LUANG UNIVERSITY**

2013

©COPYRIGHT BY MAE FAH LUANG UNIVERSITY

**DEVELOPMENT OF SILVER NANOPARTICLES-LOADED
ALGINATE BEADS EMBEDDED IN GELATIN SCAFFOLDS
FOR WOUND DRESSING APPLICATIONS**

PORNTIPA PANKONGADISAK

**THIS THESIS IS A PARTIAL FULFILLMENT OF
THE REQUIREMENTS FOR THE DEGREE OF
MASTER OF SCIENCE
IN
MATERIALS SCIENCE**

**SCHOOL OF SCIENCE
MAE FAH LUANG UNIVERSITY**

2013

©COPYRIGHT BY MAE FAH LUANG UNIVERSITY

**DEVELOPMENT OF SILVER NANOPARTICLES-LOADED
ALGINATE BEADS EMBEDDED IN GELATIN SCAFFOLDS
FOR WOUND DRESSING APPLICATIONS**

PORNTIPA PANKONGADISAK

THIS THESIS HAS BEEN APPROVED
TO BE A PARTIAL FULFILLMENT OF THE REQUIREMENTS
FOR THE DEGREE OF MASTER OF SCIENCE

IN
MATERIALS SCIENCE

2013

THESIS COMMITTEE

CHAIRPERSON

(Prof. Dr. Pitt Supaphol)

ADVISOR

(Dr. Orawan Suwantong)

CO-ADVISOR

(Dr. Uracha Rungsardthong Ruktanonchai)

EXAMINER

(Dr. Nattakan Soykeabkaew)

©COPYRIGHT BY MAE FAH LUANG UNIVERSITY

ACKNOWLEDGEMENTS

I would like to express my very great appreciation and thanks to my advisor Dr. Orawan Suwantong from School of Science, Mae Fah Luang University and co-advisor Dr. Uracha Rungsardthong Ruktanonchai from National Nanotechnology Center, National Science and Technology Development Agency, you have been a tremendous mentor for me. I would also like to thank my committee members, Professor Dr. Pitt Supaphol from The Petroleum and Petrochemical College, Chulalongkorn University and Dr. Nattakan Soykeabkaew from School of Science, Mae Fah Luang University for serving as my committee members even at hardship.

I would like to thank STIC staffs at Mae Fah Luang University for their supports in the analysis and testing of the samples has accomplished in my research. I would especially like to thank Thailand Institute of Scientific and Technological Research (TISTR) for support the *Escherichia coli* TISTR 780 and the *Staphylococcus aureus* TISTR 1466. I wish to thank all members in my research group and my entire friend for their support and encouragement to succeed in thesis. Moreover, a special thanks to my family. Words cannot express how grateful I am to my mother and father for all of the sacrifices that you've made on my behalf. Your prayer for me was what sustained me thus far.

Finally, I would like to acknowledge the financial support from the Research, Development and Engineering (RD&E) fund through The National Nanotechnology Center (NANOTEC), The National Science and Technology Development Agency (NSTDA), Thailand (P-11-00986) to Mae Fah Luang University (MFU) and Thailand Graduate Institute of Science and Technology (TGIST) (TG-55-99-55-048M). This research would not be carried out successfully without all financial supports.

Porntipa Pankongadisak

Thesis Title	Development of Silver Nanoparticles-Loaded Alginate Beads Embedded in Gelatin Scaffolds for Wound Dressing Applications
Author	Porntipa Pankongadisak
Degree	Master of Science (Materials Science)
Advisor	Dr. Orawan Suwantong
Co-Advisor	Dr. Uracha Rungsardthong Ruktanonchai

ABSTRACT

Wound infection is a main problem for wound healing process that caused from bacterial infection. From this problem, wound dressing is developed by incorporating an antibacterial agent which has an activity to kill bacteria. Silver nanoparticles (AgNPs) are mostly used as antibacterial agents that have strong antibacterial activity for using in small amount. In this research, the AgNPs-loaded alginate beads embedded in gelatin scaffolds were fabricated for use as wound dressings. The AgNPs-loaded calcium alginate beads were obtained by either electrospraying or emulsification/external gelation method. The silver (Ag^+) ions in alginate solution reduced to AgNPs were prepared by UV irradiation technique. The size and shape of beads were observed using optical microscope (OM) and scanning electron microscope (SEM). Gelatin scaffolds were fabricated from 5% w/v of gelatin solution and crosslinked with genipin. The AgNPs-loaded calcium alginate beads embedded in gelatin scaffolds were fabricated by freeze-drying method. The morphology, mechanical properties and thermal properties of these scaffolds were characterized by SEM, universal testing machine (UTM) and thermogravimetric

analysis (TGA), respectively. Moreover, these scaffolds were investigated for their water swelling and weight loss behaviors in the phosphate buffer solution (PBS) at 37 °C for 1, 3, 5 and 7 days. The release characteristics of Ag⁺ ions from both the AgNPs-loaded calcium alginate beads and the AgNPs-loaded calcium alginate beads embedded in gelatin scaffolds were carried out in either deionized water (DI) or PBS at 37 °C for 7 days. Lastly, the AgNPs-loaded calcium alginate beads embedded in gelatin scaffolds were tested for their cytotoxicity and antibacterial activity.

Keywords: Silver nanoparticles/Calcium alginate beads/Electrospraying/Gelatin scaffolds/Emulsification method/Internal gelation method

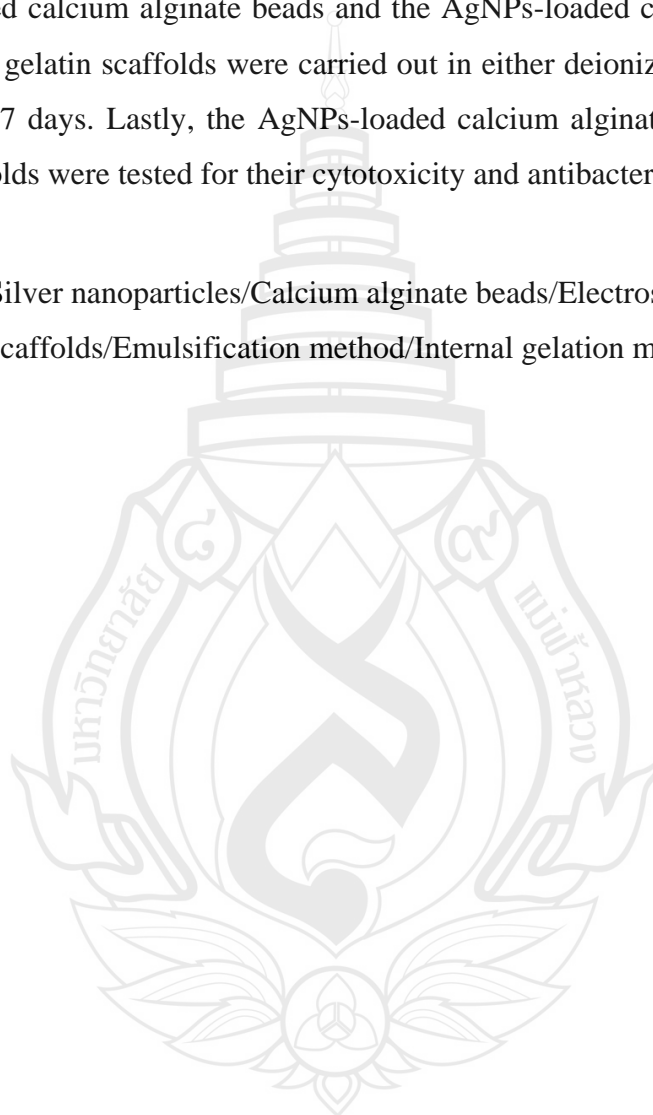


TABLE OF CONTENTS

	Page
ACKNOWLEDGEMENTS	(3)
ABSTRACT	(4)
LIST OF TABLES	(10)
LIST OF FIGURES	(12)
ABBREVIATIONS AND SYMBOLS	(15)
CHAPTER	
1 INTRODUCTION	1
1.1 Background and Significance of the Research Problem	1
1.2 Research Objectives	2
1.3 Scope of Research	2
2 LITERATURE REVIEW	3
2.1 Wound Dressing	3
2.2 Drug Delivery System to the Wound	8
2.3 Microspheres as Drug Carriers	11
2.4 Alginate	12
2.5 Gelatin	12
2.6 Silver Nanoparticles	13
3 METHODOLOGY	15
3.1 Materials	15
3.2 Equipment	16
3.3 Methodology	18

TABLE OF CONTENTS (continued)

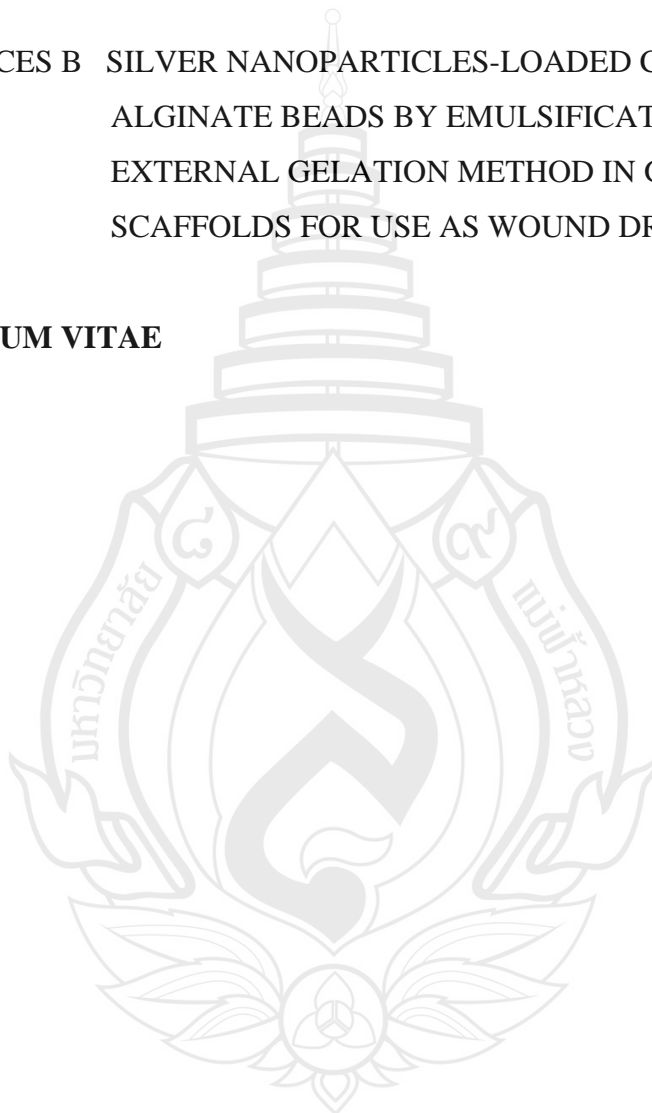
	Page
CHAPTER	
4 PREPARATION AND CHARACTERIZATION OF SILVER NANOPARTICLES-LOADED CALCIUM ALGINATE BEADS EMBEDDED IN GELATIN SCAFFOLDS	25
4.1 Abstract	25
4.2 Introduction	26
4.3 Experimental Details	28
4.4 Results and Discussion	32
4.5 Conclusions	36
4.6 Acknowledgements	36
5 DEVELOPMENT OF SILVER NANOPARTICLES-LOADED CALCIUM ALGINATE BEADS EMBEDDED IN GELATIN SCAFFOLDS FOR USE AS WOUND DRESSINGS	54
5.1 Abstract	54
5.2 Introduction	55
5.3 Experimental Details	57
5.4 Results and Discussion	63
5.5 Discussion	69
5.6 Conclusions	72
5.7 Acknowledgements	72

TABLE OF CONTENTS (continued)

	Page
CHAPTER	
6 SILVER NANOPARTICLES-LOADED CALCIUM ALGINATE BEADS BY EMULSIFICATION/EXTERNAL GELATION METHOD IN GELATIN SCAFFOLDS FOR USE AS WOUND DRESSINGS	81
6.1 Abstract	81
6.2 Introduction	82
6.3 Experimental Details	85
6.4 Results and Discussion	91
6.5 Conclusions	97
6.6 Acknowledgements	98
7 CONCLUSIONS	106
REFERENCES	108
APPENDICES	128
APPENDICES A DEVELOPMENT OF SILVER NANOPARTICLES-LOADED CALCIUM ALGINATE BEADS EMBEDDED IN GELATIN SCAFFOLDS FOR USE AS WOUND DRESSINGS	129

TABLE OF CONTENTS (continued)

	Page
APPENDICES B SILVER NANOPARTICLES-LOADED CALCIUM ALGINATE BEADS BY EMULSIFICATION/ EXTERNAL GELATION METHOD IN GELATIN SCAFFOLDS FOR USE AS WOUND DRESSINGS	132
CURRICULUM VITAE	135



LIST OF TABLES

Table	Page
4.1 Representative OM and SEM Images Illustrating the Effect of the Concentration of the Alginate and the Applied Voltage on the Morphology of the Obtained Beads as Well as the Average Values of Bead Diameters	40
4.2 Representative OM and SEM Images Illustrating the Effect of the Concentration of the Alginate Solutions on the Morphology of the Obtained Beads at an Applied Voltage of 12 kV/15 cm as Well as the Average Values of Bead Diameters	44
4.3 Representative OM and SEM Images Illustrating the Effect of the Applied Voltage on the Morphology of the Obtained Beads at a Fixed Alginate Concentration of 1.5% w/v as Well as the Average Values of Bead Diameters	45
4.4 Representative OM and SEM Images of the AgNPs-Loaded Calcium Alginate Beads at Various Concentrations of AgNO ₃	48
4.5 Shear Viscosity and Electrical Conductivity of the AgNPs-Containing Alginate Solutions at Various Concentrations of AgNO ₃ (n = 3)	49
4.6 Representative SEM Images of the Genipin-Crosslinked Gelatin Scaffolds With Different Genipin Concentrations as Well as the Average Values of Pore Sizes	50
4.7 Representative SEM Images of the AgNPs-Loaded Calcium Alginate Beads Embedded in Gelatin Scaffolds as Well as the Average Values of Pore Sizes	51
5.1 Selected TEM Images of AgNPs in Sodium Alginate Solutions at Various Concentrations of AgNO ₃ Including Diameters of the Individual AgNPs (n = 200)	73

LIST OF TABLES (continued)

Table	Page
5.2 Selected OM and SEM Images of the Neat Calcium Alginate Beads and the AgNPs-Loaded Calcium Alginate Beads at Various Concentrations of AgNO ₃ Including Diameters of the Individual Beads (n = 120) and Shear Viscosity and Electrical Conductivity of the Neat and the AgNPs-containing Alginate Solutions (n = 3)	74
5.3 Selected SEM Images, Pore Sizes, and Compressive Modulus of the Neat Calcium Alginate Beads Embedded in Gelatin Scaffolds and the AgNPs-Loaded Calcium Alginate Beads Embedded in Gelatin Scaffolds (Sizes of the Scale Bar: 200 µm)	76
5.4 Antibacterial Activity of the AgNPs-Loaded Calcium Alginate Beads Embedded in Gelatin Scaffolds (n = 3)	80
6.1 Selected OM and SEM Images of the Neat Calcium Alginate Beads and the AgNPs-Loaded Calcium Alginate Beads at Various Concentrations of AgNO ₃ Including Diameters of the Individual Beads (n = 120)	99
6.2 Compressive Modulus of the Neat Calcium Alginate Beads Embedded in Gelatin Scaffolds and the AgNPs-Loaded Calcium Alginate Beads Embedded in Gelatin Scaffolds (n = 6)	101
6.3 Antibacterial Activity of the AgNPs-Loaded Calcium Alginate Beads Embedded in Gelatin Scaffolds (n = 3)	105

LIST OF FIGURES

Figure	Page
2.1 Basic Diagram of Skin Structure	9
3.1 A Schematic Photograph of Electrospraying Apparatus	16
3.2 A Schematic Photograph of UV Irradiation Box	17
4.1 Scheme Preparations of Calcium Alginate Beads by Electrospraying Method	37
4.2 Scheme Preparations of AgNPs-Loaded Calcium Alginate Beads by Electrospraying Method	38
4.3 Schematic Illustrations of the Intermolecular Crosslinking Structures of Genipin With Gelatin	39
4.4 Selected TEM Image of the 2%AgNPs-Loaded Calcium Alginate Beads	47
4.5 Indirect Cytotoxicity Evaluation of Genipin-Crosslinked Gelatin Scaffolds With Different Genipin Concentrations After 24 h of Cell Culture (n = 3). * $p < 0.05$ Compared With Control	52
4.6 (a) Water Swelling and (b) Weight Loss Behaviors of AgNPs-Loaded Calcium Alginate Beads Embedded in Gelatin Scaffolds in PBS (n = 3). * $p < 0.05$ Compared With Submersion Time at Day 1 for Any Given Type of Sample, and [#] $p < 0.05$ Compared With 1%AgNPs-Loaded Beads Embedded in Gelatin Scaffolds for Any Given Submersion Time Point	53
5.1 Thermogravimetric Analytical Thermograms of the Neat Calcium Alginate Beads Embedded in Gelatin Scaffolds and the AgNPs-Loaded Calcium Alginate Beads Embedded in Gelatin Scaffolds	77

LIST OF FIGURES (continued)

Figure	Page
5.2 (a) Water Swelling and (b) Weight Loss Behaviors of the Neat Calcium Alginate Beads Embedded in Gelatin Scaffolds and the AgNPs-Loaded Calcium Alginate Beads Embedded in Gelatin Scaffolds (n = 4). * $p < 0.05$ Compared With the Neat Calcium Alginate Beads Embedded in Gelatin Scaffolds at a Given Time Point and [#] $p < 0.05$ Compared With 1 Day Submersion Time of a Given Scaffold	78
5.3 Cumulative release profiles of Ag ⁺ ions from the AgNPs-loaded calcium alginate beads embedded in gelatin scaffolds, reported as the weight of Ag ⁺ ions released divided by the actual weight of the beads, by total immersion method in (a) DI and (b) PBS at the physiological temperature of 37 °C (n = 3).	79
5.4 Indirect Cytotoxicity Evaluation of the AgNPs-Loaded Calcium Alginate Beads Embedded in Gelatin Scaffolds (n = 3)	80
6.1 Selected TEM Images of the 4% AgNPs-Loaded Calcium Alginate Beads	100
6.2 Selected SEM Images of the 2% AgNPs-Loaded Calcium Alginate Beads Embedded in Gelatin Scaffolds Under Magnification of 50x (a) and Magnification of 500x With the White Arrows Indicating the Embedded Beads in Scaffolds (b)	100
6.3 Thermogravimetric Analytical Thermograms of the Neat Calcium Alginate Beads Embedded in Gelatin Scaffolds and the AgNPs-Loaded Calcium Alginate Beads Embedded in Gelatin Scaffolds	102

LIST OF FIGURES (continued)

Figure	Page
6.4 (a) Water Swelling and (b) Weight Loss Behaviors of the Neat Calcium Alginate Beads Embedded in Gelatin Scaffolds and the AgNPs-Loaded Calcium Alginate Beads Embedded in Gelatin Scaffolds (n = 4). * $p < 0.05$ Compared With the Neat Calcium Alginate Beads Embedded in Gelatin Scaffolds at a Given Time Point and [#] $p < 0.05$ Compared With 1 Day Submersion Time of a Given Scaffold	103
6.5 Cumulative release profiles of Ag ⁺ ions from the AgNPs-loaded calcium alginate beads embedded in gelatin scaffolds, reported as the weight of Ag ⁺ ions released divided by the actual weight of the beads, by total immersion method in (a) DI and (b) PBS at the physiological temperature of 37 °C (n = 3).	104
6.6 Indirect Cytotoxicity Evaluation of the AgNPs-Loaded Calcium Alginate Beads Embedded in Gelatin Scaffolds (n = 3). * $p < 0.05$ Compared With the Viability of NHDF Cells Cultured With the Fresh Culture Medium as Control	105

ABBREVIATIONS AND SYMBOLS

AgNPs	Silver nanoparticles
EHDS	Electrohydrodynamic spraying
Na ⁺	Sodium ions
Ca ²⁺	Calcium (II) ions
% w/v	Percent weight by volume
AgNO ₃	Silver nitrate
CaCl ₂	Calcium chloride
kV	Kilovolts or 1000 volts
kN	Kilo-newton or unit of force
cm	Centimeter scale
mm	Millimeter scale
μm	Micrometer scale
M	Molarity unit
UV	Ultraviolet-visible light
h	Hour
°C	Degree Celsius
OM	Optical Microscopy
SEM	Scanning Electron Microscopy
TGA	Thermogravimetric Analysis
AAS	Atomic Absorption Spectroscopy
PP	Polypropylene
PBS	Phosphate buffer saline
DI	Deionized water
TCPS	Tissue-culture polystyrene
NHDF	Normal human dermal fibroblasts
DMEM	Dulbecco's modified Eagle's medium

ABBREVIATIONS AND SYMBOLS (continued)

FBS	Fetal bovine serum
SFM	Serum-free medium
MTT	3-(4,5-Dimethylthiazol-2-yl)-2,5-diphenyltetrazolium bromide
pH	measure of acidity or alkalinity
ml	Milliliter or unit of volume
mg	Milligram
μL	Microliter or unit of volume
% w/w	Percent weight by weight
mg.mL^{-1}	Milligram per milliliter or unit of concentration
mm.min^{-1}	Millimeter per minute or unit of speed
$^{\circ}\text{C.min}^{-1}$	Degree Celsius per minute or unit of heating rate
mPa.s	Millipascal seconds or unit of shear viscosity
$\mu\text{S.cm}^{-1}$	Microsiemens per centimeter or unit of electrical conductivity
kPa	kilopascal or unit of compressive modulus
CFU/ml	Colony-forming units per milliliter
DMSO	Dimethyl sulfoxide
NA	Nutrient agar
M	Weight of sample after submersion in the testing solution
M_i	Initial weight of the sample in its dry state
M_d	Weight of the sample after submersion in the testing solution in its dry state

CHAPTER 1

INTRODUCTION

1.1 Background and Significance of the Research Problem

Wound of the skin can be caused by the fire burn, infection, inflammation or even ulceration of chronic diseases. The skin is dehydrated and could be easily infected by bacteria which can lead to wound infections. Currently, it is still a major problem in term of public health and medical field in Thailand and worldwide. For the traditional treatment, using the antibiotics has limitation such as very short life of medication. To solve this limitation, then the application of antibiotics in the form of polymer beads is used. The expectation of this solution is to help extend the duration of drug releasing and to develop a wound dressing materials for treating a patient with a wound, preventing water loss out of body, and protecting bacterial infection. At present, Thailand has to import the medical materials from abroad. Since the cost of the importing medical materials is high, then this cannot meet the needs of people who have low income. In this research, alginate and gelatin are used to fabricate the medical materials. The advantages of gelatin and alginate are low cost, good biocompatibility, high water adsorbing ability, biodegradability and low toxicity. Thus, many researchers try to develop the medical materials for reducing the import of medical materials from abroad.

In this research, the development of wound dressing material using freeze-drying method was used to fabricate the scaffolds. The electrospraying and the emulsification/external gelation methods were used to prepare the calcium alginate beads. The incorporation of AgNPs into the calcium alginate beads was used to inhibit bacteria from penetrating through skin wound due to its small size and high surface area. Thus, in this research, we developed the wound dressing materials by embedding the AgNPs-loaded calcium alginate beads in the gelatin scaffolds to reduce the burst release and sustain the release of Ag⁺ ions for a long period of time.

1.2 Research Objectives

1.2.1 To produce the AgNPs-loaded calcium alginate beads embedded in gelatin scaffolds

1.2.2 To study the release characteristics of Ag^+ ions from the scaffolds, the antibacterial activity of the scaffolds, and the cytotoxicity of the scaffolds

1.2.3 To develop the AgNPs-loaded calcium alginate beads embedded in gelatin scaffolds for use in wound dressing and drug delivery applications

1.2 Scope of Research

1.3.1 Find the optimal condition (i.e., concentration, applied voltage) to produce the neat calcium alginate beads and the AgNPs-loaded calcium alginate beads by electrospraying method

1.3.2 Find the optimal condition to produce the neat calcium alginate beads and the AgNPs-loaded calcium alginate beads by emulsification/external gelation method

1.3.3 Study the morphology and size of both the neat calcium alginate beads and the AgNPs-loaded calcium alginate beads by SEM

1.3.4 Find the optimal condition (i.e., the concentration of gelatin solution, the concentration of crosslinking agent) to produce the scaffolds by freeze-drying method

1.3.5 Characterize the morphology, the mechanical properties and the thermal properties of the samples by SEM, UTM, and TGA, respectively

1.3.6 Determine the actual amount of silver in the samples by atomic absorption spectrophotometer (AAS) and the release characteristics of Ag^+ ions from the samples in either DI or PBS medium by AAS

1.3.7 Study the antibacterial activity of the samples by AATCC test method

1.3.8 Study the cytotoxicity of the samples using normal human dermal fibroblast (NHDF) cells by indirect cytotoxicity

CHAPTER 2

LITERATURE REVIEW

2.1 Wound Dressing

2.1.1 Mechanism of Wound Healing

Wound healing is a complex process that involves the association of cells, cytokine mediators, and extracellular matrix to repair the tissue. The phase of normal wound healing is divided into four phases: hemostasis, inflammatory, proliferative and remodeling (Mackay & Miller, 2003).

2.1.1.1 Hemostasis

This process is a short period of time that prevents excessive blood loss in the body. Bleeding is observed when skin is injured, promoted to clean bacteria out from wound and prevented blood loss in the body at short time. Bleeding will activate haemostasis which is exudates such as clotting factors. Fibrinogen in the exudates elicits the clotting mechanism resulting in coagulation of exudates. Haemostasis and fibrinogen will form fibrin network and produces a clot in the wound causing bleeding to stop.

2.1.1.2 Inflammation

The inflammatory phase of wound repair is the process to reduce the risk of infection by stopping blood loss. White cell or fluid containing plasma proteins, blood cells and antibodies are sent into the wound site causing pain, swelling, fever, and redness around the wound site. Neutrophils and macrophages are killer to clean, scavenge for bacteria and prepare the injury site for healing. This process will occur 2-4 days after the injury depending on the stage of wound.

2.1.1.3 Proliferation

The proliferative phase is the wound beginning to rebuild itself during skin or organ that overlaps with the ending of the inflammatory phase. The wound begins to contract and the skin or organ that is repaired to return to its normal size by

regeneration of new tissue and blood vessel. Collagen is also deposited in the affected area. Fibroblasts have begun to enter and collect in the wound by around day 3 after the injury. Granulation tissue will begin to be seen in the wound by the end of the first week, this tissue will continue to grow until the wound is healed.

2.1.1.4 Remodeling

The remodeling phase is the end process and broader peak than another phase (or also called the maturation phase), which is overlap on proliferative phase (2-3 weeks post injury). This process involves the collagen and its associated extracellular matrix. The initial deposition of collagen is created the weak collagen fibers with random orientation. The new collagen fibers are produced which show greater wound tensile strength after the decomposition of old collagen fibers. Re-growing of tissue is occurred by rearranging itself that depends on severity of the wound. The remodeling may continue for months up to two years and achieve 40-70 percent of undamaged tissue at four weeks.

2.1.2 Types and Properties of Wound Dressing

The wound dressing is work on the basis of forming dry, protective barriers which prevent bacterial contamination and absorb exudates. Wound dressing can maintain the moist at the wound, protect the exudates from leakage, thermal insulation, eliminate cell death in the wound, reduce trauma or pain at dressing change, resist the toxicity around the wound, and keep the gas change. Properties of dressing should have moisture vaporization, rapidly rate of healing and should reduce the amount of bacterial. There are four types of wound assessment: necrotic, slough, granulating, and epithelializing. Necrotic is a form of cell injury that results in devitalized tissue and black in color from dehydration and cell death. Slough is a layer or mass of dead tissue separated from surrounding living tissue, as in a wound, a sore, or an inflammation wound. Granulating is actually a healing process whereby lumpy, pinky tissues comprising of connective tissues and capillaries forming around the surface of a wound. Epithelializing occurs as epithelial cells migrate over granulation tissue from the wound margins, hair follicles and sweat glands within the wound. Wound dressing has been used in medical applications such as semi-permeable film and pad, non-adherent contact, hydrocolloid, alginate, hydrofibre, foams, hydrogel,

antimicrobial, deodorizing, larval therapy, topical negative pressure therapy and protease-modulating matrix (Watson & Hodgkin, 2005).

2.1.3 Scaffolds for Wound Dressing

The scaffold is one type of wound dressing that is a substrate for the implanted cells and a physical support to control the restoration of a tissue or an organ (Parveen, Krishnakumar & Sahoo, 2006). In addition to facilitating cell attachment, promoting cell growth, and allowing the retention of differentiated cell functions, the scaffold should be biocompatible, biodegradable, highly porous with a large surface/volume ratio, mechanically strength, and malleable (Chen, Ushida & Tateishi, 2002). Many natural and synthetic polymers can be used to produce the scaffolds. Natural polymers have been widely used for medical applications including collagen, fibroin, gelatin, chitosan, alginate, and hyaluronic acid (Adekogbe & Ghanem, 2005; Woei et al., 2001). While synthetic polymers also have been widely used such as polycaprolactone (PCL), polylactic acid (PLA), polyglycolic acid (PGA), and poly(lactide-co-glycolide) (PLGA) (Gunatillake & Adhikari, 2003). Moreover, several processing techniques have been developed to fabricate polymeric scaffolds including fiber bonding, electrospinning, solvent casting/particulate leaching, gas foaming/high pressure processing, and freeze drying, etc.

2.1.4 Scaffolds Fabrication Techniques

2.1.4.1 Fiber Bonding

Fiber bonding technique is developed to bind the fibers together at points of intersection that shows a high surface area to volume ratio and high porosity to a cell adhesion. In 1993, Mikos et al. used PGA and PLLA polymers to prepare fiber bonded scaffolds. PGA fibers were arranged in the form of nonwoven mesh and then embedded in a PLLA/CH₂Cl₂ solution. After evaporation of the solvent, PGA-PLLA composite matrix was obtained. Then, the matrix was heated above the melting temperature of both polymers. PLLA was dissolved in CH₂Cl₂ and then solvent was removed leaving out from the PGA fibers. Therefore, the fibers will be bonded at their cross-point (Mikos et al., 1993). The disadvantages of this technique are poor mechanical properties, lack of control over porosity and pore size, the availability of suitable solvent, immiscibility of two polymers in the melt state, and the required

relative melting temperatures of the polymers. Solvent residue in the scaffold may be harmful to the cell and organs.

2.1.4.2 Electrospinning

Electrospinning is a modern method for preparing highly porous non-woven mats and ultrafine fibers with nano- and microscale in diameter of fibers. This process uses electrostatic to form the fibers. Many biocompatible polymers can be eletrospun into nanofiber such as PGA, PLGA, and PCL (Yoshimoto, Shin, Terai & Vacanti, 2003). Electrospun fibers are produced by dissolving the polymer in solvent and then the polymer solution is poured into a syringe. The polymer is ejected through a metal capillary that is applied a high voltage at capillary. When charges within the polymer fluid reach a critical value, a pendant droplet at the tip of the nozzle changes its shape from spherical into conical shape or Taylor cone (Frenot & Chronakis, 2003). While nanofibers of polymer are ejected through the air, the solvent is evaporated from the fibers. Thus the dry fibers are obtained on a grounded collector (Doshi & Reneker, 1995). Many factors affect the fiber thickness, fiber diameter, and average pore diameter including polymer concentration, type of solvent, ejection rate, applied voltage, capillary diameter, collecting plate material, and the distance between the capillary and the collecting plate (Pham, Sharma & Mikos, 2006). The fibrillar scaffold composed of α,β -poly(*N*-2-hydroxyethyl)-DL-aspartamide graft with polylactic acid (PHEA-g-PLA) was prepared by electrospining. The electrospun PHEA-g-PLA copolymer fiber showed the fiber diameter about 1 μm (Pitarresi, Palumbo, Fiorica, Calascibetta & Giammona, 2010). Electrospinning process can control over pore sizes, porosity, and fiber thickness, but its mechanical properties are limited.

2.1.4.3 Solvent Casting/Particulate Leaching

Solvent casting/particulate leaching technique is developed to control porosity, pore diameter, and crystallinity by adjusting the processing parameters and the type, amount, and size of porogen. This technique is the casting of polymer/porogen/organic solvent mixture solution followed by solvent evaporation and leaching out the porogen to obtain a polymeric scaffold with an interconnected porous network (Lu & Mikos, 1996). The disadvantages of this technique are thin membranes and residual solvents or porogen materials (Yang, Leong, Du & Chua,

2001). 3D PLGA porous scaffolds have been fabricated by solvent casting/particulate leaching method. PLGA porous scaffolds can be used as templates for cell seeding. These scaffolds showed the pore size in the range of 250-425 μm and a rectangular shape of morphology (Jayasuriva, Assad, Jayatissa & Ebraheim, 2006).

2.1.4.4 Gas Foaming/Particulate Leaching

Gas foaming/particulate leaching is a method to produce pores with high inter-connectivity. An effervescent salt (e.g., ammonium bicarbonate) as a gas foaming agent added into the polymer gel paste. Then a gel paste mixture is cast into the mold. After solvent evaporation, it is immersed in hot water. The ammonia and carbondioxide leach out from the polymer matrix resulting in the high porosity of polymer matrix (Nam, Yoon & Park, 2000). This technique can control porosity and pore size, and can also enhance mechanical properties. However, a drawback of this process is the residual solvent and porogen. Macroporous PCL scaffolds have been prepared by improved gas foaming/salt leaching method. The semi-solidified polymer-ammonium bicarbonate salt mixture in citric acid solution was used to prepare these scaffolds at room temperature. The porous structure is obtained due to an acid-base gas evolving reaction between ammonium bicarbonate and citric acid. The PCL scaffold showed the pore size in the range of 200-300 μm and porosity in the range of 86–96.8% (Lim, Gwon, Shin, Jeun & Nho, 2008).

2.1.4.5 Freeze-Drying

Freeze-drying is based on the formation of ice crystals that induce porosity through ice sublimation and desorption. The kinetics of the freezing stage control the porosity and the interconnectivity of scaffold by removing water or solvent from emulsion to yield the highly inter-connected pores of scaffold (Liapis, Pikal & Bruttini, 1996). This process can prepare the porosity up to 90%, and diameter of scaffold in a range of 15-35 μm . Advantages of this process are highly porous structure and highly pore interconnectivity. But this process is limited to produce small pore size (Whang, Thomas & Healy, 1995). Porous gelatin scaffolds have been fabricated by using water as a porogen and freeze-drying technique. The fast freezing process can produce the scaffolds with small pore size. While large pore size of scaffolds was obtained from the slow freezing process (Kang, Tabata & Ikada, 1999).

2.2 Drug Delivery System to the Wound

The controlled drug delivery systems occurred less than 25 years ago by using synthetic polymers. The structure of synthetic polymer is necessary to verify the motivation for attaining controlled released (Langer, 1998). The aims of controlled drug release are improving the effectiveness of drug therapy, increasing therapeutic activity reducing the number of drug administration required during treatment, or eliminating the need for specialized drug administration.

2.2.1 Mechanism of Drug Delivery System

Human skin consists of two distinct layers: the stratified vascular cellular epidermis and an underlying dermis of connective tissue (Barry, Gidda, Scotchford & Howdle, 2004). A fatty subcutaneous layer resides beneath the dermis. Hairy skin develops hair follicles and sebaceous glands, and the highly vascularized dermis supports the apocrine and eccrine sweat glands, which pass through pores in the epidermis to reach the skin surface. For drug permeation, the most important component in this complex membrane is the stratum corneum, or horny layer, which usually provides the rate-limiting or slowest step in the penetration process (Barry et al., 2004). The mechanisms of drug transportation by crossing the intact skin have not yet been completely elucidated. However, possible macro-routes may comprise the transdermal pathway or via the hair follicles and sweat glands. The appendageal route may be significance for short diffusional times and for polar molecules. Recently, it was believed that, for polar molecules, the probable route was via the hydrated keratin of the corneocyte. However, it seems more probable that the dominant pathway is via the polar region of intercellular lipid, with the lipid chains providing the nonpolar routes shown in Figure 2.1 (Langer, 2004).

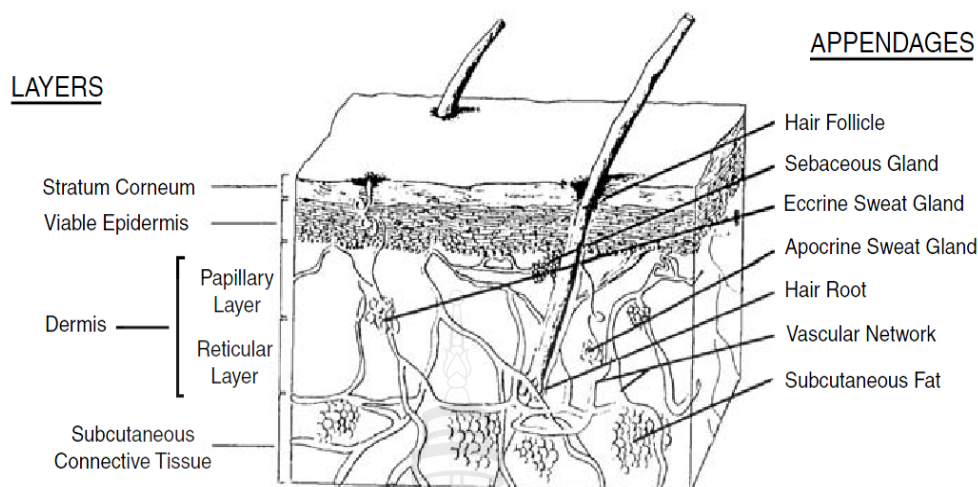


Figure 2.1 Basic Diagram of Skin Structure

Source Cleary (1984)

In 1984, Wise reported that the relative importance of these routes depends upon numerous factors, such as the time-scale of permeation, the physicochemical properties of the penetrant (e.g., pKa, molecular size, stability, binding affinity, solubility, and partition coefficient), integrity and thickness of the stratum corneum, density of sweat glands and follicles, skin hydration, metabolism, and vehicle effects (Wise, 1984).

2.2.2 Scaffolds for Wound Dressing and Drug Delivery System

Most modern dressings are made from polymers which can serve as vehicles for the release and delivery of drugs to wound sites. The release of drugs from modern polymeric dressings to wounds has been reported in the literature with few clinical studies carried out to date. The polymeric dressings employed for controlled drug delivery to wounds include hydrogels such as poly(lactide-co-glycolide), poly(vinyl pyrrolidone), poly(vinyl alcohol) and poly(hydroxyalkylmethacrylates), polyurethane-foam, hydrocolloid and alginate dressings. Other polymeric dressings for drug delivery to wounds comprise novel formulations prepared from polymeric biomaterials such as hyaluronic acid, collagen, and chitosan. Synthetic polymers

employed as swellable dressings for controlled drug delivery including silicone gel sheets, lactic acid (Boateng, Matthews, Stevens & Eccleston, 2007). Some of these novel polymeric dressings for drug delivery exist as patents (Burrell & Morris, 1998). Composite dressings comprising both synthetic and naturally occurring polymers have also been reported for controlled drug delivery to wound sites (Sakchai, Churrerat & Srisagul, 2006). The sustained release tissue engineered polymeric scaffolds for controlled delivery of growth factors and genetic material to wound sites have been reported by Yerushalmi, et al. 1994 (Yerushalmi, Arad & Margalit, 1994). The modern dressings for drug delivery to wounds may be applied in the form of gels, films and foams whilst the novel polymeric dressings produced in the form of films and porous sponges such as freeze-dried wafers or discs or as tissue engineered polymeric scaffolds (Kumar, Muzzarelli, Muzzarelli, Sashiwa & Domb, 2004). Zhang & Zhang (2002) prepared macroporous chitosan scaffolds reinforced by calcium phosphates (CaP) particles such as β -tricalcium phosphate (β -TCP) and CaP invert glasses using a thermally induced phase-separation technique. These porous composite materials were loaded with gentamicin sulphate (GS) by immersing them in GS-containing PBS solutions. *In vitro* tests showed that, in comparison with GS-loaded pure chitosan scaffolds, the initial high burst release of GS was decreased through incorporating CaP crystals and glass particles into the scaffolds, and a sustained release for more than three weeks was achieved (Zhang & Zhang, 2002). The highest sustained release was observed from the particle-containing composite, which was suggested to occur owing to a higher extent of chitosan cross-linking. Moreover, there were no apparent morphological differences for osteoblastic cells grown on the pure chitosan scaffolds and those grown on composite scaffolds. The cells attached and migrated on these scaffolds, suggesting a good cellular compatibility (Zhang & Zhang, 2002; Habraken, Wolke & Jansen, 2007). A new design of a tissue engineering (TE) scaffold with controlled drug-delivery capability has been developed by Shi et al., (2009). The scaffold is based on mesoporous silica–HA (HMS–HA) composite particles used as fillers in PLGA microspheres. HMS–HA particles were produced using dodecylamine as a template and GS-loaded PLGA microspheres were prepared using a double emulsion solvent evaporation technique (water/oil/water). PLGA/HMS–HA–GS composite microspheres were prepared using

a single emulsion solvent evaporation method. Afterwards, PLGA or PLGA/HMS–HA–GS microsphere sintered scaffolds were fabricated by pouring PLGA or PLGA/HMS–HA–GS microspheres into cylindrical moulds, and subsequently sintering at 70 °C for 2 h. The results showed that the presence of HA in PLGA/HMS–HA scaffolds could balance the decreased pH values caused by the acidic degradation product of PLGA. Moreover, HMS–HA improved the cytocompatibility and bioactivity of PLGA. It was also claimed that the compressive strength and elastic modulus of PLGA/HMS–HA scaffolds were higher than those of pure PLGA scaffolds, showing similar mechanical properties to human cancellous bone. In *vitro* drug-delivery testing in the simulated body fluid (SBF) of the PLGA/HMS–HA scaffolds showed that PLGA reduced the GS release from HMS–HA particles and the release rate for nearly one month (Shi et al., 2009).

2.3 Microspheres as Drug Carriers

2.3.1 Electrospraying

Electrohydrodynamic spraying or electrospraying is a process of liquid atomization involving the electrical forces. In this process, the liquid flowing out from a capillary nozzle maintained at high electric potential is applied by the electric field to be dispersed to form droplets (Cloupeau & Prunet, 1994). The size of electrospray droplets is wide range from hundreds micrometers down to tens nanometers (Jaworek, 2007). The charge and size of droplet can be controlled by the flow rate of the liquid and the voltage at the capillary nozzle. A recent report, bovine serum albumin (BSA) as the protein model drug was loaded in the alginate microparticles by electrospraying technique. It was found that this technique can be applied to prepare alginate in micron size and alginate can encapsulate BSA (Suksamran et al., 2009).

2.3.2 Emulsification/external gelation

An emulsification/external gelation method is a process for preparing small diameter alginate beads. It is a safe method for mass preparation of beads (Chen & Subirade, 2006). This method need to disperse the polymer, drug/protein and divalent cations into an oil phase (such as paraffin oil or organic solvents) in formation of an emulsifier. Then the beads are obtained by removing the residual oil or organic

solvents (Chan, Lee & Heng, 2006; Liu et al., 2002; Quong, Neufeld, Skjåk-Braek & Poncelet, 1998). The several parameters used in this method can change the physical properties of alginate beads such as size, size distribution, morphology, and swelling features. This method can prepare chitosan beads with good morphology. The emulsion system using liquid paraffin oil as a continuous phase and 0.5-4% of Span 80 as a surfactant was used to prepare the beads. When the stirring speed was 700 rpm, the average size diameter of chitosan beads was 297 μm (Al-Helw, Al-Angary, Mahrous & Al-Dardari, 1998). The smallest average diameters of chitosan beads using 1% Span 80 in paraffin oil as continuous phase were $10.2 \pm 0.21 \mu\text{m}$ when increasing the stirring speed to 3000 rpm was used (Chourasia & Jain, 2004).

2.4 Alginate

Alginate is a natural polysaccharide which extracted from brown seaweed, composed of β -D-mannuronic acid (M) and α -L-guluronic acid (G) (Wells & Sheardown, 2007). The commonly applications of alginate are biomedical applications such as living cell encapsulant matrices, wound dressings and intranasal delivery devices. In addition to encapsulate angiogenic growth factors, such as basic fibroblast growth factor (bFGF) and the vascular endothelial growth factor (VEGF) to treat ischemia, the sodium alginate cross-linked with calcium was used to produce calcium alginate beads as an encapsulant (Lin, Qu, Lin & Ling, 2007). The structures of calcium alginate beads are known as the egg-box model (Hutmacher, 2000). The sodium alginate solution is dropped into a solution containing divalent metal ions, and then the cation-alginate gel beads were formed. These gel beads were not reversed to solution but dissolved in the cation-sequestering agent (Torres et al., 2005). Calcium alginate beads have been used in controlled drug delivery system for ophthalmic drug delivery (Pasparakis & Bouropoulos, 2006).

2.5 Gelatin

Gelatin (Gel) is a natural polymer denatured form of collagen and contains a number of functional groups such as amino acids that found in animal tissue. Collagen is the major protein component of extracellular matrices in animal (ECM) (Sai &

Babu, 2000). Collagen has highly antigenicity due to its animal origin but gelatin has relatively low-antigenic and lower cost (Lien, Li & Huang, 2008). This material has the limitation of low mechanical strength and is effectively used only as incorporated component with others polymers to modify the biological or mechanical properties (Ding, Lee & Wang, 2005). Gelatin has been blended with other organic or inorganic biomaterials to fabricate 3-D scaffolds, hydrogels, and films. There are several properties of gelatin such as biological origin, biodegradability, and biocompatibility. It is suitable used for wound dressing, drug delivery system, and tissue engineering applications (Zhong, Zhang & Lim, 2010). A novel method of gelatin for crosslinking the scaffolds was successfully fabricated using glutaraldehyde (GTA) as a crosslinking agent. The structure of these scaffolds showed uniformly distributed and interconnected pores (Lien et al., 2008).

2.6 Silver Nanoparticles

Silver nanoparticles (AgNPs) are well known as a broad spectrum antibiotic with strong antibacterial properties (Son, Youk, Lee & Park, 2004). In recent year, it has been widely used as biomedical devices, such as fibers, films, gels, and beads due to its antibacterial properties (Jin, Jeon, Kim & Youk, 2007; Wei, Sun, Qian, Ye & Ma, 2009; Akhavan & Ghaderi, 2010; Bryaskova, Pencheva, Kale, Lad. & Kantardjiev, 2010; Chun et al., 2010; Kim, Lee, Lee & Shin, 2010). AgNPs are attached into the cell wall resulting to bacteria damage. It penetrates inside the cell bacteria by interacting with phosphorus- and sulfur-containing biomolecule including DNA and proteins. Another, silver (Ag^+) ions are released from AgNPs and bound to the cell wall and outer cell causing the alteration to functionality of the cell membrane (Sambhy, 2006). Many researchers have been synthesized the AgNPs by controlling shape, size and size distribution. The system for producing AgNPs is composed of salt precursor (i.e., silver nitrate (AgNO_3), reducing agent, and stabilizer. The reduction of Ag^+ ions to AgNPs was obtained by a chemical method using reducing agents such as sodium borohydride, formamide, dimethylformamide, triethanolamine, hydrazine, etc. Although these reducing agent is simple and effective, but they have a problem to environmental hazard from the residual reducing agent. Another technique, using γ -

ray irradiation, UV irradiation, microwave, and ultrasonic have been a choice to solve this problem and to eliminate the reducing agent. Long-chain fatty acids (stearic, palmitic, and lauric acids), lauryl amine, poly(vinyl pyrrolidone), poly(vinyl alcohol), amphiphilic block copolymer poly(ester amide), soluble starch, etc. were used as a stabilizer to prevent the aggregation of AgNPs formed (Yoksan & Chirachanchai, 2009). The AgNPs-loaded poly(vinyl alcohol) (PVA) fiber mats were prepared by electrospray method. The reduction of Ag^+ ions to AgNPs was obtained by UV-irradiation technique. The results showed that these fiber mats showed an excellent antibacterial activity above 99.9%. Thus, these fiber mats were good materials for used as a wound dressing (Hong, 2007).



CHAPTER 3

METHODOLOGY

3.1 Materials

3.1.1 Materials for Fabrication of AgPNs-Loaded Calcium Alginate Beads Embedded in Gelatin Scaffolds

Silver nitrate (AgNO_3 ; $\geq 99.9\%$ purity) was purchased from Fisher Scientific (USA). Sodium alginate was purchased from Carlo Erba (Italy). Gelatin (Type A, porcine skin, ~ 180 Bloom) and Span 80 were purchased from Fluka Analytical (Switzerland). Genipin powder (98% purity) was obtained from Shanghai Angoal Chemical (China). Nitric acid (HNO_3) (65% w/w) was obtained from Merck (Germany). Low-viscosity alginic acid sodium salt and medium-viscosity grade of hydroxypropyl methylcellulose (HPMC) were purchased from Sigma (USA). Paraffin oil, calcium chloride (CaCl_2), and isopropyl alcohol ($\text{C}_3\text{H}_8\text{O}$) were purchased from Ajax Chemicals (Australia). All chemicals were analytical reagent grade and used without further purification.

3.1.2 Materials for Preparation of Buffer Solution

Sodium chloride (NaCl), anhydrous disodium hydrogen orthophosphate (Na_2HPO_4) and sodium dihydrogen orthophosphate (NaH_2PO_4) were purchased from Ajax Chemicals (Australia). All chemicals were analytical reagent grade and used without further purification.

3.1.3 Materials for Cell Culture

Normal human dermal fibroblasts (NHDF) were used as reference cells. Dulbecco's modified Eagle's medium (DMEM; Sigma-Aldrich, USA), supplemented by 10% fetal bovine serum (FBS; Invitrogen Corp., USA), 1% L-glutamine

(Invitrogen Corp., USA) and 1% antibiotic and antimycotic formulation [containing penicillin G sodium, streptomycin sulfate, (Invitrogen Corp., USA)].

3.2 Equipment

3.2.1 Equipment for Electrospraying Process

3.2.1.1 High voltage power supply from Gamma High Voltage Research Inc. (Ormond Beach, Florida), model D-UC5-30N DC is used to generate positive DC voltage.

3.2.1.2 Syringe with volume size 10 mL is served as a container for polymer solutions.

3.2.1.3 Stainless steel needle with gauge number 24 (or the inner diameter of 0.55 mm) is used as the electrode to conduct the electrical from power supply to the solutions.

3.2.1.4 Crosslinking bath as a collector which placed on hotplate stirrer HTS-1003 and attached with aluminum sheet.

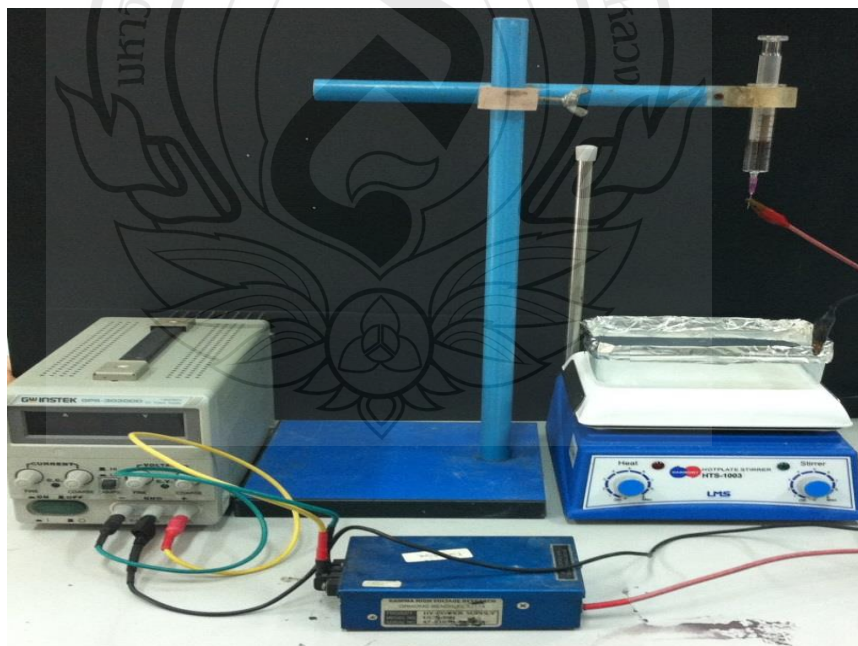


Figure 3.1 A Schematic Photograph of Electrospraying Apparatus

3.2.2 Equipment for UV Irradiation Method

3.2.2.1 UV LEDs lamp at 254 nm

3.2.2.2 UV exposure box with the dimension length \times width \times height of box: $60 \times 40 \times 35$ cm

3.2.2.3 Schott stirring hot plate is used for stirring solutions



Figure 3.2 A Schematic Photograph of UV Irradiation Box

3.2.3 Equipment for Characterization of Materials

3.2.3.1 A CyberScan con 200 conductivity meters was used to characterize the conductivity of the as-prepared solutions.

3.2.3.2 A Brookfield/RVDV-II+P viscometer was used to characterize the viscosity of the as-prepared solutions.

3.2.3.3 A JEOL JEM-2100 transmission electron microscope was used to observe the shapes and sizes of the AgNPs in samples.

3.2.3.4 A Motic BA300 optical microscope was used to observe the shapes and sizes of the samples.

3.2.3.5 An EDAX model: LEO 1450 VP scanning electron microscope was used to investigate the morphology of the samples.

3.2.3.6 A Polaron SC-762 sputtering device was used to coat each sample with a thin layer of gold prior to observation by scanning electron microscopy (SEM).

3.2.3.7 An Instron Machine Model 5566 universal testing machine was used to investigate the compressive modulus of the samples.

3.2.3.8 A Perkin-Elmer Pyris Diamond thermogravimetric analyzer was used to investigate the thermal behavior of the samples.

3.2.3.9 A Varian SpectraAA-300/A Hitachi Z-5000 atomic absorption spectroscope was used to determine the amount of Ag^+ ions in the sample solutions.

3.2.3.10 A SpectraMax M2 Microplate Reader was used to measure the absorbance of solution from MTT assay at wavelength of 570 nm.

3.3 Methodology

3.3.1 Preparation of Neat and AgNPs-Loaded Calcium Alginate Beads by Electrospraying Method

Firstly, the optimal condition for producing calcium alginate beads was carried out by electrospraying method. The concentration of sodium alginate solution was 0.5, 1.0, and 1.5% w/v and the applied voltage was 8, 10, 12, and 15 kV. The prepared sodium alginate solutions were then extruded dropwise through a needle placed into a glass syringe capped with a 24-gauge blunt needle (an internal diameter of needle is 0.55 mm) into a 0.5 M CaCl_2 solution under an applied electric field. The distance between tip to collector was fixed at 15 cm. The calcium alginate beads were collected in CaCl_2 solution with gentle stirring for 30 min. The obtained calcium alginate beads were washed with deionized water and then lyophilized for 20 h.

For the preparation of the AgNPs-loaded calcium alginate beads, the base sodium alginate solution was prepared at a fixed concentration of 1.5% w/v. The AgNPs-loaded sodium alginate solutions were prepared by adding 0, 1, 2, 3, 4, and 8% w/w AgNO_3 (based on the weight of sodium alginate) into the base sodium alginate solutions. According to the previous method (Darroudi, Ahmad, Zak, Zamiri,

& Hakimi, 2011; Martinez-Gutierrez et al., 2010), the Ag^+ ions in the alginate solution was reduced to AgNPs by UV irradiation at 254 nm for 1 h. Prior to electrospraying, the solutions were characterized for their viscosity and conductivity at room temperature (26 ± 1 °C) using a Brookfield/RVDV-II+P viscometer and a CyberScan con 200 conductivity meter, respectively. These solutions were then extruded dropwise through a needle into a 0.5 M CaCl_2 solution under a fixed electric field of 12 kV/15 cm using the electrospraying method. The obtained AgNPs-loaded calcium alginate beads were left in the CaCl_2 solution for 30 min. These beads were separated from CaCl_2 solution and then washed with deionized water. Finally, the beads were lyophilized for 20 h. It should be noted that the calcium alginate beads containing 1, 2, 3, 4, and 8% w/w of AgNO_3 were hereafter denoted as 1%, 2%, 3%, 4% and 8% AgNPs-loaded calcium alginate beads, respectively.

3.3.2 Preparation of Neat and AgNPs-Loaded Calcium Alginate Beads by Emulsification/External Gelation Method

For an aqueous phase of the system, 5% w/v of an aqueous solution containing sodium alginate and hydroxypropyl methylcellulose (HPMC) (9:1) was used to produce the calcium alginate microbeads by emulsification/external gelation method (Wan, Heng & Chan, 1992; Lemoine, Wauters, Bouchend'homme & Pr  at, 1998). An aqueous solution was dispersed into paraffin oil containing 5% v/v of Span 80 with a ratio of 1:4 (i.e., the volume of aqueous phase/the volume of oil phase) by using a magnetic stirrer at 1200 rpm for 30 min. In case of the AgNPs-loaded calcium alginate beads, 2 and 4% w/w AgNO_3 solutions (based on the weight of sodium alginate and HPMC) were added in an aqueous solution containing sodium alginate and HPMC. Then, the Ag^+ ions in an aqueous solution were reduced to AgNPs by UV irradiation at 254 nm for 1 h. After emulsification, 10% w/v CaCl_2 solution was slowly added in the mixture solution and then the mixture solution was continuously mixed for 2 h. 100% isopropyl alcohol was then added to harden the beads. The beads were centrifuged, and washed twice with isopropyl alcohol and water, respectively. Finally, the microbeads were lyophilized for 20 h.

3.3.3 Preparation of Neat Calcium Alginate Beads Embedded in Gelatin Scaffolds and AgNPs-Loaded Alginate Beads Embedded in Gelatin Scaffolds

The neat calcium alginate beads embedded in the gelatin scaffolds were prepared by adding 1 or 10% w/w of dry calcium alginate beads (based on the weight of the gelatin powder) into 5% w/w of gelatin solutions. These solutions were crosslinked with 3% w/w genipin solution and then poured into polypropylene (PP) mold at room temperature and left it for 24 h. The neat calcium alginate beads embedded in gelatin scaffolds were obtained by lyophilization. While, the AgNPs-loaded calcium alginate beads embedded in gelatin scaffolds were prepared by adding 1 or 10 % w/w of dry 1%, 2%, 3%, 4%, and 8% AgNPs-loaded calcium alginate beads (based on the weight of gelatin powder) into 5% w/v gelatin solutions. These solutions were crosslinked and then poured into PP mold at room temperature and left it for 24 h. Finally, the AgNPs-loaded calcium alginate beads embedded in gelatin scaffolds were obtained by lyophilization.

3.3.4 Characterization of Samples

The shapes and sizes of both the neat and the AgNPs-loaded calcium alginate beads were investigated by Motic BA300 optical microscope (OM) and a LEO 1450 VP scanning electron microscope (SEM). Prior to SEM observation, each sample was coated with a thin layer of gold using a Polaron SC-7620 sputtering device. The diameters of the beads were measured from OM and SEM images using a Motic Image Plus 2.0 and a SemAphore 4.0 software, respectively.

The shapes and sizes of AgNPs in the AgNPs-loaded sodium alginate solutions after UV irradiation at 254 nm for 1 h were observed by a JEOL JEM-2100 transmission electron microscope (TEM) operated at 200 kV accelerating voltage. For the morphological observation, each sample was deposited on carbon-coated copper grids. The diameters of the AgNPs were measured directly from TEM images using a SemAphore 4.0 software. While, the morphology of AgNPs in the AgNPs-loaded calcium alginate beads were also investigated by a TEM. Prior to TEM observation, the dispersion of the AgNPs-loaded calcium alginate beads in ethanol solution was placed on carbon-coated copper grid. The sample grid was kept in desiccator cabinet until the solvent was slowly evaporated.

The neat calcium alginate beads embedded in the gelatin scaffolds and the AgNPs-loaded calcium alginate beads embedded in the gelatin scaffolds were also characterized for their morphological appearance by SEM. Each sample was coated with a thin layer of gold using a Polaron SC-7620 sputtering device prior to the observation under SEM. Pore size of the scaffolds was measured directly from SEM images using SemAphore 4.0 software. These values were averaged to obtain the pore size of the particular pore.

The compressive modulus of both the neat calcium alginate beads embedded in the gelatin scaffolds and the AgNPs-loaded calcium alginate beads embedded in the gelatin scaffolds in dry state was investigated with Instron Machine Model 5566 universal testing machine using a 1 kN load cell at room temperature. The samples were compressed at the crosshead speed of $1.0 \text{ mm} \cdot \text{min}^{-1}$ until the samples were about 70% deformed from their original height. The obtained data were modified by connecting with computer for controlling apparatus and analyzing the results.

The thermal behavior of both the neat calcium alginate beads embedded in the gelatin scaffolds and the AgNPs-loaded calcium alginate beads embedded in the gelatin scaffolds (3-5 mg) was carried out by a Perkin–Elmer Pyris Diamond Thermogravimetric Analyzer (TGA) under a nitrogen atmosphere, with a heating rate of $10 \text{ }^{\circ}\text{C} \cdot \text{min}^{-1}$ from 25-600 $^{\circ}\text{C}$.

The water swelling and the weight loss behaviors of both the neat calcium alginate beads embedded in the gelatin scaffolds and the AgNPs-loaded calcium alginate beads embedded in the gelatin scaffolds were investigated in a phosphate buffer solution (PBS, see in section 3.3.5.1 for the preparation of phosphate buffer solution) at the physiological temperature of 37 $^{\circ}\text{C}$ for 1, 3, 5, and 7 days. The measurements of each sample were calculated according to the following equations:

$$\text{Water swelling (\%)} = \frac{M - M_d}{M_d} \times 100, \quad (3.1)$$

$$\text{and} \quad \text{Weight loss (\%)} = \frac{M_i - M_d}{M_i} \times 100, \quad (3.2)$$

where M is the weight of each sample after submersion in a buffer solution for a certain period of time (1, 3, 5, and 7 days), M_d is the weight of each sample after

submersion in the buffer solution for a certain period of time (1, 3, 5, and 7 days) in its dry state, and M_i is the initial weight of each sample in its dry state.

3.3.5 Release Characteristics of Ag^+ Ions from AgNPs-Loaded Calcium Alginate Beads and AgNPs-Loaded Calcium Alginate Beads Embedded in Gelatin Scaffolds

3.3.5.1 Preparation of Phosphate Buffer Solution

6.177 g of anhydrous disodium hydrogen orthophosphate and 1.014 g of sodium dihydrogen orthophosphate were dissolved in ~100 mL of distilled water. 8.7 g of sodium chloride was then added into the 20 mL of this solution. Finally, distilled water (DI) was added into the solution to fill the volume up to 1,000 mL and adjust pH to 7.4.

3.3.5.2 Actual Silver Content

The actual amount of silver in both the AgNPs-loaded calcium alginate beads and the AgNPs-loaded calcium alginate microbeads embedded in the gelatin scaffolds was first determined. Each sample was immersed in 20 mL of PBS until the sample was completely dissolved. These solutions were determined using a Varian SpectrAA-300/a Hitachi Z-5000 atomic absorption spectroscope (AAS). The obtained data was calculated to determine the actual amount of silver in both AgNPs-loaded calcium alginate beads and the AgNPs-loaded calcium alginate beads embedded in the gelatin scaffolds.

3.3.5.3 Silver Release Assay

The release characteristics of Ag^+ ions from both the AgNPs-loaded calcium alginate beads and the AgNPs-loaded calcium alginate beads embedded in the gelatin scaffolds were investigated by total immersion method in the PBS (pH 7.4) and DI (pH 7.0) at 37 °C. After a specified immersion time ranging between 0 and 7 days, 2 or 3 mL of the sample solution was withdrawn and equal amount of fresh medium was refilled. The released amount of Ag^+ ions in each sample solutions was determined using AAS. The obtained data were calculated to determine the cumulative amount of Ag^+ ions released from both the AgNPs-loaded calcium alginate beads and the AgNPs-loaded calcium alginate beads embedded in the gelatin scaffolds.

3.3.6 Antibacterial Evaluation of AgNPs-Loaded Calcium Alginate Beads Embedded in Gelatin Scaffolds

The AATCC Test Method 100 (Antibacterial Finishes on Textile Materials: Assessment of The American Association of Textile Chemists and Colorists) or Colonies count was used to investigate the antibacterial activity of the AgNPs-loaded calcium alginate beads embedded in the gelatin scaffolds against *Escherichia coli* TISTR 780 and *Staphylococcus aureus* TISTR 1466. First, 1.0 mL of culture medium (10^5 CFU/mL) was added into each sample and then kept it in incubator at 37 °C for 24 h. For control, the neat calcium alginate beads embedded in the gelatin scaffolds were tested. After 24 h incubation, the bacteria were eluted from each sample by adding 5 mL of sterile DI into each sample with vigorously shaking for 5 minutes at room temperature. The eluted solutions were then made a series dilution by using 0.1% peptone. The series diluted solutions were spread (in triplicate) on nutrient agar (NA) plate. These plates were incubated at 37 °C for 24 h. Finally, the colonies on agar plate were photographed and counted (range of 30-300 colonies) to evaluate the antibacterial activity. The number of bacteria presented in the sample was determined (on agar plate) and the percentage of reduction was also calculated.

The percent reduction of bacteria (R, %) was calculated by the following equation:

$$R (\%) = \frac{100 (B - A)}{B} \quad (3.3)$$

where A is the number of bacteria recovered from the treated test sample (AgNPs-loaded calcium alginate beads embedded in gelatin scaffolds) after incubation at 37 °C for 24 h and B is the number of bacteria recovered from the untreated test sample (neat calcium alginate beads embedded in gelatin scaffolds) after incubation at 37 °C for 24 h.

3.3.7 Indirect Cytotoxicity Evaluation of AgNPs-Loaded Calcium Alginate Beads and AgNPs-Loaded Calcium Alginate Beads Embedded in Gelatin Scaffolds

The indirect cytotoxicity evaluation of the AgNPs-loaded calcium alginate beads and the AgNPs-loaded calcium alginate beads embedded in the gelatin

scaffolds was investigated in adaptation from the ISO 10993-5 standard test method in a 96-well tissue-culture polystyrene plate (TCPS; Corning Costar[®], USA) using normal human dermal fibroblasts (NHDF; 7th passage). The cells were cultured in Dulbecco's modified Eagle's medium (DMEM; Sigma-Aldrich, USA), supplemented by 10% fetal bovine serum (FBS; Invitrogen Corp., USA), 1% L-glutamine (Invitrogen Corp., USA) and 1% antibiotic and antimycotic formulation [containing penicillin G sodium, streptomycin sulfate, and amphotericin B (Invitrogen Corp., USA)]. The AgNPs-loaded calcium alginate beads and AgNPs-loaded calcium alginate beads embedded in the gelatin scaffolds (47 ± 1 mg) were sterilized by UV radiation for ~1 h and then were immersed in 1 mL of serum-free medium (SFM; containing DMEM, 1% L-glutamine, 1% lactalbumin, and 1% antibiotic and antimycotic formulation) for 24 h in incubation to produce extraction media. NHDF cells were separately cultured in wells of TCPS at 10,000 cells/well in serum-containing DMEM for 24 h to allow cell attachment. The cells were then starved with SFM for 24 h. After that, the medium was replaced with an extraction medium and cells were re-incubated for 24 h. The viability of the cells cultured by each of the extraction medium was determined with 3-(4,5-dimethylthiazol-2-yl)-2,5-diphenyltetrazolium bromide (MTT) assay, with the viability of the cells cultured by fresh SFM was used as control.

The MTT assay is based on the reduction of the yellow tetrazolium salt to purple formazan crystals by dehydrogenase enzymes secreted from the mitochondria of metabolically active cells. The amount of purple formazan crystals formed is proportional to the number of viable cells. First, each culture medium was aspirated and replaced with 25 μ L/well of MTT solution at 5 mg·mL⁻¹ for a 96-well TCPS. The plate was incubated for 2 h at 37 °C. The solution was then aspirated and 100 μ L/well of dimethyl sulfoxide (DMSO) was added to dissolve the formazan crystals. After 3 min of rotary agitation, the absorbance at the wavelength of 570 nm representing the viability of the cells was measured using a SpectraMax M2 Microplate Reader.

CHAPTER 4

PREPARATION AND CHARACTERIZATION OF SILVER NANOPARTICLES-LOADED CALCIUM ALGINATE BEADS EMBEDDED IN GELATIN SCAFFOLDS

4.1 Abstract

Silver nanoparticles (AgNPs)-loaded alginate beads embedded in gelatin scaffolds were successfully prepared. The AgNPs-loaded calcium alginate beads were prepared by electrospraying method. The effect of alginate concentration and applied voltage on shape and diameter of beads was studied. The diameter of dry AgNPs-loaded calcium alginate beads at various concentrations of AgNO₃ were ranged between 154 and 171 µm. The AgNPs-loaded calcium alginate beads embedded in gelatin scaffolds were fabricated by freeze-drying method. The water swelling and weight loss behaviors of the AgNPs-loaded alginate beads embedded in gelatin scaffolds increased with an increase in the submersion time. Moreover, the genipin-crosslinked gelatin scaffolds were proven to be non-toxic to normal human dermal fibroblasts, suggesting their potential uses as wound dressings.

Keywords: Alginate beads/ Electrospraying/Gelatin/Scaffolds/Silver nanoparticles

4.2 Introduction

Metal nanoparticles, produced from silver, gold, and copper have been reported and well known for their antibacterial properties. Silver nanoparticles (AgNPs) are widely used as antibacterial agents due to their non-toxicity and strong antibacterial activity (Sharma, Yngard & Lin, 2009). AgNPs can be synthesized by chemical reduction using sodium borohydride (NaBH_4), formamide, and triethanolamine. The advantages of this method are its simplicity and effectiveness. However, its disadvantages such as biological toxicity and environmental hazard of residual reducing agents have been reported. Other methods such as X-ray irradiation, UV irradiation and microwave were also used to synthesize AgNPs since they can eliminate the purification step for removing the residual reducing agents (Yoksan & Chirachanchai, 2009).

Electrohydrodynamic spraying or electrospraying is a technique that has been reported to produce polymer beads for controlled release (Ciach, 2006; Ding et al., 2005; Xie, Lim, Phua, Hua & Wang, 2006). It is a process of liquid atomization with electrical forces. In this process, the liquid flowing out from a capillary nozzle which is maintained at high electric potential is applied by the electric field to be dispersed into droplets (Cloupeau, 1994). The size of droplets can be varied from hundreds micrometers down to tens nanometers. The shape and size of droplets can be controlled by the flow rate of the liquid and the voltage at the capillary nozzle (Jaworek & Sobczyk, 2008). Recently, several parameters affecting the shape of alginate beads produced by electrospraying/extrusion were studied. The results showed that higher voltage, higher calcium chloride concentration, shorter width of electrical field and slower extrusion rates resulted in small size of alginate beads (Shi, He, Teh, Morsi & Goh, 2011). Moreover, bovine serum albumin (BSA) was used as a protein model drug and loaded in the alginate beads by electrospraying method. The results showed that the higher amount of initial BSA and the slower releasing rate of BSA from the formulation were observed (Suksamran et al., 2009).

Alginate is a natural polysaccharide extracted from brown seaweed. It is composed of β -D-mannuronic acid (M) and α -L-guluronic acid (G) (Augst, Kong & Mooney, 2006). It is cross-linked with calcium ions to form gel, known as “the egg-

box model” (Martinez et al., 2012; Thu, Zulfakar & Ng, 2012). Generally, it can be used as living cell encapsulant matrices (Rebelatto, Guimond, Bowersock & HogenEsch, 2011), wound dressings (Ouwerx, Velings, Mestdagh & Axelos, 1998) and intranasal drug delivery devices (Rousseau et al., 2004). In addition, it can encapsulate angiogenic growth factors, such as basic fibroblast growth factor (bFGF) and the vascular endothelial growth factor (VEGF) to treat ischemia.

Polymeric scaffolds are substrates for the implanted cells with good physical support to control the tissue restoration or improve the functional tissue regeneration (Chen et al., 2002). In addition, the polymeric scaffolds can support cell adhesion, migration, proliferation and differentiation (Yarlagadda, Chandrasekharan & Shyan, 2005). Scaffolds should have three-dimensional architecture, highly porous with a large surface area/volume ratio, and well interconnected open pore structure. Moreover, they should be mechanically strong, malleable, biocompatible, and biodegradable (Freed et al., 2004; Hutmacher, 2001; Ma & Choi, 2001). Freeze-drying used to produce the polymeric scaffolds involves the formation of ice crystals inside polymer solution during freezing, and those ice crystals act as porogen particles during lyophilization, resulting in the forming of a porous three-dimensional polymeric scaffolds (Kang et al., 1999). Gelatin is widely used in medical applications as scaffold materials because of its biocompatibility, low immunogenicity, and biodegradability (Kim et al., 2009).

The aim of this work is to develop a method for controlling and sustaining release of AgNPs from the AgNPs-loaded calcium alginate beads embedded in gelatin scaffolds. The effect of alginate concentration and the applied voltage on the morphology and size of the calcium alginate beads was studied. The calcium alginate beads incorporated with AgNPs were obtained by electrospraying method. UV irradiation technique was used to reduce the silver (Ag^+) ions in alginate solution to AgNPs. Moreover, the AgNPs-loaded calcium alginate beads embedded in gelatin scaffolds were fabricated by freeze drying method. The shape and size of both the neat and the AgNPs-loaded calcium alginate beads were observed by optical microscope (OM) and scanning electron microscope (SEM). The morphological appearance of both neat and the AgNPs-loaded calcium alginate beads embedded in gelatin scaffolds was also studied. The water swelling and weight loss behaviors of

the AgNPs-loaded calcium alginate beads embedded in gelatin scaffolds were investigated. Lastly, the indirect cytotoxicity of the genipin-cross-linked gelatin scaffolds with different genipin concentrations was investigated.

4.3 Experimental Details

4.3.1 Materials

Gelatin (Type A, porcine skin, ~180 Bloom) was purchased from Fluka Analytical (Switzerland). Genipin powder (98% purity) was obtained from Shanghai Angoal Chemical (China). Sodium alginate was purchased from Carlo Erba (Italy). Silver nitrate (AgNO_3 ; $\geq 99.9\%$ purity) was purchased from Fisher Scientific (USA). Calcium chloride (CaCl_2), sodium chloride, anhydrous disodium hydrogen orthophosphate and sodium dihydrogen orthophosphate (Ajax Chemicals, Australia) were analytical reagent grade and used without further purification.

4.3.2 Preparation of both Neat and AgNPs-Loaded Calcium Alginate Beads

Firstly, the optimal condition for producing calcium alginate beads was carried out by electrospraying method (Figure 4.1). The concentration of sodium alginate solution was 0.5, 1.0, and 1.5% w/v and the applied voltage was 8, 10, 12, and 15 kV. The prepared sodium alginate solutions were then extruded dropwise through a needle placed into a glass syringe capped with a 24-gauge blunt needle (an internal diameter of needle is 0.55 mm) into a 0.5 M CaCl_2 solution under an applied electric field. The distance between tip to collector was fixed at 15 cm. The calcium alginate beads were collected in CaCl_2 solution with gentle stirring for 30 min. The obtained calcium alginate beads were washed with deionized water and then lyophilized for 20 h.

For the AgNPs-loaded calcium alginate beads, the preparation was presented in Figure 4.2. The base sodium alginate solution was prepared at a fixed concentration of 1.5% w/v. The AgNPs-loaded sodium alginate solutions were prepared by adding 1, 2, and 3% w/w AgNO_3 (based on the weight of sodium alginate) into the base sodium alginate solutions. According to the previous method (Darroudi et al., 2011), the Ag^+ ions in the alginate solution was reduced to AgNPs by UV irradiation at 254

nm for 1 h. Prior to electrospraying, the solutions were characterized for their viscosity and conductivity at room temperature (26 ± 1 °C) using a Brookfield/RVDV-II+P viscometer and a CyberScan con 200 conductivity meter, respectively. These solutions were then extruded dropwise through a needle into a 0.5 M CaCl_2 solution under a fixed electric field of 12 kV/15 cm using the electrospraying method. The obtained AgNPs-loaded calcium alginate beads were left in the CaCl_2 solution for 30 min. Finally, these beads were separated from CaCl_2 solution and then washed with deionized water. It should be noted that the calcium alginate beads containing 1, 2, and 3% w/w of AgNO_3 are hereafter denoted as 1%, 2%, and 3% AgNPs-loaded calcium alginate beads, respectively.

4.3.3 Preparation of Genipin-Crosslinked Gelatin Scaffolds and AgNPs-Loaded Calcium Alginate Beads Embedded in Gelatin Scaffolds

Gelatin powder was dissolved in boiled deionized water to prepare the base gelatin solution at a fixed concentration of 5% w/v. Genipin was used as a cross-linking agent to cross-link the amino acid groups of gelatin as shown in Figure 4.3 (Chang, Tsai, Liang & Sung, 2001). Various concentrations of genipin (i.e., 3, 4, 5, and 6% w/w based on the weight of gelatin powder) were added into gelatin solutions and then, the solutions were stirred at room temperature for 1 h. These solutions were then poured into polypropylene (PP) mold and lyophilized to form scaffolds by freeze-drying method.

The dry 1%, 2%, and 3% AgNPs-loaded calcium alginate beads were used to embed in the gelatin scaffolds. The AgNPs-loaded calcium alginate beads embedded in gelatin scaffolds were prepared by adding 1% w/w of the AgNPs-loaded calcium alginate beads (based on the weight of gelatin powder) into 5% w/v of gelatin solutions. These solutions were then poured into PP mold and cross-linked at room temperature for 24 h. The AgNPs-loaded calcium alginate beads embedded in gelatin scaffolds were obtained by lyophilization.

4.3.4 Morphological Observation

The shape and size of both the neat and the AgNPs-loaded calcium alginate beads were investigated by Motic BA300 optical microscope (OM) using the

magnification of 4x and a LEO 1450 VP scanning electron microscope (SEM). For the morphological observation, each sample was coated with a thin layer of gold using a Polaron SC-7620 sputtering device. The diameters of the beads were measured directly from OM and SEM images using a Motic Images Plus 2.0 and a SemAphore 4.0 software, respectively.

The shape and size of AgNPs in the AgNPs-loaded calcium alginate beads were investigated by a JEOL JEM-2100 transmission electron microscope (TEM). The dispersion of the AgNPs-loaded calcium alginate beads in ethanol solution was placed on carbon-coated copper grid. The sample grid was kept in desiccator cabinet until the solvent was slowly evaporated.

The genipin-cross-linked gelatin scaffolds and the AgNPs-loaded calcium alginate beads embedded in the gelatin scaffolds were characterized for their morphological appearance by SEM. Each sample was coated with a thin layer of gold using a Polaron SC-7620 sputtering device prior to the observation under SEM. Pore sizes of the scaffolds were measured directly from SEM images using a SemAphore 4.0 software. More than 30 pores of each sample group were measured.

4.3.5 Indirect Cytotoxicity Evaluation of Genipin-Crosslinked Gelatin Scaffolds

The indirect cytotoxicity evaluation of genipin-cross-linked gelatin scaffolds was conducted in adaptation from the ISO 10993-5 standard test method in a 96-well tissue-culture polystyrene plate (TCPS; Corning Costar®, USA) using normal human dermal fibroblasts (NHDF; 7th passage). The ISO 10993-5 standard test method is the test method to assess the *in vitro* cytotoxicity of medical devices. First, the cells were cultured in Dulbecco's modified Eagle's medium (DMEM; Sigma-Aldrich, USA), supplemented by 10% fetal bovine serum (FBS; Invitrogen Corp., USA), 1% L-glutamine (Invitrogen Corp., USA) and 1% antibiotic and antimycotic formulation [containing penicillin G sodium, streptomycin sulfate, and amphotericin B (Invitrogen Corp., USA)]. The genipin-cross-linked gelatin scaffolds that had been cross-linked with 3, 4, 5, and 6% w/w of genipin (47 ± 1 mg) were sterilized by UV radiation for ~1 h and then were immersed in 1 mL of serum-free medium (SFM; containing DMEM, 1% L-glutamine, 1% lactalbumin, and 1% antibiotic and

antimycotic formulation) for 24 h in incubation to produce extraction media. NHDF cells were separately cultured in wells of TCPS at 10,000 cells/well in serum-containing DMEM for 24 h to allow cell attachment. The cells were then starved with SFM for 24 h. After that, the medium was replaced with an extraction medium and cells were re-incubated for 24 h. The viability of the cells cultured by each of the extraction medium was determined with 3-(4,5-dimethylthiazol-2-yl)-2,5-diphenyltetrazolium bromide (MTT) assay, with the viability of the cells cultured by fresh SFM was used as control.

The MTT assay is based on the reduction of the yellow tetrazolium salt to purple formazan crystals by dehydrogenase enzymes secreted from the mitochondria of metabolically active cells. The amount of purple formazan crystals formed is proportional to the number of viable cells. First, each culture medium was aspirated and replaced with 25 μL /well of MTT solution at 5 $\text{mg}\cdot\text{mL}^{-1}$ for a 96-well TCPS. The plate was incubated for 2 h at 37 °C. The solution was then aspirated, and 100 μL /well of dimethyl sulfoxide (DMSO) was added to dissolve the formazan crystals. After 3 min of rotary agitation, the absorbance at the wavelength of 570 nm representing the viability of the cells was measured using a SpectraMax M2 Microplate Reader.

4.3.6 Water Swelling and Weight Loss Behaviors of AgNPs-loaded Calcium Alginate Beads Embedded in Gelatin Scaffolds

The water swelling and the weight loss behaviors of the AgNPs-loaded calcium alginate beads embedded in gelatin scaffolds were investigated in a phosphate buffer solution (PBS) at the physiological temperature of 37 °C for 1, 3, and 5 days. The measurements of each sample were calculated according to the following equations:

$$\text{Water swelling (\%)} = \frac{M - M_d}{M_d} \times 100, \quad (4.1)$$

and

$$\text{Weight loss (\%)} = \frac{M_i - M_d}{M_i} \times 100, \quad (4.2)$$

where M is the weight of each sample after submersion in a buffer solution for a certain period of time (1, 3, and 5 days), M_d is the weight of each sample after submersion in the buffer solution for a certain period of time (1, 3, and 5 days) in its dry state, and M_i is the initial weight of each sample in its dry state.

4.3.7 Statistical Analysis

Data were presented as means \pm standard errors of means. Statistical analysis was carried out by the one-way analysis of variance (one-way ANOVA) and Scheffe's post hoc test in SPSS (IBM SPSS, USA). The statistical significance was accepted at $p < 0.5$.

4.4 Results and Discussion

4.4.1 Neat and AgNPs-Loaded Calcium Alginate Beads

The effect of the concentration of the alginate solutions (i.e., 0.5, 1.0, and 1.5% w/v) and the applied voltage (i.e., 8, 10, 12, and 15 kV over a fixed collection distance of 15 cm) on morphology and size of the calcium alginate beads was reported (see Table 4.1). The shapes and diameters of both the wet and dry calcium alginate beads were observed by OM and SEM, respectively. The results are shown in Table 4.2 and Table 4.3. The results showed that the diameters of all dry calcium alginate beads were smaller than the diameters of the wet calcium alginate beads because the water molecules in dry beads diffused out from the beads. The effect of the concentration of the alginate solution at the fixed applied voltage of 12 kV on the diameters of beads is also shown in Table 4.2. According to the obtained results, the diameters of the dry calcium alginate beads obtained under these conditions ranged between 40 and 170 μm . For a given applied voltage, increasing concentration of alginate solution caused the diameters of the beads to increase. Moreover, the beads became more spherical when the alginate concentration was increased. The effect of the applied voltage at the fixed alginate concentration of 1.5% w/v on the diameters of beads is also shown in Table 4.3. According to this result, the diameters of the dry calcium alginate beads obtained under these conditions ranged between 148 and 276 μm . For a given concentration, increasing the applied voltage caused the diameters of

the beads to decrease, except for alginate concentration of 0.5% w/v and the applied voltage of 15 kV (Table 4.1). The increase of the applied voltage could overcome the surface tension force of the alginate droplet, resulting in the decrease of the bead diameters while the increase of the alginate concentration increased the surface tension force of the alginate droplet, resulting in the increase of the bead diameters. Hence, the factors affecting the diameters and shapes of the calcium alginate beads were the concentration of the alginate solution and the applied voltage. To further investigate the electrospraying of the AgNPs-loaded calcium alginate beads, the alginate concentration of 1.5% w/v and the applied voltage of 12 kV over a fixed collection distance of 15 cm were chosen as the model condition. As mentioned, Shi et al. (2011) reported that the higher applied voltages could allow the alginate beads to become smaller because the high applied voltage provided the stronger electrical force on the surface of the alginate droplets to small inject formed. The high concentration of the alginate solution was viscous and sticky that affected the solution and could not regurgitate round shape. For the low concentration of the solution, the alginate molecules were not enough on the surface layer. The shrinkage of the bead surface occurred after gelation; thus, the tear-like structure of the beads was observed. The results indicated that the concentration of the alginate solution affected the shape of the beads significantly (Shi et al., 2011).

According to Table 4.2 and 4.3, the 1.5% w/v alginate solution that was electrosprayed under the fixed applied voltage of 12 kV/15 cm was chosen as the model condition for further investigation. Because it was easy to spray and the shape of the beads was more spherical. The AgNPs-loaded calcium alginate beads were prepared by adding varying amounts of the AgNO_3 (i.e., 1, 2, and 3% w/w based on the weight of sodium alginate powder) to the 1.5% w/v alginate solution. Before electrospraying, the base sodium alginate solutions containing varying amounts of the AgNO_3 were irradiated by UV irradiation for 1 h. The Ag^+ ions in the alginate solutions were reduced to AgNPs. After electrospraying, the AgNPs were obtained within the calcium alginate beads as shown in Figure 4.4. The shapes and diameters of both the wet and dry AgNPs-loaded calcium alginate beads were observed by OM and SEM, respectively, and the results are shown in Table 4.4. The diameters of the wet 1%, 2%, and 3% AgNPs-loaded calcium alginate beads were 573.46 ± 17.64 , 512.27

± 13.13 and 462.86 ± 12.59 μm , respectively, while the diameters of the dry 1%, 2%, and 3% AgNPs-loaded calcium alginate beads were 171.33 ± 21.39 , 166.89 ± 16.65 , and 153.71 ± 15.16 μm , respectively. From Table 4.4, increasing of the AgNO_3 concentrations decreased the diameters of the AgNPs-loaded calcium alginate beads. These results could be supported by the shear viscosity and electrical conductivity of the AgNPs-containing alginate solutions, results as shown in Table 4.5. From Table 4.5, the shear viscosity of the solutions decreased with increasing AgNO_3 concentration while the electrical conductivity of the solutions increased with increasing the AgNO_3 concentration. The increased electrical conductivity of the AgNPs-containing alginate solutions was a direct result of an increase in the amount of Ag^+ ions within the AgNPs-containing alginate solutions. This increase in the number of charge carriers caused both electrostatic and coulombic repulsive forces to overcome the surface tension of the solutions, leading to the smaller diameters of the beads (Shi et al., 2011).

4.4.2 Genipin-Cross-linked Gelatin Scaffolds and AgNPs-Loaded Calcium Alginate Beads Embedded in Gelatin Scaffolds

Representative SEM images of the gelatin scaffolds prepared from 5% w/v of gelatin solution and cross-linked with various concentrations of genipin (i.e., 3, 4, 5, and 6% w/w based on the weight of gelatin powder) are shown in Table 4.6. The results showed that the interconnected porous structure of all scaffolds was obtained. The pore size of these scaffolds ranged between 179.38 ± 49.68 μm and 203.30 ± 70.93 μm . In addition, the gelatin scaffolds that had been cross-linked with 5% w/w of genipin showed the larger size of interconnected porous structure than other scaffolds. However, increasing the concentration of genipin did not affect the pore size of scaffolds. Tonda-Turo et al. (2011) reported that the mean pore size of the pure 2.5% w/v of gelatin scaffolds and the gelatin scaffolds cross-linked with genipin was about 140 and 120 μm , respectively (Tonda-Turo et al., 2011), while, Abbasi, Eslamian, Heyd & Rousseau (2008) reported that the increase of the genipin concentration caused the pore size of gelatin matrices to decrease. The representative SEM images of the AgNPs-loaded calcium alginate beads embedded in gelatin scaffolds are shown in Table 4.7. The results showed that the interconnected porous

structure of all scaffolds was obtained. The pore size of these scaffolds ranged between $154.70 \pm 37.30 \mu\text{m}$ and $245.06 \pm 68.38 \mu\text{m}$ while the pore size of the gelatin scaffolds unembedded with the AgNPs-loaded calcium alginate beads was $179.38 \pm 49.68 \mu\text{m}$ (see Table 4.6). However, embedding of the AgNPs-loaded calcium alginate beads into the gelatin scaffolds did not affect the pore size of the scaffolds. To be used as scaffold materials or wound dressings, the pore size of polymeric scaffolds should facilitate cell seeding, attachment and also allow liquid flow to transport nutrients through the porosity of materials. Thus, the optimal pore size of scaffolds was in the range between 100 and 500 μm (Ikada, 2006).

4.4.3 Indirect Cytotoxicity Evaluation of Genipin-Cross-linked Gelatin Scaffolds

To assess the toxicity of the genipin-cross-linked gelatin scaffolds, indirect cytotoxicity evaluation was carried out. The gelatin scaffolds cross-linked with various genipin concentrations (i.e., 3, 4, 5, and 6% w/w based on the weight of gelatin powder) were evaluated for their cytotoxicity. The viability of the NHDF cultured with the extraction media from these samples in comparison with that of the cells cultured with the fresh culture medium is shown in Figure 4.5. Obviously, the viability of the cells cultured with all the extraction media from the genipin-cross-linked gelatin scaffolds with various genipin concentrations ranged between ~85 and ~100%, indicating that all the genipin-cross-linked gelatin scaffolds were proven non-toxic to NHDF, indicating their potential uses for wound dressings.

4.4.4 Water Swelling and Weight Loss Behaviors of AgNPs-Loaded Calcium Alginate Beads Embedded in Gelatin Scaffolds

The water swelling and the weight loss behaviors of the 1%, 2%, and 3% AgNPs-loaded calcium alginate beads embedded in gelatin scaffolds after submersion in PBS at 37 °C for 1, 3, and 5 day were investigated and the results are shown in Figure 4.6. At 1 day after submersion in PBS, the water swelling of the 1%, 2%, and 3% AgNPs-loaded beads embedded in gelatin scaffolds was ~744, ~738, and ~752%, respectively (see Figure 4.6a). At 3 days, the value increased to ~805, ~796, and ~802%, respectively. At 5 days, the value also increased to ~889, ~909, and ~942%, respectively. Thus, the water swelling of all the AgNPs-loaded calcium alginate beads

embedded in gelatin scaffolds increased with increasing submersion time. However, the increasing of AgNO_3 content for loading in the gelatin scaffolds did not much affect the water swelling of these scaffolds.

The weight loss behavior of the AgNPs-loaded calcium alginate beads embedded in gelatin scaffolds after submersion in PBS at 37 °C for 1, 3, and 5 day is shown in Figure 4.6b. At 1 day after submersion in PBS, the weight loss of the 1%, 2%, and 3% AgNPs-loaded beads embedded in gelatin scaffolds was ~7, ~8, and ~7%, respectively, while at 3 days, the value were ~8, ~8, and ~8%, respectively. At 5 days, the value significantly increased to ~14, ~15, and ~17%, respectively. Similar to the water swelling behavior, the weight loss of all AgNPs-loaded calcium alginate beads embedded in gelatin scaffolds increased with increasing submersion time, except at day 3, the weight loss of all the AgNPs-loaded calcium alginate beads embedded in gelatin scaffolds was slightly increased. Similarly, the increased AgNO_3 content for loading in the gelatin scaffolds did not much affect the weight loss of these scaffolds.

4.5 Conclusions

In this study, the AgNPs-loaded calcium alginate beads embedded in gelatin scaffolds were successfully prepared. The calcium alginate beads incorporated with AgNPs were obtained by electrospraying method. Factors affecting the shapes and diameters of the calcium alginate beads were the concentration of alginate solution and the applied voltage. Besides, the genipin-cross-linked gelatin scaffolds were proven non-toxic to NHDF, suggesting their potential uses for wound dressings.

4.6 Acknowledgements

The authors would like to acknowledge the financial support from the Research, Development and Engineering (RD&E) fund through The National Nanotechnology Center (NANOTEC), The National Science and Technology Development Agency (NSTDA), Thailand (P-11-00986) to Mae Fah Luang

University (MFU) and Thailand Graduate Institute of Science and Technology (TGIST) (TG-55-99-55-048M).

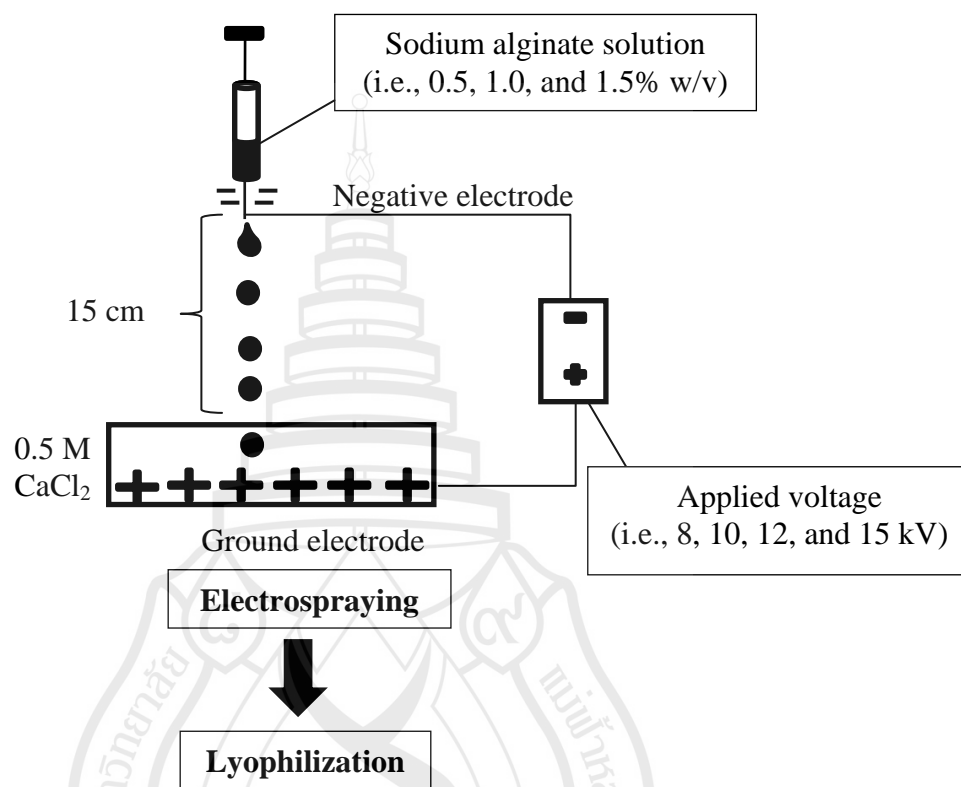


Figure 4.1 Scheme Preparations of Calcium Alginate Beads by Electrospaying Method

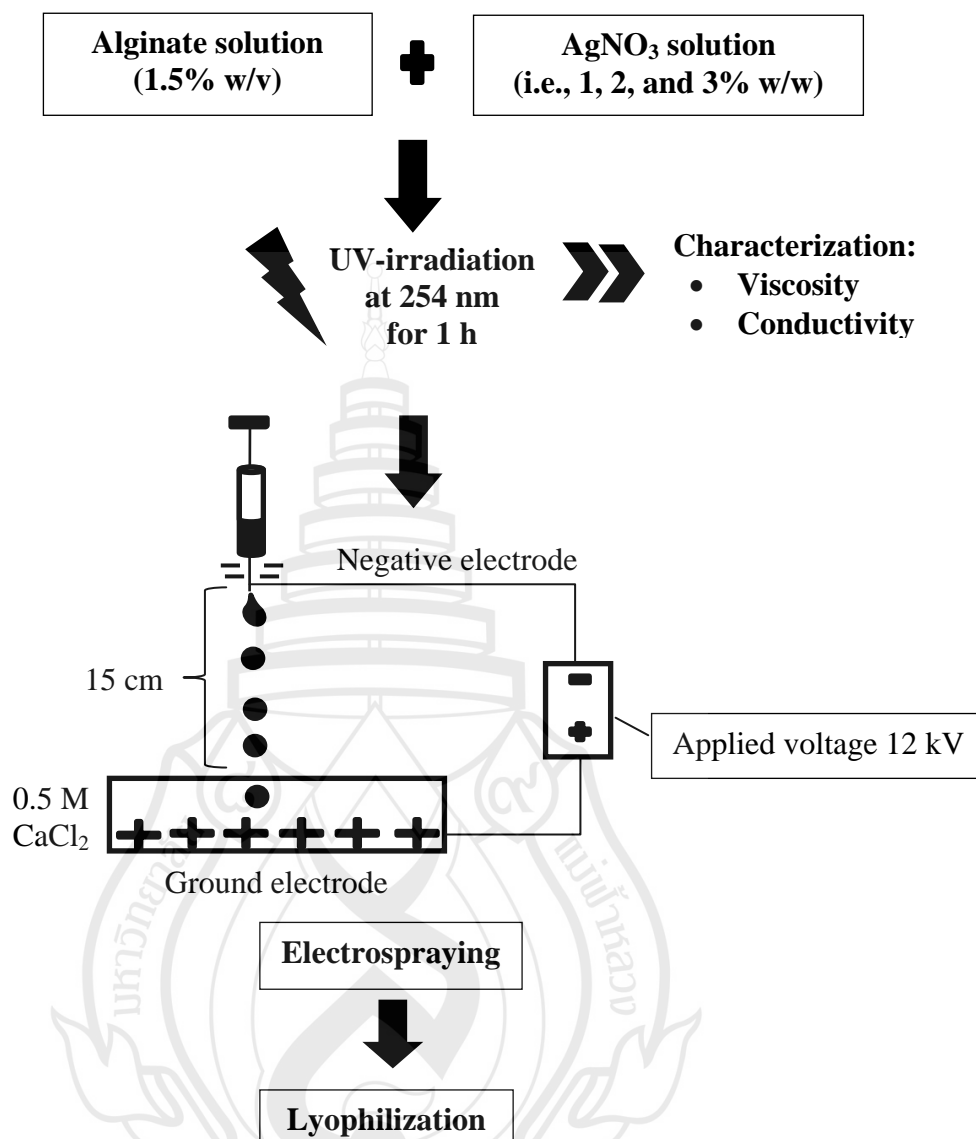


Figure 4.2 Scheme Preparations of AgNPs-Loaded Calcium Alginate Beads by Electro spraying Method

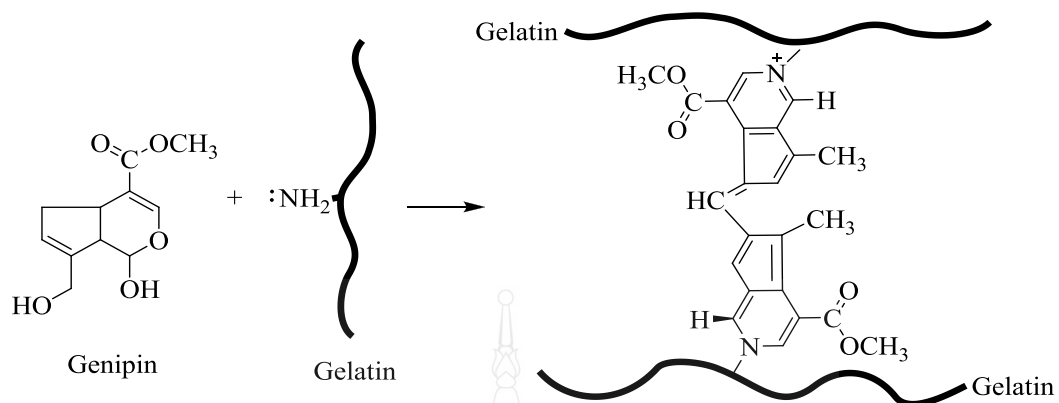


Figure 4.3 Schematic Illustrations of the Intermolecular Crosslinking Structures of Genipin with Gelatin

Table 4.1 Representative OM and SEM Images Illustrating the Effect of the Concentration of the Alginate and the Applied Voltage on the Morphology of the Obtained Beads as Well as the Average Values of Bead Diameters

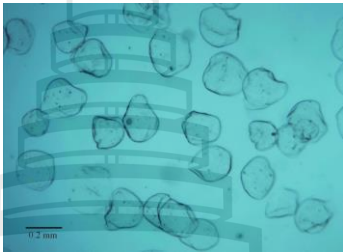
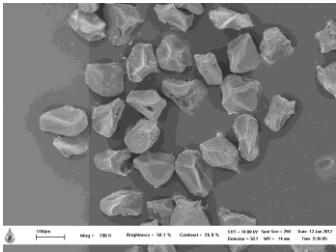
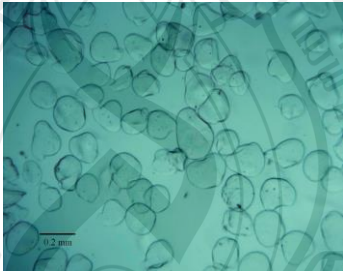
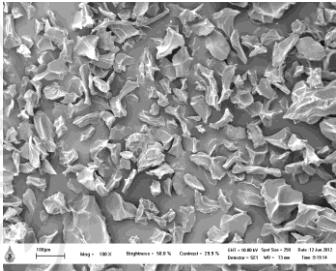
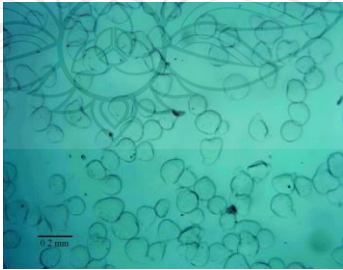
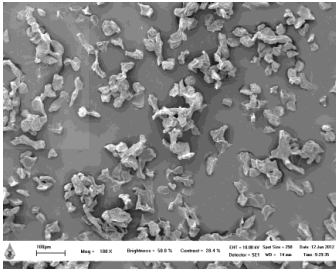
Alginate solution (% w/v)	Applied voltage (kV)	Observed by	
		OM	SEM
0.5	8		
	Bead diameters (μm)	224 ± 24.57	124.96 ± 13.83
	10		
	Bead diameters (μm)	151.63 ± 25.69	69.10 ± 8.21
	12		
	Bead diameters (μm)	123.19 ± 17.85	39.63 ± 4.83

Table 4.1 (continued)

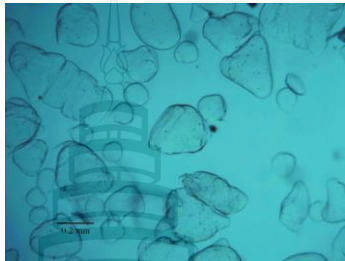
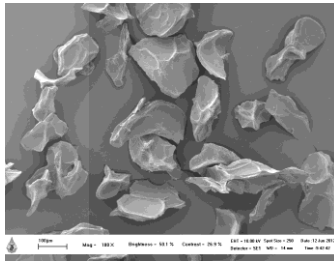
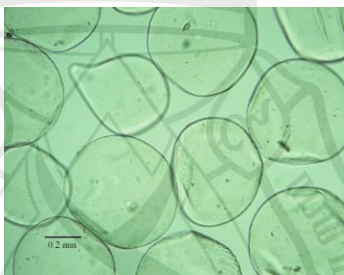
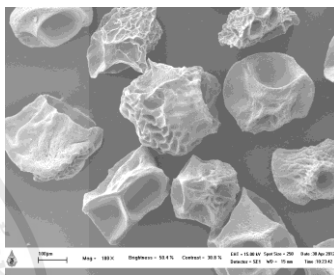
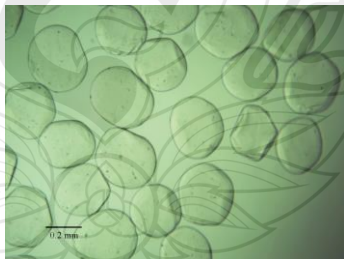
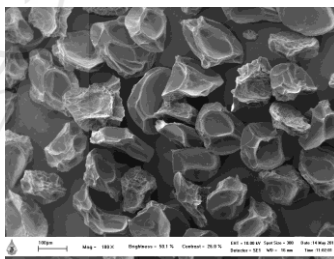
Alginate solution (% w/v)	Applied voltage (kV)	Observed by	
		OM	SEM
0.5	15		
	Bead diameters (µm)	221.51 ± 74.03	115.76 ± 18.87
1.0	8		
	Bead diameters (µm)	344.94 ± 39.32	246.39 ± 31.23
	10		
	Bead diameters (µm)	321.52 ± 26.70	170.50 ± 28.05

Table 4.1 (continued)

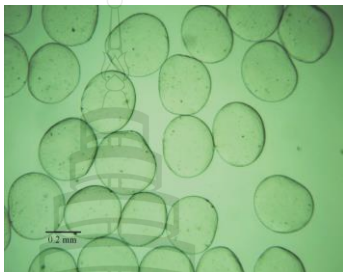
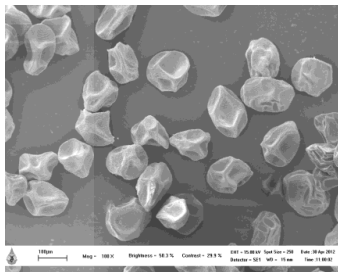
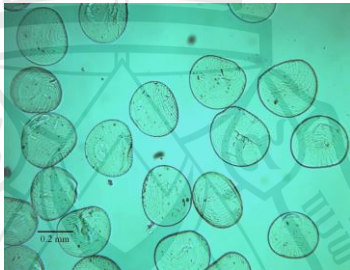
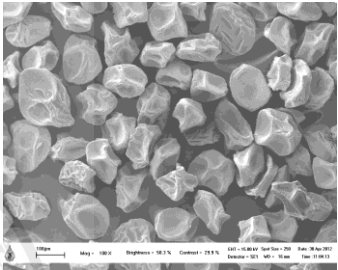

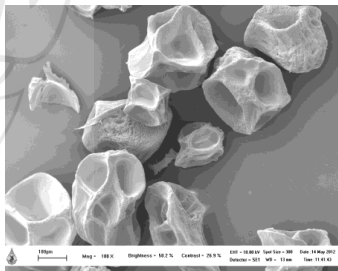
Alginate solution (% w/v)	Applied voltage (kV)	Observed by	
		OM	SEM
1.0	12		
	Bead diameters (μm)	306.63 ± 22.83	167.94 ± 27.23
1.0	15		
	Bead diameters (μm)	295.87 ± 21.48	133.55 ± 24.92
1.5	8		
	Bead diameters (μm)	618.83 ± 17.35	275.96 ± 41.67

Table 4.1 (continued)


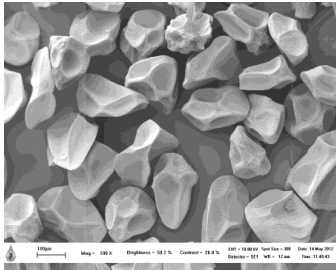
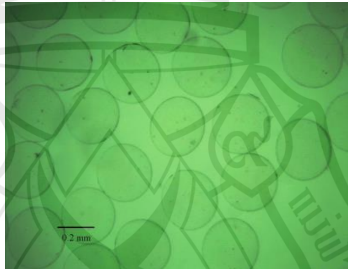
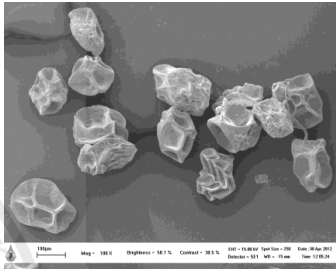

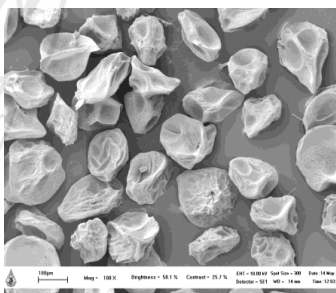
Alginate solution (% w/v)	Applied voltage (kV)	Observed by	
		OM	SEM
1.5	10		
	Bead diameters (μm)	383.27 ± 16.39	193.06 ± 26.96
	12		
	Bead diameters (μm)	331.51 ± 8.70	170.11 ± 21.12
	15		
	Bead diameters (μm)	316.02 ± 20.19	147.72 ± 17.14

Table 4.2 Representative OM and SEM Images Illustrating the Effect of the Concentration of the Alginate Solutions on the Morphology of the Obtained Beads at an Applied Voltage of 12 kV/15 cm as Well as the Average Values of Bead Diameters


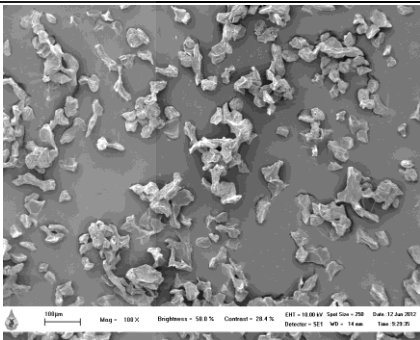
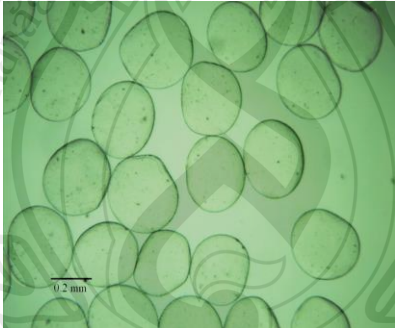
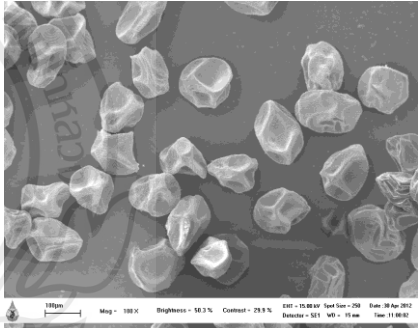
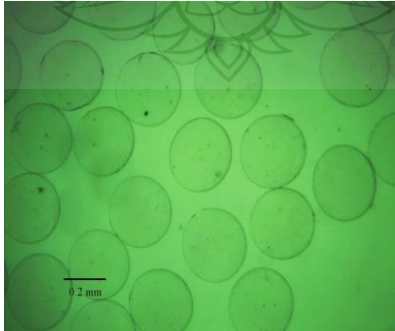
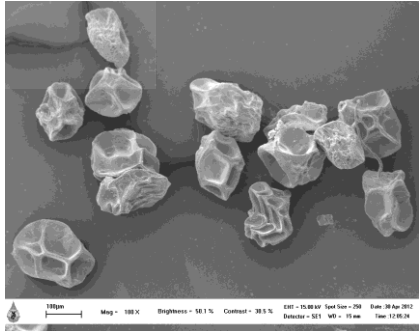
Alginate solution (% w/v)	Observed by	
	OM	SEM
0.5		
Bead diameters (μm)	123.19 ± 17.85	39.63 ± 4.83
1.0		
Bead diameters (μm)	306.63 ± 22.83	167.94 ± 27.23
1.5		
Bead diameters (μm)	331.51 ± 8.70	170.11 ± 21.1

Table 4.3 Representative OM and SEM Images Illustrating the Effect of the Applied Voltage on the Morphology of the Obtained Beads at a Fixed Alginate Concentration of 1.5 % w/v as Well as the Average Values of Bead Diameters

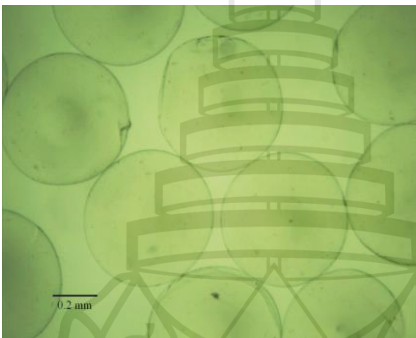
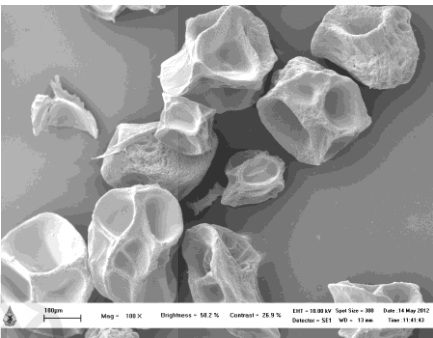
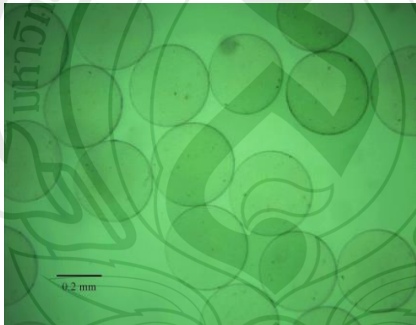
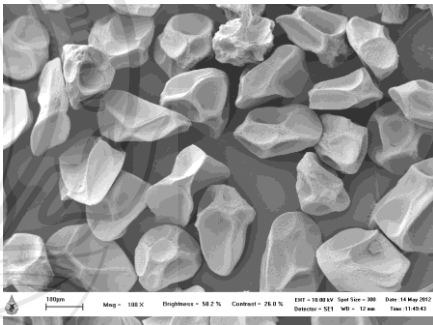
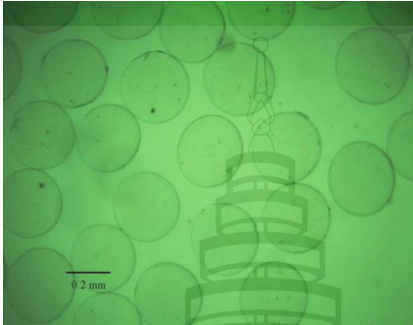
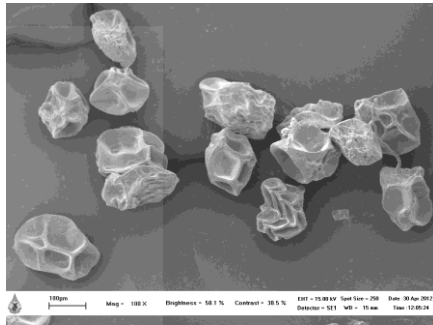

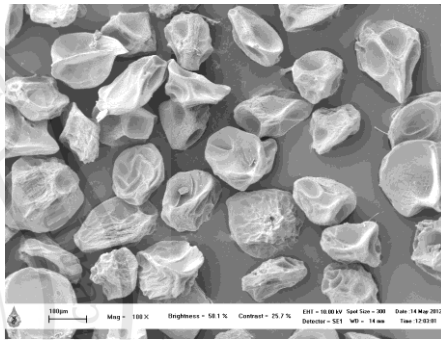
Applied voltage (kV)	Observed by	
	OM	SEM
8		
Bead diameters (μm)	618.83 ± 17.35	275.96 ± 41.67
10		
Bead diameters (μm)	383.27 ± 16.39	193.06 ± 26.96

Table 4.3 (continued)

Applied voltage (kV)	Observed by	
	OM	SEM
12		
Bead diameters (μm)	331.51 ± 8.70	170.11 ± 21.12
15		
Bead diameters (μm)	316.02 ± 20.19	147.72 ± 17.14

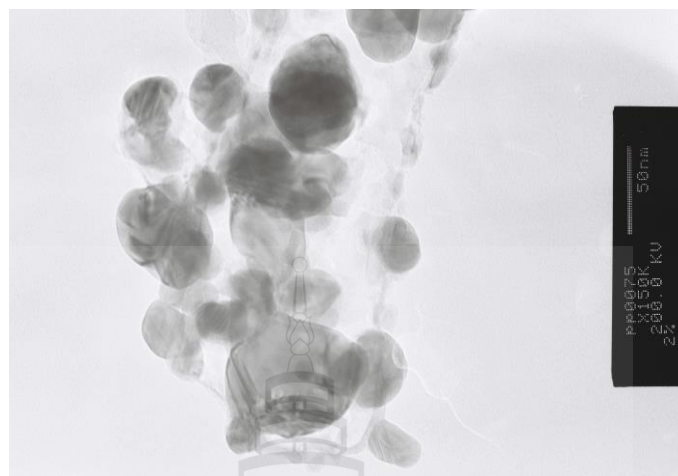


Figure 4.4 Selected TEM Image of the 2% AgNPs-Loaded Calcium Alginate Beads

Table 4.4 Representative OM and SEM Images of the AgNPs-Loaded Calcium Alginate Beads at Various Concentrations of AgNO₃

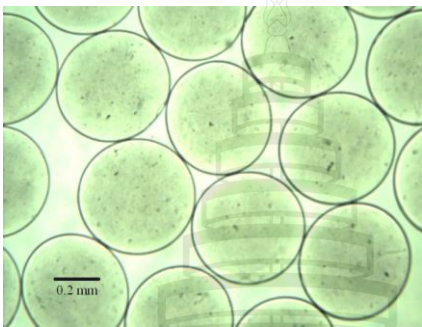
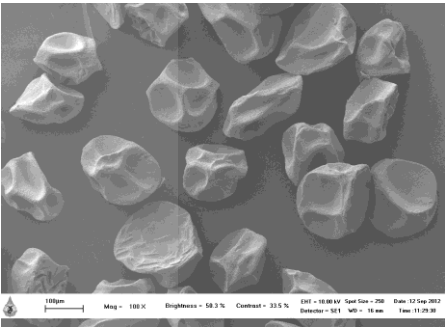
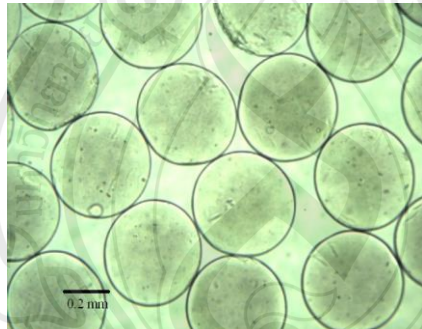
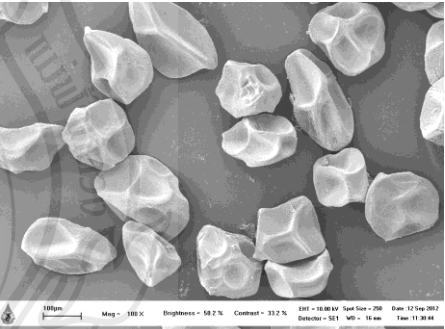
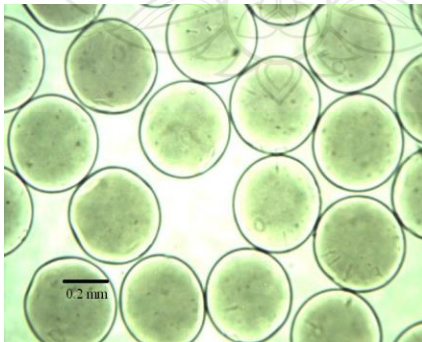
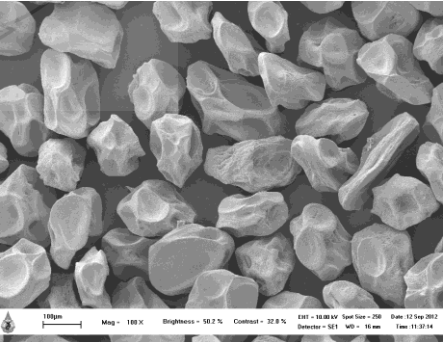
Concentration of AgNO ₃ (% w/w)	Observed by	
	OM	SEM
1		
Diameters (µm)	573.46 ± 17.64	171.33 ± 21.39
2		
Diameters (µm)	512.27 ± 13.13	166.89 ± 16.65
3		
Diameters (µm)	462.86 ± 12.59	153.71 ± 15.16

Table 4.5 Shear Viscosity and Electrical Conductivity of the AgNPs-Containing Alginate Solutions at Various Concentrations of AgNO₃ (n = 3)

Type of alginate solution	Shear viscosity (mPa s)	Electrical conductivity ($\mu\text{S cm}^{-1}$)
with 1% AgNO ₃ (based on weight of alginate)	96.9 \pm 1.2	1850 \pm 12
with 2% AgNO ₃ (based on weight of alginate)	96.4 \pm 1.6	1872 \pm 20
with 3% AgNO ₃ (based on weight of alginate)	90.4 \pm 1.4	1919 \pm 13

Table 4.6 Representative SEM Images of the Genipin-Crosslinked Gelatin Scaffolds with Different Genipin Concentrations As Well As the Average Values of Pore Sizes

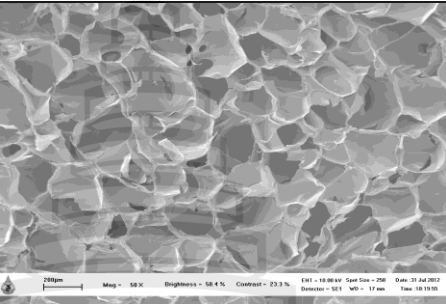
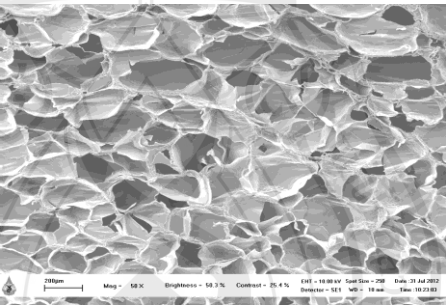
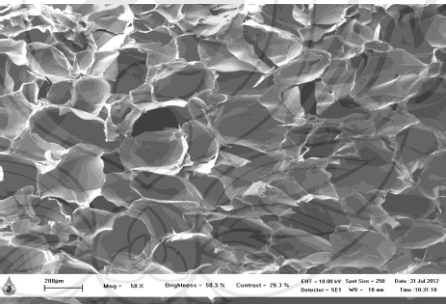
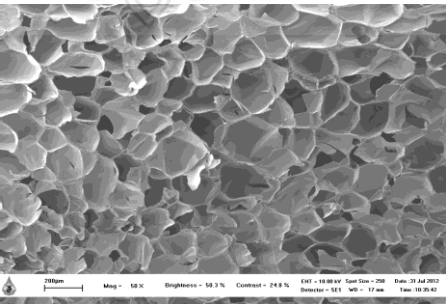
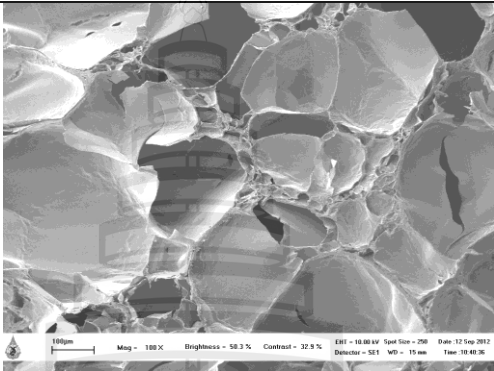
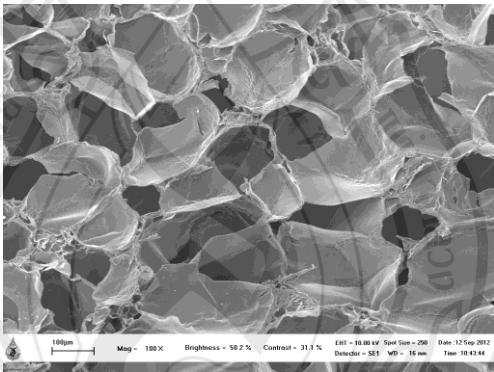
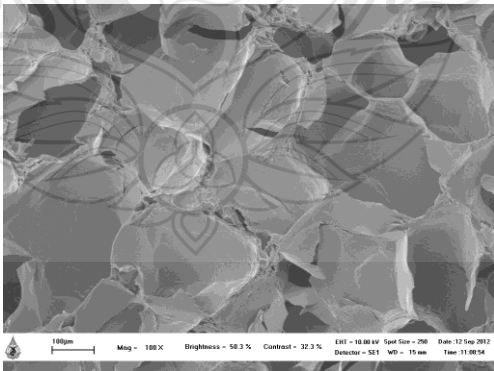
Genipin concentration (% w/w, based on weight of gelatin)	Representative SEM images of scaffolds	Pore sizes (μm)
3		179.38 ± 49.68
4		184.21 ± 59.15
5		203.30 ± 70.93
6		179.60 ± 49.37

Table 4.7 Representative SEM Images of the AgNPs-Loaded Calcium Alginate Beads Embedded in Gelatin Scaffolds As Well As the Average Values of Pore Sizes

Concentration of AgNO ₃ (% w/w)	Representative SEM images of scaffolds	Pore sizes (μm)
1		245.06 ± 68.38
2		154.70 ± 37.30
3		184.44 ± 60.20

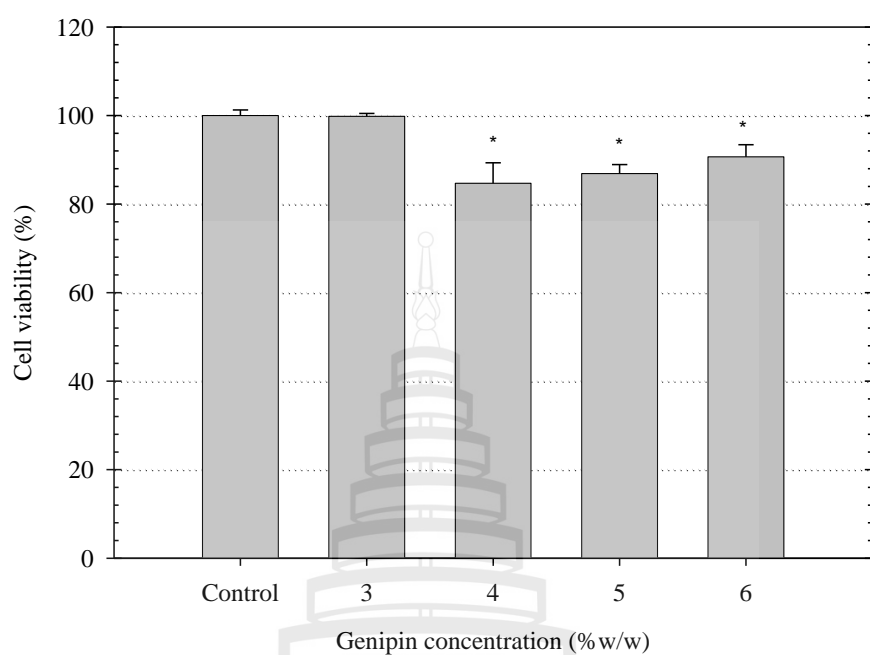
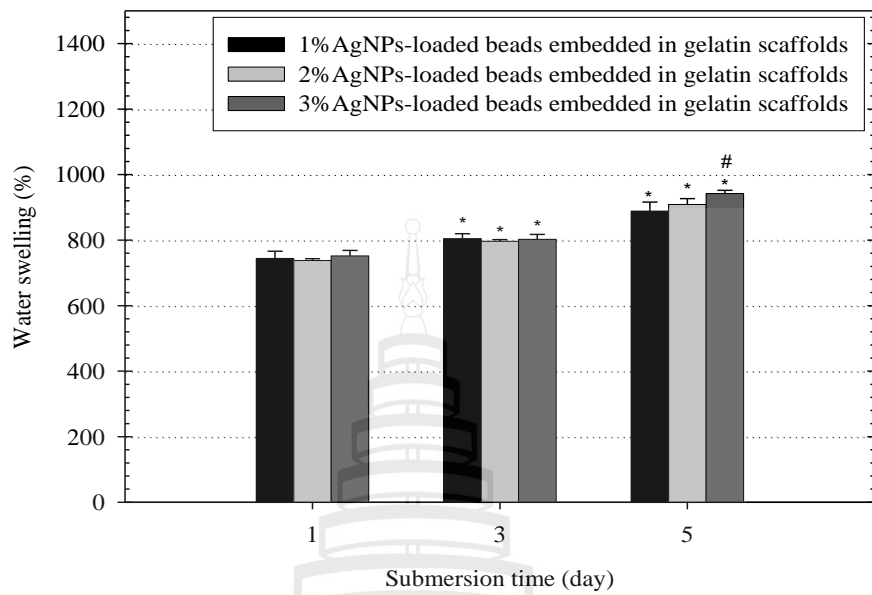


Figure 4.5 Indirect Cytotoxicity Evaluation of Genipin-Crosslinked Gelatin Scaffolds with Different Genipin Concentrations after 24 h of Cell Culture (n = 3). * $p < 0.05$ Compared With Control

(a)



(b)

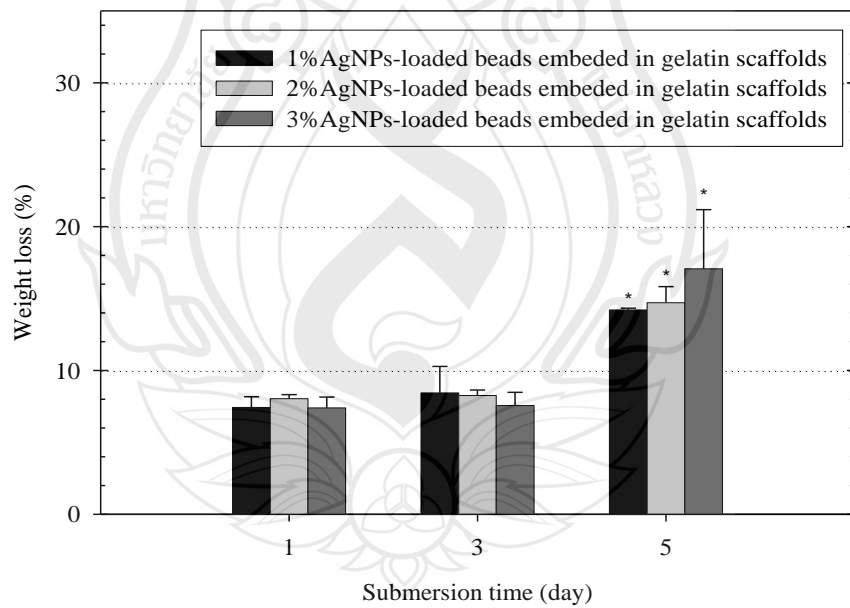


Figure 4.6 (a) Water Swelling and (b) Weight Loss Behaviors of AgNPs-Loaded Calcium Alginate Beads Embedded In Gelatin Scaffolds in PBS ($n = 3$).

* $p < 0.05$ Compared With Submersion Time at Day 1 for Any Given Type of Sample, and # $p < 0.05$ Compared with 1% AgNPs-Loaded Beads Embedded in Gelatin Scaffolds for Any Given Submersion Time Point

CHAPTER 5

DEVELOPMENT OF SILVER NANOPARTICLES- LOADED CALCIUM ALGINATE BEADS EMBEDDED IN GELATIN SCAFFOLDS FOR USE AS WOUND DRESSINGS

5.1 Abstract

The silver nanoparticles (AgNPs)-loaded calcium alginate beads embedded in gelatin scaffolds were developed to sustain and maintain the release of silver (Ag^+) ions over an extended time period. UV irradiation technique was used to reduce the Ag^+ ions in alginate solution to AgNPs. The average AgNPs sizes ranged between ~20 and ~22 nm. The AgNPs-loaded calcium alginate beads were prepared by electrospraying of the sodium alginate solution containing AgNPs into calcium chloride (CaCl_2) solution. The AgNPs-loaded calcium alginate beads were then embedded into gelatin scaffolds. The release characteristics of Ag^+ ions from both the AgNPs-loaded calcium alginate beads and the AgNPs-loaded calcium alginate beads embedded in gelatin scaffolds were carried out in either deionized water (DI) or phosphate buffer solution (PBS) at 37 °C for 7 days. Moreover, the AgNPs-loaded calcium alginate beads embedded in gelatin scaffolds were tested for their antibacterial activity and cytotoxicity.

Keywords: Wound dressing/Silver nanoparticles/Alginate/Gelatin/Bead/Drug delivery system

5.2 Introduction

Nowadays there are many chronic wound patients in the worldwide. Chronic wound is a wound that needs more time to heal. It can be classified into three main categories which are pressure ulcers, diabetic and venous ulcers (Fonder et al., 2008). The delayed wound healing or non-healing chronic wound is caused by bacteria infection. Therefore, strategies for wound healing of chronic wounds have become a significantly important role (Guo & DiPietro, 2010). Silver nanoparticles (AgNPs) have been known as antibacterial agents. Thus, AgNPs have been widely used in several biomedical applications (Durán, Marcato, De Souza, Alves & Esposito, 2007; Schierholz, Lucas, Rump & Pulverer, 1998; Jung, Kim, Burm & Park, 2013; Stevanović et al., 2014). AgNPs can enter into cells and then release the silver (Ag^+) ions to interact with their enzymes and proteins to inhibit the bacterial respiration and the transport of important substances within the cells. They interact with DNA to inhibit the cell proliferation and bind to the cell wall of bacteria to change the functionality of the cell membrane, thus prohibiting bacterial regeneration (Kim et al., 2007; Kim, Lee, Ryu, Choi & Lee, 2011; Prabhu & Poullose, 2012).

Accordingly, incorporation of AgNPs into polymer matrices have been widely used as wound dressing materials (Abdelgawad, Hudson & Rojas, 2014; Maneerung, Tokura & Rujiravanit, 2008; Rujitanaroj, Pimpha & Supaphol, 2008; Sudheesh Kumar et al., 2010). The impregnation of AgNPs into bacterial cellulose for antimicrobial wound dressing was prepared by Maneerung et al. The results showed that the materials showed a strong antimicrobial activity against both *Staphylococcus aureus* and *Escherichia coli* (Maneerung et al., 2008). The release characteristics of Ag^+ ions and the antibacterial activity of the AgNPs-loaded electrospun gelatin fiber mats were studied by Rujitanaroj et al. The results showed that the cumulative release of Ag^+ ions from the AgNPs-loaded electrospun gelatin fiber mats in the acetate buffer and distilled water initially showed rather rapidly in the first submersion time, and then increased gradually, while those in simulated body fluid showed more gradually over the submersion time. Moreover, these samples inhibited the bacterial growth, especially *Pseudomonas aeruginosa* (Rujitanaroj et al., 2008). The β -chitin/AgNPs

composite scaffolds were prepared by Sudheesh Kumar et al. They studied the antibacterial activity of these scaffolds and the results showed that these scaffolds exhibited the higher activity against *Escherichia coli* than *Staphylococcus aureus* (Sudheesh Kumar et al., 2010). The chitosan/AgNPs/polyvinyl alcohol nanofiber mats were fabricated by electrospinning. The incorporation of AgNPs into these fiber mats resulted in the strong antibacterial activity against *Escherichia coli* making them had the potential for use as wound dressings (Abdelgawad et al., 2014).

Electrohydrodynamic spraying or electrospraying method is a process of liquid atomization with electrical forces. The liquid flowing out from a capillary nozzle is subjected to an electric field, causes elongation of the meniscus to form the jet. The jet deforms and disrupts into small droplets due to electrical force. The size of electrospray droplets can be varied from tens nanometer to hundreds micrometer (Jaworek & Sobczyk, 2008). The encapsulation or incorporation of drugs into polymer beads has been reported for use in drug delivery systems (Xie et al., 2006; Ciach, 2006; Suksamran et al., 2009; Islam et al., 2011). For example, bovine serum albumin (BSA), a protein model drug, was loaded in the alginate beads by electrospraying method. The release profiles of BSA from 1 mg·mL⁻¹ alginate medium viscosity and applied voltage at 20 kV showed the slowest release rate and sustained release (Suksamran et al., 2009). A similar work, pullulan/AgNPs composite nanobeads were prepared by electrospraying method. These materials were tested for the antibacterial activity against both *Staphylococcus aureus* and *Escherichia coli* and the results showed that these materials had the strong antibacterial activity against both bacteria (Islam et al., 2011).

Alginate is a naturally occurring anionic polysaccharide and derived from brown seaweed and bacteria. It is a binary copolymer of 1, 4 linked β -D-mannuronic acid (M) and α -L-guluronic acid (G) (Skjåk-Braek, Grasdalen & Smidsrød, 1989; Martinsen, Skjåk-Braek & Smidsrød, 1989; Draget, Østgaard & Smidsrød, 1990). It is used for many biomedical applications, due to its low cost, low toxicity, and good biocompatibility (Suksamran et al., 2009; Wee & Gombotz, 1998; Augst et al., 2006). Moreover, it can form gels by the binding of divalent cations such as calcium ions (LeRoux, Guilak & Setton, 1999). Gelatin is a natural biopolymer which is a derivative of collagen by hydrolysis reaction (Bogue, 1923). It has been widely used

for drug delivery and wound dressing applications because it has good biocompatibility, high water absorbing ability, biodegradability and low cost. (Tabata, Hijikata & Ikada, 1994; Hong et al., 2001; Takahashi, Miyoshi & Boki, 1993).

In this study, we developed the AgNPs-loaded calcium alginate beads embedded in gelatin scaffolds for wound dressing and drug delivery applications. Electrospraying method was used to prepare the AgNPs-loaded calcium alginate beads. The Ag^+ ions in alginate solution were reduced to AgNPs by UV irradiation technique. Besides, the AgNPs-loaded calcium alginate beads embedded in gelatin scaffolds were fabricated by freeze-drying method. The embedding of the AgNPs-loaded calcium alginate beads into gelatin scaffolds was used to control and sustain the release of Ag^+ ions for treating, especially, chronic wounds. The AgNPs-loaded calcium alginate beads embedded in gelatin scaffolds were characterized for their morphology, compressive modulus, water swelling, and weight loss behaviors. Moreover, the release characteristics of Ag^+ ions from these scaffolds were investigated. The antibacterial activity against bacteria and the indirect cytotoxicity of these scaffolds were also investigated.

5.3 Experimental Details

5.3.1 Materials

Gelatin (Type A, porcine skin, ~180 Bloom) was purchased from Fluka Analytical (Switzerland). Genipin powder (98% purity) was obtained from Shanghai Angoal Chemical (China). Sodium alginate was purchased from Carlo Erba (Italy). Silver nitrate (AgNO_3 ; $\geq 99.9\%$ purity) was purchased from Fisher Scientific (USA). Calcium chloride (CaCl_2), sodium chloride, anhydrous disodium hydrogen orthophosphate and sodium dihydrogen orthophosphate (Ajax Chemicals, Australia) were analytical reagent grade and used without further purification.

5.3.2 Preparation of Neat and AgNPs-Loaded Calcium Alginate Beads

The base sodium alginate solution was prepared at a fixed concentration of 1.5% w/v. The neat and the AgNPs-loaded sodium alginate solutions were prepared by adding 0, 4, and 8% w/w AgNO_3 (based on the weight of sodium alginate) into the

base sodium alginate solution. The Ag^+ ions in the alginate solution were reduced to AgNPs by UV irradiation at 254 nm for 1 h (Martinez-Gutierrez et al., 2010). Prior to electrospraying, the solutions were characterized for their viscosity and conductivity, at room temperature (26 ± 1 °C), using a Brookfield/RVDV-II+P viscometer and a CyberScan con 200 conductivity meter, respectively. These solutions were then extruded dropwise through a needle placed into a glass syringe capped with a 24-gauge blunt needle (an internal diameter of needle is 0.55 mm) into a 0.5 M CaCl_2 solution under a fixed electric field of 12 kV/15 cm using an electrospraying method. The obtained neat and AgNPs-loaded calcium alginate beads were left in CaCl_2 solution for 30 min. These beads were separated from CaCl_2 solution and then washed with deionized water (DI). Finally, the beads were lyophilized for 20 h. It should be noted that the calcium alginate beads containing 4 and 8% w/w of AgNO_3 were hereafter denoted as 4% and 8% AgNPs-loaded calcium alginate beads, respectively.

5.3.3 Preparation of Neat Calcium Alginate Beads Embedded in Gelatin Scaffolds and AgNPs-Loaded Calcium Alginate Beads Embedded in Gelatin Scaffolds

The neat calcium alginate beads embedded in gelatin scaffolds were prepared by adding 10% w/w of dry calcium alginate beads (based on the gelatin powder) into 5% w/v gelatin solutions. These solutions were crosslinked with 3% w/w genipin solution (Pankongadisak, Ruktanonchai, Supaphol & Suwantong, 2014) and then poured into polypropylene (PP) mold at room temperature for 24 h. The neat calcium alginate beads embedded in gelatin scaffolds were obtained by lyophilization. While, the 4% and 8% AgNPs-loaded calcium alginate beads embedded in gelatin scaffolds were prepared by adding 10% w/w of the dry 4% and 8% AgNPs-loaded calcium alginate beads (based on the weight of gelatin powder) into 5% w/v gelatin solutions. These solutions were crosslinked and then poured into PP mold at room temperature for 24 h. Finally, the AgNPs-loaded calcium alginate beads embedded in gelatin scaffolds were obtained by lyophilization.

5.3.4 Morphological Observation

The shapes and sizes of AgNPs in the AgNPs-loaded sodium alginate solutions after UV irradiation at 254 nm for 1 h were observed by a JEOL JEM-2100

transmission electron microscope (TEM) operated at 200 kV accelerating voltage. For the morphological observation, each sample was deposited on C-coated Cu grids. The diameters of the AgNPs were measured directly from TEM images using a SemAphore 4.0 software.

The shapes and sizes of both the neat and the AgNPs-loaded calcium alginate beads were investigated by Motic BA300 optical microscope (OM) using the magnification of 4x and a LEO 1450 VP scanning electron microscope (SEM), respectively. Prior to SEM observation, each sample was coated with a thin layer of gold using a Polaron SC-7620 sputtering device. The diameters of the beads were measured directly from SEM images using SemAphore 4.0 software.

The neat calcium alginate beads embedded in gelatin scaffolds and the AgNPs-loaded calcium alginate beads embedded in gelatin scaffolds were also characterized for their morphological appearance by SEM. Each sample was coated with a thin layer of gold using a Polaron SC-7620 sputtering device prior to the observation under SEM. Pore size of the scaffolds was measured directly from SEM images using SemAphore 4.0 software. These values were averaged to obtain the pore size of the particular pore.

5.3.5 Mechanical Test

The compressive modulus of both the neat calcium alginate beads embedded in gelatin scaffolds and the AgNPs-loaded calcium alginate beads embedded in gelatin scaffolds was investigated with Instron Machine Model 5566 universal testing machine using a 1 kN load cell at room temperature. The samples ($n = 6$) were compressed at the crosshead speed of $1.0 \text{ mm} \cdot \text{min}^{-1}$ until the samples were about 70% deformed from their original height. The obtained data were modified by connecting with computer for controlling apparatus and analyzing the results.

5.3.6 Thermal Test

The thermal behavior of both the neat calcium alginate beads embedded in gelatin scaffolds and the AgNPs-loaded calcium alginate beads embedded in gelatin scaffolds (3-5 mg) was carried out by a Perkin–Elmer Pyris Diamond Thermogravimetric Analyzer (TGA) under a nitrogen atmosphere, with a heating rate of $10 \text{ }^{\circ}\text{C} \cdot \text{min}^{-1}$ from 25-600 $^{\circ}\text{C}$.

5.3.7 Water Swelling and Weight Loss Behaviors of Neat Calcium Alginate Beads Embedded in Gelatin Scaffolds and AgNPs-Loaded Calcium Alginate Beads Embedded in Gelatin Scaffolds

The water swelling and the weight loss behaviors of both the neat calcium alginate beads embedded in gelatin scaffolds and the AgNPs-loaded calcium alginate beads embedded in gelatin scaffolds were investigated in a phosphate buffer solution (PBS, see below for the preparation of phosphate buffer solution) at 37 °C for 1, 3, 5, and 7 days. The measurements of each sample were calculated according to the following equations (Tungprapa et al., 2007):

$$\text{Water swelling (\%)} = \frac{M - M_d}{M_d} \times 100, \quad (5.1)$$

and

$$\text{Weight loss (\%)} = \frac{M_i - M_d}{M_i} \times 100, \quad (5.2)$$

where M is the weight of each sample after submersion in a buffer solution for a certain period of time (1, 3, 5, and 7 days), M_d is the dry weight of each sample after being submerged in the buffer solution for a certain period of time (1, 3, 5, and 7 days) and then dried in the oven, and M_i is the initial weight of each sample in its dry state.

5.3.8 Release Characteristics of Ag⁺ Ions from AgNPs-Loaded Calcium Alginate Beads and AgNPs-Loaded Calcium Alginate Beads Embedded in Gelatin Scaffolds

5.3.8.1 Preparation of Phosphate Buffer Solution

6.177 g of anhydrous disodium hydrogen orthophosphate and 1.014 g of sodium dihydrogen orthophosphate were dissolved in ~100 mL of distilled water. 8.7 g of sodium chloride was then added into the 20 mL of this solution. Finally, distilled water (DI) was added into the solution to fill the volume up to 1,000 mL and adjust pH to 7.4.

5.3.8.2 Actual Silver Content

The actual amount of silver in both the AgNPs-loaded calcium alginate beads and the AgNPs-loaded calcium alginate beads embedded in gelatin scaffolds was first determined. Each sample was immersed in 20 mL of PBS for ~30 days until the sample was completely dissolved. These solutions were then determined using a Varian SpectrAA-300 Atomic Absorption Spectroscopy (AAS). The obtained data was calculated to determine the actual amount of silver in both AgNPs-loaded calcium alginate beads and the AgNPs-loaded calcium alginate beads embedded in gelatin scaffolds.

5.3.8.3 Silver Release Assay

The release characteristics of Ag^+ ions from both the AgNPs-loaded calcium alginate beads and the AgNPs-loaded calcium alginate beads embedded in gelatin scaffolds were investigated by total immersion method. Each sample was immersed in 20 mL of the PBS (pH 7.4) and DI (pH 7.0) at 37 °C. After a specified immersion time ranging between 0 and 7 days, 2 mL of the sample solution was withdrawn and equal amount of fresh medium was refilled. The released amount of Ag^+ ions in each sample solutions was determined using AAS. The obtained data were calculated to determine the cumulative amount of Ag^+ ions released from both the AgNPs-loaded calcium alginate beads and the AgNPs-loaded calcium alginate beads embedded in gelatin scaffolds.

5.3.9 Antibacterial Evaluation of AgNPs-Loaded Calcium Alginate Beads Embedded in Gelatin Scaffolds

The AATCC Test Method 100 (Antibacterial Finishes on Textile Materials: Assessment of The American Association of Textile Chemists and Colorists) or Colonies count was used to investigate the antibacterial activity of the AgNPs-loaded calcium alginate beads embedded in gelatin scaffolds against *Escherichia coli* TISTR 780 and *Staphylococcus aureus* TISTR 1466. First, 1.0 mL of culture medium (10^5 CFU/mL) was added into each sample and then kept it in incubator at 37 °C for 24 h. For control, the neat calcium alginate beads embedded in gelatin scaffolds were tested. After 24 h incubation, the bacteria were eluted from each sample by adding 5 mL of sterile DI into each sample with vigorously shaking for 5 min at room

temperature. The eluted solutions were then made a series dilution by using 0.1% peptone. The series diluted solutions were spread (in triplicate) on nutrient agar (NA) plate. These plates were incubated at 37 °C for 24 h. Finally, the colonies on agar plate were photographed and counted (range of 30-300 colonies) to evaluate the antibacterial activity. The number of bacteria presented in the sample was determined (on agar plate) and the percentage of reduction was also calculated.

The percent reduction of bacteria (R, %) was calculated by the following equation:

$$R (\%) = \frac{100 (B - A)}{B} \quad (6.3)$$

where A is the number of bacteria recovered from the treated test sample (AgNPs-loaded calcium alginate beads embedded in gelatin scaffolds) after incubation at 37 °C for 24 h and B is the number of bacteria recovered from the untreated test sample (neat calcium alginate beads embedded in gelatin scaffolds) after incubation at 37 °C for 24 h.

5.3.10 Indirect Cytotoxicity Evaluation of AgNPs-Loaded Calcium Alginate Beads Embedded in Gelatin Scaffolds

The indirect cytotoxicity evaluation of the AgNPs-loaded calcium alginate beads embedded in gelatin scaffolds was investigated in adaptation from the ISO 10993-5 standard test method in a 96-well tissue-culture polystyrene plate (TCPS; Corning Costar®, USA) using normal human dermal fibroblasts (NHDF; 7th passage). The cells were cultured in Dulbecco's modified Eagle's medium (DMEM; Sigma-Aldrich, USA), supplemented by 10% fetal bovine serum (FBS; Invitrogen Corp., USA), 1% L-glutamine (Invitrogen Corp., USA) and 1% antibiotic and antimycotic formulation [containing penicillin G sodium, streptomycin sulfate, and amphotericin B (Invitrogen Corp., USA)]. The 4% and 8% AgNPs-loaded calcium alginate beads embedded in gelatin scaffolds (47 ± 1 mg) were sterilized by UV radiation for ~1 h and then were immersed in 1 mL of serum-free medium (SFM; containing DMEM, 1% L-glutamine, 1% lactalbumin, and 1% antibiotic and antimycotic formulation) for 24 h in incubation to produce extraction media. NHDF cells were separately cultured

in wells of TCPS at 10,000 cells/well in serum-containing DMEM for 24 h to allow cell attachment. The cells were then starved with SFM for 24 h. After that, the medium was replaced with an extraction medium and cells were re-incubated for 24 h. The viability of the cells cultured by each of the extraction medium was determined with 3-(4,5-dimethylthiazol-2-yl)-2,5-diphenyltetrazolium bromide (MTT) assay (MTT assay is available in Supplementary information), with the viability of the cells cultured by fresh SFM was used as control.

The MTT assay is based on the reduction of the yellow tetrazolium salt to purple formazan crystals by dehydrogenase enzymes secreted from the mitochondria of metabolically active cells. The amount of purple formazan crystals formed is proportional to the number of viable cells. First, each culture medium was aspirated and replaced with 25 μL /well of MTT solution at 5 $\text{mg}\cdot\text{mL}^{-1}$ for a 96-well TCPS. The plate was incubated for 2 h at 37 $^{\circ}\text{C}$. The solution was then aspirated and 100 μL /well of dimethyl sulfoxide (DMSO) was added to dissolve the formazan crystals. After 3 min of rotary agitation, the absorbance at the wavelength of 570 nm representing the viability of the cells was measured using a SpectraMax M2 Microplate Reader.

5.3.11 Statistical analysis

The results were represented as means \pm standard errors of means. Statistical analysis was carried out by the one-way analysis of variance (one-way ANOVA) and Scheffe's post hoc test in SPSS (IBM SPSS, USA). The statistical significance was accepted at $p < 0.05$.

5.4 Results and Discussion

5.4.1 Neat and AgNPs-Loaded Calcium Alginate Beads

The AgNPs-loaded calcium alginate beads were prepared by adding varying amounts of the AgNO_3 (i.e., 4 and 8% w/w based on the weight of sodium alginate powder) to the 1.5% w/v alginate solution. After UV irradiation, the AgNPs in sodium alginate solutions were obtained and the results are shown in Table 5.1. Irregular shape of AgNPs with the wide size distribution was obtained. The average diameters of AgNPs in the 4% and 8% AgNPs-sodium alginate solutions were $22.39 \pm$

5.97 nm and 19.47 ± 5.48 nm, respectively. Moreover, the shapes and diameters of both the wet and dry AgNPs-loaded calcium alginate beads were observed by OM and SEM, respectively and the results are shown in Table 5.2. The diameters of the wet neat, 4%, and 8% AgNPs-loaded calcium alginate beads observed by OM were 485.38 ± 16.35 , 439.52 ± 23.33 and 411.21 ± 14.89 μm , respectively. While the diameters of the dry neat, 4%, and 8% AgNPs-loaded calcium alginate beads observed by SEM were 149.02 ± 12.93 , 143.31 ± 12.30 and 139.96 ± 11.11 μm , respectively.

5.4.2 Neat Calcium Alginate Beads Embedded in Gelatin Scaffolds and AgNPs-Loaded Calcium alginate Beads Embedded in Gelatin Scaffolds

Selected SEM images of the neat calcium alginate beads embedded in gelatin scaffolds and the AgNPs-loaded calcium alginate beads embedded in gelatin scaffolds are shown in Table 5.3. The results showed that the interconnected porous structure of all scaffolds was obtained. The pore size of the neat calcium alginate beads embedded in gelatin scaffolds, the 4% AgNPs- and the 8% AgNPs-loaded calcium alginate beads embedded in gelatin scaffolds was 239.49 ± 51.41 μm , 245.89 ± 50.41 μm and 264.28 ± 57.39 μm . Hence, embedding of the AgNPs-loaded calcium alginate beads into gelatin scaffolds caused the pore size of the scaffolds to increase. DeFail, Edington, Matthews, Lee & Marra (2006) prepared the doxorubicin-loaded poly(D,L-lactide-co-glycolide) or PLGA microspheres embedded within gelatin scaffolds. They found that the PLGA microspheres were embedded homogenously distribution within the gelatin pores (DeFail et al., 2006). Banerjee, Mishra & Maiti (2009) reported that the microarchitecture of 10% w/w PLGA microsphere loaded gelatin scaffold showed no regular pore structure with the pore diameter of 30-150 μm (Banerjee et al., 2009).

5.4.3 Mechanical Property of Neat Calcium Alginate Beads Embedded in Gelatin Scaffolds and AgNPs-Loaded Calcium Alginate Beads Embedded in Gelatin Scaffolds

The scaffolds should have the desirable mechanical strength and stable shape. The strength is an important characteristic of the biomaterials. For *in vivo* applications, the compressive modulus is the relevant property. Thus, the compressive test is accepted to evaluate the mechanical strength of the polymeric scaffolds. For this purpose, the compressive modulus of both the neat calcium alginate beads

embedded in gelatin scaffolds and the AgNPs-loaded calcium alginate beads embedded in gelatin scaffolds was investigated. The compressive modulus was obtained from the stress-strain curves and calculated between 2 and 6% strain, since the extent is small in the first region of compressive deformation that considered as elastic region (Zhou, Gong & Gao, 2005). The compressive modulus of both the neat calcium alginate beads embedded in gelatin scaffolds and the AgNPs-loaded calcium alginate beads embedded in gelatin scaffolds is shown in Table 5.3. The compressive modulus of the neat calcium alginate beads embedded in gelatin scaffolds, the 4%AgNPs- and the 8%AgNPs-loaded calcium alginate beads embedded in gelatin scaffolds was 2.88 ± 1.30 , 2.50 ± 0.69 , and 2.63 ± 0.64 kPa, respectively. The incorporation of AgNPs in gelatin/carboxymethyl chitosan hydrogels resulted in the interruption of dispersed AgNPs on the hydrogels, leading to the slightly decrease in the compressive modulus (Zhou et al., 2012).

5.4.4 Thermal Property of Neat Calcium Alginate Beads Embedded in Gelatin Scaffolds and AgNPs-Loaded Calcium Alginate Beads Embedded in Gelatin Scaffolds

Thermal behaviors of both the neat calcium alginate beads embedded in gelatin scaffolds and the AgNPs-loaded calcium alginate beads embedded in gelatin scaffolds were investigated by TGA and the results are shown in Figure 5.1. From Figure 5.1, all scaffolds showed various weight loss processes. The first step was in the temperature range of about 50-150 °C, corresponding to the loss of moisture. The second step covered the temperature ranges of about 250-500 °C, corresponding to the thermal degradation of polymers (i.e., gelatin or alginate). The thermal degradation of gelatin scaffolds were observed in the temperature range 50-220 °C and 250-600 °C were due to loss of water and loss of gelatin respectively (Gautam, Dinda, & Mishra, 2013). Moreover, the alginate scaffolds showed decomposition in the range of 50–100 °C and 220-280 °C due to loss of moisture content and loss of alginate control scaffold, respectively (Srinivasan, Jayasree, Chennazhi, Nair, & Jayakumar, 2012). From the TGA thermogram results, the thermal degradation temperature of the AgNPs-loaded calcium alginate beads embedded in gelatin scaffolds was lower than that of the neat calcium alginate beads embedded in gelatin scaffolds. Moreover, the

increase of AgNPs contents embedded in the scaffolds slightly decreased the thermal degradation temperature of the scaffolds. Thus, the thermal stability of the neat calcium alginate beads embedded in gelatin scaffolds was higher than that of the AgNPs-loaded calcium alginate beads embedded in gelatin scaffolds.

5.4.5 Water Swelling and Weight Loss Behaviors of Neat Calcium Alginate Beads Embedded in Gelatin Scaffolds and AgNPs-Loaded Calcium Alginate Beads Embedded in Gelatin Scaffolds

The water swelling and the weight loss behaviors of both the neat calcium alginate beads embedded in gelatin scaffolds and the AgNPs-loaded calcium alginate beads embedded in gelatin scaffolds after submersion in PBS at 37 °C for 1, 3, 5, and 7 day were investigated and the results are shown in Figure 5.2. At 1 day after submersion in PBS, the water swelling of the neat calcium alginate beads embedded in gelatin scaffolds, the 4%AgNPs- and 8%AgNPs-loaded beads embedded in gelatin scaffolds was ~571, ~580, and ~613%, respectively (see Figure 5.2a) At 3 days, the value increased to ~794, ~799, and ~851%, respectively. At 5 days, the value also increased to ~922, ~920, and ~970%, respectively. Moreover, at 7 days, the value increased to ~966, ~953, and ~981%, respectively. Thus, the water swelling of all scaffolds increased with increasing submersion time. However, the increasing of AgNO₃ content embedded in gelatin scaffolds did not significantly affect the water swelling of these scaffolds.

The weight loss behavior of both the neat calcium alginate beads embedded in gelatin scaffolds and the AgNPs-loaded calcium alginate beads embedded in gelatin scaffolds after submersion in PBS at 37 °C for 1, 3, 5, and 7 day is shown in Figure 5.2b. At 1 day after submersion in PBS, the weight loss of the neat calcium alginate beads embedded in gelatin scaffolds, the 4%AgNPs- and the 8%AgNPs-loaded beads embedded in gelatin scaffolds was ~12, ~12, and ~12%, respectively, while, at 3 days, the value increased to ~16, ~17, and ~18%, respectively. At 5 days, the value significantly increased to ~17, ~20, and ~23%, respectively. At 7 days, the value also increased to ~21, ~21, and ~23%, respectively. Similarly, the weight loss of all scaffolds increased with increasing submersion time. Moreover, the increased AgNO₃

content embedded in gelatin scaffolds did not significantly affect the weight loss of these scaffolds.

5.4.6 Release Characteristics of Ag⁺ Ions from AgNPs-Loaded Calcium Alginate Beads and AgNPs-Loaded Calcium Alginate Beads Embedded in Gelatin Scaffolds

The actual amounts of silver in both the AgNPs-loaded calcium alginate beads and the AgNPs-loaded calcium alginate beads embedded in gelatin scaffolds were determined prior to investigating the release characteristics of Ag⁺ ions from these samples. From the results, it was found that the actual amounts of silver in the 4%AgNPs- and the 8%AgNPs-loaded calcium alginate beads were 8.41 ± 1.00 and 11.56 ± 0.97 mg/g (based on the actual weight of beads), respectively, while the actual amounts of silver in the 4%AgNPs- and the 8%AgNPs-loaded calcium alginate beads embedded in gelatin scaffolds were 9.03 ± 2.26 and 12.07 ± 1.60 mg/g, respectively.

The AgNPs will be oxidized to Ag⁺ under the presented oxygen condition through the oxidation of Zero-valent Ag (Ag⁰). The equation of oxidation reaction of AgNPs is (Liu & Hurt, 2010):



The release characteristics of Ag⁺ ions from both the AgNPs-loaded calcium alginate beads and the AgNPs-loaded calcium alginate beads embedded in gelatin scaffolds were carried out by the total immersion method over a period of 7 days in either the DI or the PBS medium at 37 °C. The cumulative release profiles of Ag⁺ ions from all scaffolds were reported as the weight of Ag⁺ ions released (in mg) divided by the actual weight of the beads (in g) (see Figure 5.3). The cumulative amounts of Ag⁺ ions released from all scaffolds into the DI medium gradually increased within the first submersion time, increased more gradually afterwards, and then reached a plateau value at the longest submersion investigated time. On the other hand, the cumulative amounts of Ag⁺ ions released from all scaffolds into the PBS medium rapidly increased within the first submersion time, increased more gradually afterwards, and then reached a plateau value at the early submersion investigated time. Moreover, the cumulative amounts of Ag⁺ ions released from all scaffolds in the

PBS medium were higher than those in the DI medium. In addition, the cumulative amounts of Ag^+ ions released from the AgNPs-loaded calcium alginate beads in both types of medium were greater than those from the AgNPs-loaded calcium alginate beads embedded in gelatin scaffolds at all submersion investigated time. Specifically, the maximum cumulative amounts of Ag^+ ions released from the 4%AgNPs-loaded calcium alginate beads, the 8%AgNPs-loaded calcium alginate beads, the 4%AgNPs-loaded calcium alginate beads embedded in gelatin scaffolds, and the 8%AgNPs-loaded calcium alginate beads embedded in gelatin scaffolds upon submersion in the DI medium were ~ 0.9 , ~ 1.1 , ~ 0.1 , and ~ 0.4 mg/g, respectively, on average. On the other hand, the maximum cumulative amounts of Ag^+ ions released from the 4%AgNPs-loaded calcium alginate beads, the 8%AgNPs-loaded calcium alginate beads, the 4%AgNPs-loaded calcium alginate beads embedded in gelatin scaffolds, and the 8%AgNPs-loaded calcium alginate beads embedded in gelatin scaffolds upon their submersion in the PBS medium were ~ 8.2 , ~ 11.7 , ~ 6.9 , and ~ 10.7 mg/g, respectively, on average.

5.4.7 Antibacterial Evaluation of AgNPs-Loaded Calcium Alginate Beads Embedded in Gelatin Scaffolds

Two candidate bacteria (i.e., *E. coli* TISTR 780 as Gram-negative and *S. aureus* TISTR 1466 as Gram-positive) were used to evaluate the antibacterial activity of the AgNPs-loaded calcium alginate beads embedded in gelatin scaffolds. The percentage of inhibition or colony count provides a quantitative procedure for evaluation of the antibacterial activity of the AgNPs-loaded calcium alginate beads embedded in gelatin scaffolds and the results are shown in Table 5.4. According to the obtained results, the neat calcium alginate beads embedded in gelatin scaffolds (i.e., control) showed no activity against the growth of both *E. coli* TISTR 780 and *S. aureus* TISTR 1466. The 4%AgNPs-loaded calcium alginate beads embedded in gelatin scaffolds showed low activity against the growth of *E. coli* TISTR 780 with percent reduction of 68.29, while, these scaffolds showed high activity against the growth of *S. aureus* TISTR 1466 with percent reduction of 98.04. However, the 8%AgNPs-loaded calcium alginate beads embedded in gelatin scaffolds showed high activity against the growth of both *E. coli* TISTR 780 and *S. aureus* TISTR 1466 with

percent reduction of 97.76 and 99.97, respectively. From these results, both the 4%AgNPs- and the 8%AgNPs-loaded calcium alginate beads embedded in gelatin scaffolds showed antibacterial activity against both *E. coli* TISTR 780 and *S. aureus* TISTR 1466 indicating these scaffold could be used as wound dressings. Moreover, the increased AgNO₃ content embedded in gelatin scaffolds increased the activity against the growth of both *E. coli* TISTR 780 and *S. aureus* TISTR 1466.

5.4.8 Indirect Cytotoxicity Evaluation of AgNPs-Loaded Calcium Alginate Beads Embedded in Gelatin Scaffolds

To assess whether the AgNPs-loaded calcium alginate beads embedded in gelatin scaffolds could be used as wound dressings or scaffolding materials, indirect cytotoxicity evaluation was carried out on these scaffolds. The 4%AgNPs- and the 8%AgNPs-loaded calcium alginate beads embedded in gelatin scaffolds were evaluated for their cytotoxicity. The viability of NHDF cells cultured with the extraction media from these samples in comparison with that of the cells cultured with the fresh culture medium is shown in Figure 5.4. Obviously, the viability of the cells cultured with all the extraction media from the 4%AgNPS- and the 8%AgNPs-loaded calcium alginate beads embedded in gelatin scaffolds ranged between ~89 and ~105%.

5.5 Discussion

Wound healing involves re-epithelization process and wound contraction. The re-epithelization process involves keratinocyte migration and proliferation in the epidermal layer. Furthermore, wound contraction involves a cellular event which occurs in the dermal layer through myofibroblasts, minimizes the open wound area by pulling the neighboring tissue towards the wound center (Lee, Chesnoy & Huang, 2004; Eming et al., 2007; Lee, Cobain, Huard & Huang, 2007). Since AgNPs can promote wound healing and reduce wound inflammation through its strong antibacterial properties, thus, the addition of AgNPs to the wound was employed for treating skin wound. The addition of AgNPs to the wound increased the rate of wound closure through the promotion of proliferation and migration of keratinocytes.

Moreover, AgNPs accelerated the differentiation of fibroblasts into myofibroblasts, thus promoting wound contraction (Liu, et al., 2010). However, most cases of infected and chronic wounds caused by bacteria need more time to heal. Thus, the aim of this study was to develop the AgNPs-loaded calcium alginate beads embedded in gelatin scaffolds for wound dressing and drug delivery applications. In addition, the embedding of the AgNPs-loaded calcium alginate beads into gelatin scaffolds was used to control and sustain the release of Ag^+ ions for treating chronic wounds.

From Table 5.2, all dry calcium alginate beads had smaller diameters than all wet calcium alginate beads due to the diffusion out of water molecules from the beads (Pankongadisak, Ruktanonchai, Supaphol & Suwantong, 2014). The increase of the AgNO_3 concentration decreased the diameters of the AgNPs-loaded calcium alginate beads. These results could be supported by the shear viscosity and electrical conductivity of the AgNPs-containing alginate solutions as shown in Table 5.2. The shear viscosity of the solutions decreased with increasing AgNO_3 concentration, while, the electrical conductivity of the solutions increased with increasing the AgNO_3 concentration. For the low shear viscosity of the AgNPs-containing alginate solutions, the charges that initiate the spraying might be sufficient to break up the solutions into small droplets, resulting in the decreased diameter of the beads. In addition, the decreased shear viscosity of the solutions might reduce the surface tension of the solutions, thus the diameter of the beads was decreased (Jaworek & Sobczyk, 2008; Suksamran et al., 2009). The increased electrical conductivity of the AgNPs-containing alginate solutions was a direct result of an increase in the amount of Ag^+ ions within the AgNPs-containing alginate solutions. The increase in the number of charge carriers caused both electrostatic and coulombic repulsive forces to overcome the surface tension of the solutions, leading to the smaller diameters of the beads (Shi et al., 2011).

Sikareepaisan, Ruktanonchai & Supaphol (2011) studied the cumulative amounts of asiaticoside released from the asiaticoside-loaded alginate films into PBS as the releasing medium. They reported that the alginate films were broken up into small pieces over a period of time upon submersion in PBS because sodium (Na^+) ions present in the PBS medium. Thus, after submersion of the asiaticoside-loaded alginate films in the PBS medium, the ionic exchange between Ca^{2+} ions and Na^+ ions

can occur, resulting in the gradual disintegration of the alginate films (Sikareepaisan et al., 2011). Moreover, a rapid decrease of mechanical properties was observed in the presence of monovalent ions (K^+ or Na^+) because of the ion exchange between the monovalent ions and the crosslinking Ca^{2+} ions. However, the stability of the alginate hydrogel was improved by adding orthosilicic acid (OSA) to the hydrogel (Birdi, Bridson, Smit, Mohd Bohari & Grover, 2012). From these reasons, it could be confirmed that comparison between two types of releasing medium (i.e., DI and PBS medium), the higher cumulative amounts of Ag^+ ions released from these scaffolds were obtained in the PBS medium as compared with the DI medium (see Figure 5.3). Moreover, the embedding of the AgNPs-loaded calcium alginate beads into the gelatin scaffolds sustained and prolonged the release of Ag^+ ions from scaffolds into the medium. This result might be because the diffusion barrier of the gelatin scaffolds restricted the diffusion of Ag^+ ions from the beads into the medium. In 2009, Mandal and Kundu embedded the drug loaded-calcium alginate beads within silk fibroin scaffolds to control and sustain release of the drug. They found that silk coating on the calcium alginate beads acted as the mechanically stable shells and diffusion barrier to the encapsulated drug resulting in controlling the release characteristic (Mandal & Kundu, 2009).

Rattanuengsrikul, Pimpha & Supaphol (2009) prepared the AgNPs-loaded gelatin hydrogels that contained 2.5% w/w of $AgNO_3$ by solvent-casting technique. They reported that the viability of the cells cultured with the extraction media from the AgNPs-loaded gelatin hydrogels was low (i.e., 38-43%) (Rattanuengsrikul et al., 2009). To investigate that the embedding of the AgNPs-loaded calcium alginate beads into the gelatin scaffolds could reduce the toxicity of AgNPs, the indirect cytotoxicity evaluation was thus employed. According to ISO 10993-5, the cell viability greater than 80% are considered as non-toxicity; within 60-80% weak; 40-60% moderate and lower than 40% strong cytotoxicity, respectively (ISO 10993-5, 2009). From Figure 5.4, the viability of the cells cultured with all the extraction media from the AgNPs-loaded calcium alginate beads embedded in gelatin scaffolds was greater than 80% (i.e., 89-105%), indicating that all the AgNPs-loaded calcium alginate beads embedded in gelatin scaffolds were proven non-toxic to NHDF cells. This result might be due to the diffusion barrier of the gelatin scaffold that restricts the release of

Ag⁺ ions into the extraction media. Thus, these scaffolds had potential for use as wound dressings.

5.6 Conclusions

In this study, the calcium alginate beads incorporated with AgNPs were obtained by electrospraying method. UV irradiation technique was used to reduce the Ag⁺ ions in alginate solution to AgNPs. The average diameters of both the neat and the AgNPs-loaded calcium alginate beads ranged between ~140 and ~149 μm . The water swelling and weight loss behaviors of the AgNPs-loaded calcium alginate beads embedded in gelatin scaffolds increased with an increase in the submersion time. The cumulative amounts of Ag⁺ ions released from both the AgNPs-loaded calcium alginate beads and the AgNPs-loaded calcium alginate beads embedded in gelatin scaffolds in the PBS medium were higher than those in the DI medium. Moreover, the cumulative amounts of Ag⁺ ions released from the AgNPs-loaded calcium alginate beads in both types of medium were greater than those from the AgNPs-loaded calcium alginate beads embedded in gelatin scaffolds. Thus, the embedding of the AgNPs-loaded calcium alginate beads into the gelatin scaffolds could be used to sustain the release of Ag⁺ ions. Moreover, the AgNPs-loaded calcium alginate beads embedded in gelatin scaffolds showed the higher efficiency antibacterial activity with *S. aureus* TISTR 1466 than that with *E. coli* TISTR 780. Lastly, the AgNPs-loaded calcium alginate beads embedded in gelatin scaffolds were non-toxic to the NHDF cells indicating their potential uses for wound dressings.

5.7 Acknowledgements

The authors would like to acknowledge the financial support from the Research, Development and Engineering (RD&E) fund through The National Nanotechnology Center (NANOTEC), The National Science and Technology Development Agency (NSTDA), Thailand (P-11-00986) to Mae Fah Luang

University (MFU) and Thailand Graduate Institute of Science and Technology (TGIST) (TG-55-99-55-048M).

Table 5.1 Selected TEM Images of AgNPs in Sodium Alginate Solutions at various Concentrations of AgNO_3 Including Diameters of the Individual AgNPs ($n = 200$)

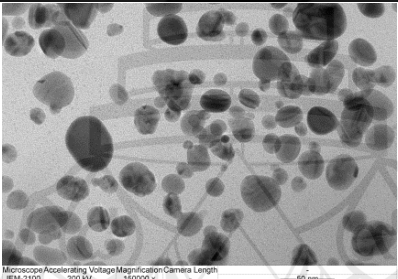
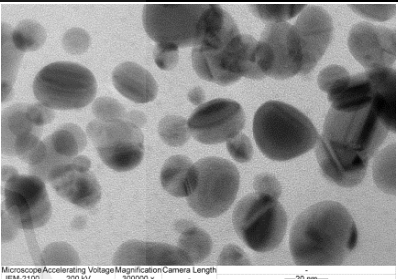
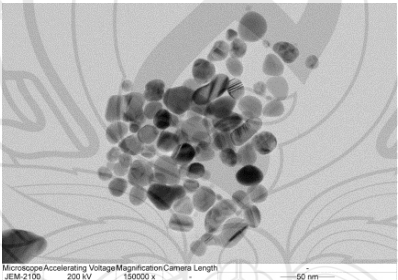
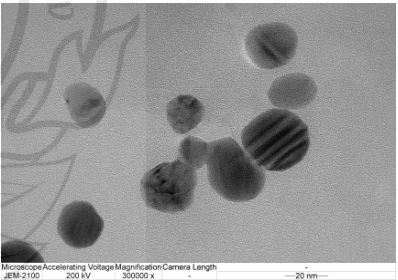
Concentration of AgNO_3 (% w/w)	TEM observation	
	150,000x	300,000x
4		
Diameters of AgNPs (nm)	22.39 ± 5.97	
8		
Diameters of AgNPs (nm)	19.47 ± 5.48	

Table 5.2 Selected OM and SEM Images of the Neat Calcium Alginate Beads and the AgNPs-Loaded Calcium Alginate Beads at Various Concentrations of AgNO₃ Including Diameters of the Individual Beads (n = 120) and Shear Viscosity and Electrical Conductivity of the Neat and the AgNPs-Containing Alginate Solutions (n = 3)

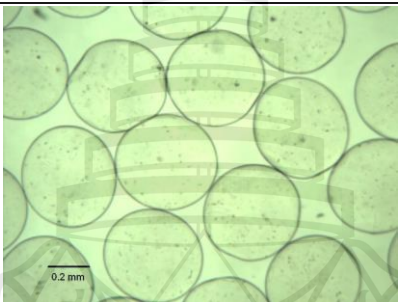
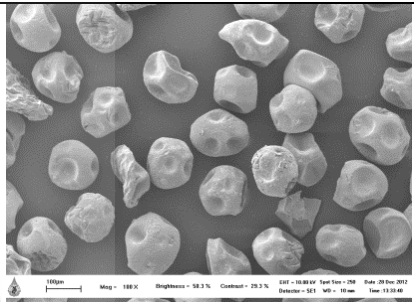
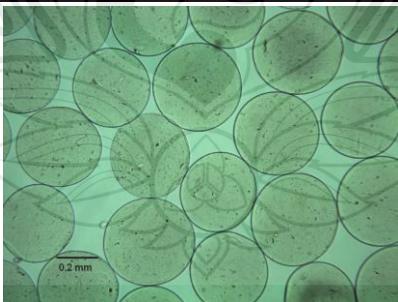
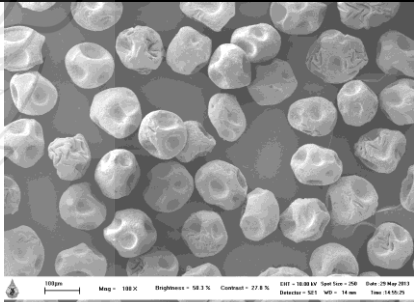
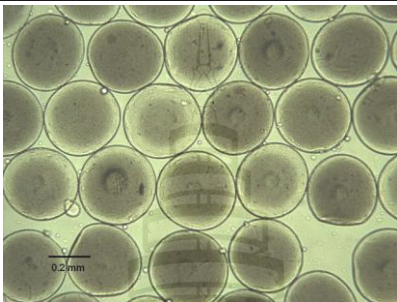
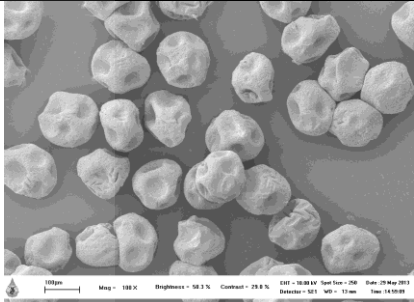
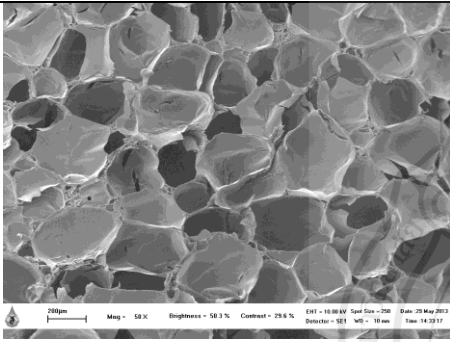
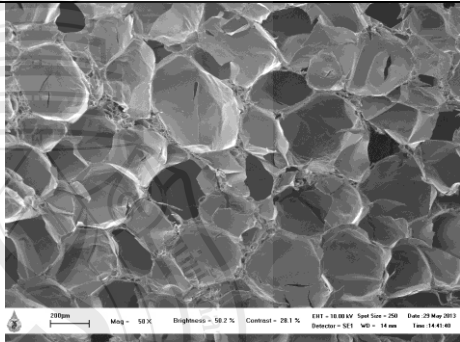
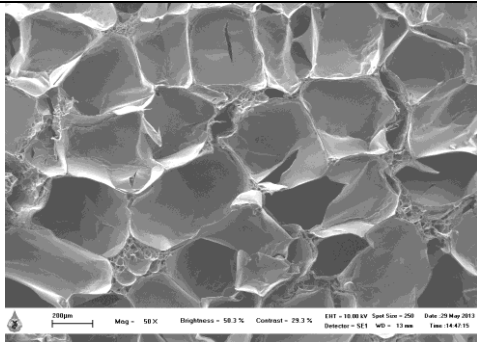
Concentration of AgNO ₃ (% w/w)	Observed by	
	OM	SEM
0		
Bead diameters (µm)	485.38 ± 16.35	149.02 ± 12.93
Shear viscosity (mPa s)	265.27 ± 1.44	
Electrical conductivity (mS cm ⁻¹)	2.76 ± 0.02	
4		
Bead diameters (µm)	439.52 ± 23.33*	143.31 ± 12.30*
Shear viscosity (mPa s)	227.43 ± 3.98*	
Electrical conductivity (mS cm ⁻¹)	2.98 ± 0.03*	

Table 5.2 (continued)

Concentration of AgNO ₃ (% w/w)	Observed by	
	OM	SEM
4		
Bead diameters (µm)	411.21 ± 14.89*	139.96 ± 11.11*
Shear viscosity (mPa s)	218.43 ± 5.22*	
Electrical conductivity (mS cm ⁻¹)	3.19 ± 0.02*	

Note. * $p < 0.05$ compared with the neat calcium alginate beads or the pure alginate solution

Table 5.3 Selected SEM Images, Pore Sizes, and Compressive Modulus of the Neat Calcium Alginate Beads Embedded in Gelatin Scaffolds and the AgNPs-Loaded Calcium Alginate Beads Embedded in Gelatin Scaffolds (Sizes of the Scale Bar: 200 μm)

Concentration of AgNO ₃ (% w/w)	0	4	8
Representative SEM images of scaffolds			
Pore sizes (μm)	239.49 ± 51.41	245.89 ± 50.41	$264.28 \pm 57.39^*$
Compressive modulus (kPa)	2.88 ± 1.30	2.50 ± 0.69	2.63 ± 0.64

Note. $*p < 0.05$ compared with the neat calcium alginate beads embedded in gelatin scaffolds

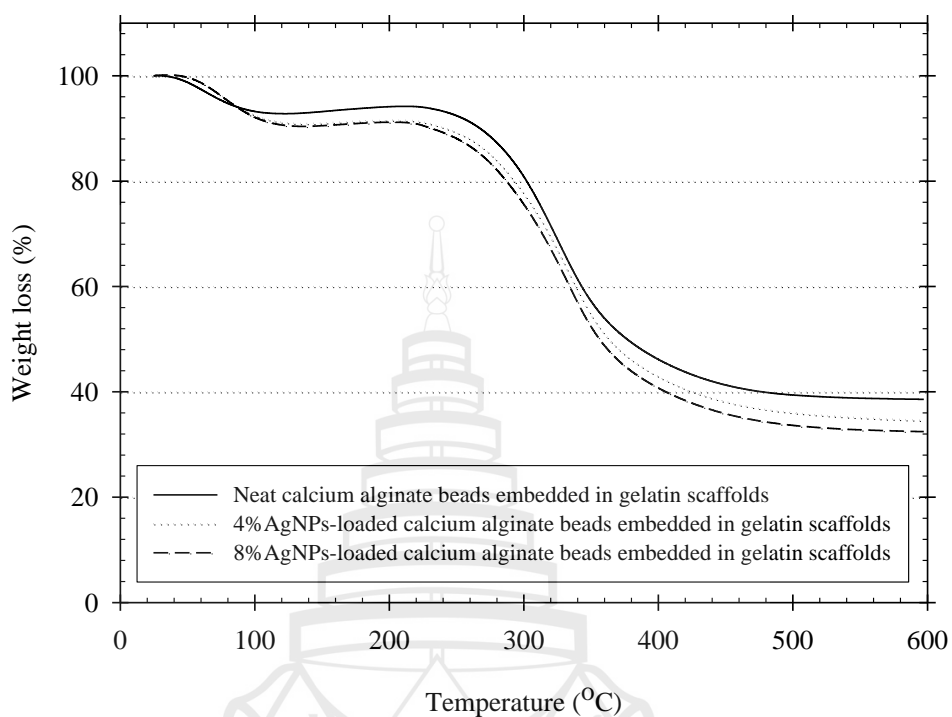
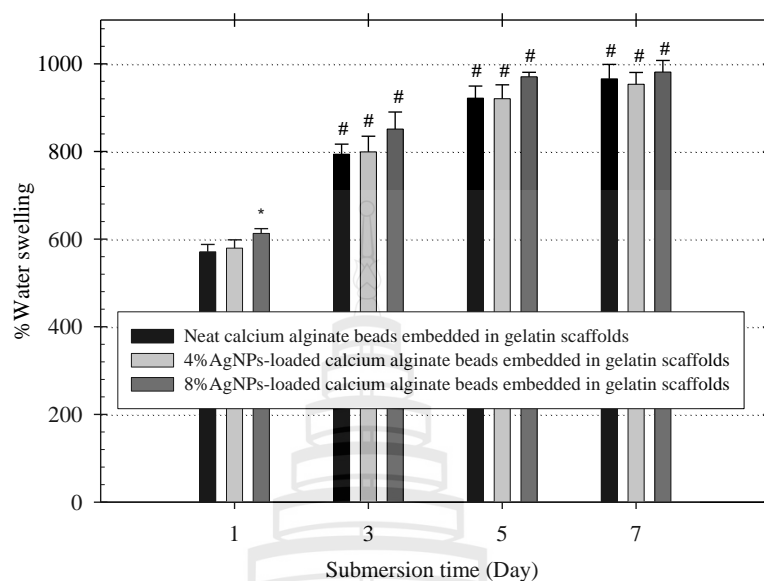


Figure 5.1 Thermogravimetric Analytical Thermograms of the Neat Calcium Alginate Beads Embedded in Gelatin Scaffolds and the AgNPs-Loaded Calcium Alginate Beads Embedded in Gelatin Scaffolds

(a)



(b)

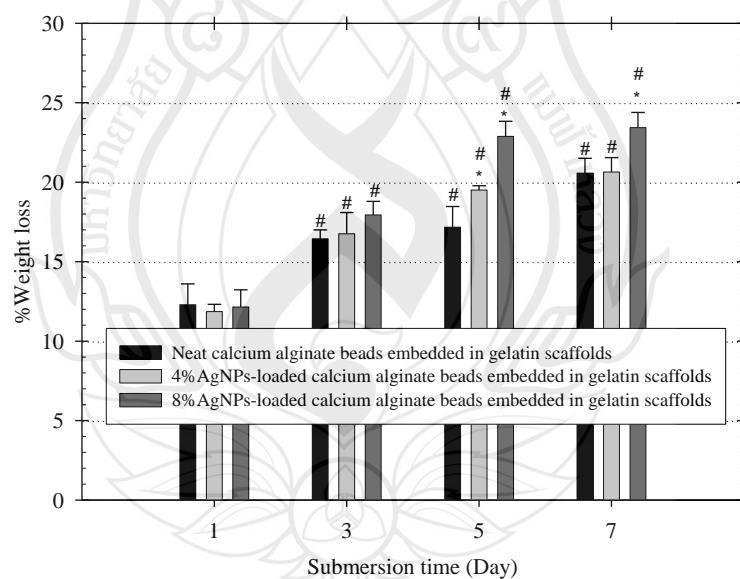


Figure 5.2 (a) Water Swelling and (b) Weight Loss Behaviors of the Neat Calcium Alginate Beads Embedded in Gelatin Scaffolds and the AgNPs-Loaded Calcium Alginate Beads Embedded in Gelatin Scaffolds ($n = 4$). * $p < 0.05$ Compared with the Neat Calcium Alginate Beads Embedded in Gelatin Scaffolds at a Given Time Point and # $p < 0.05$ Compared with 1 Day Submersion Time of a Given Scaffold

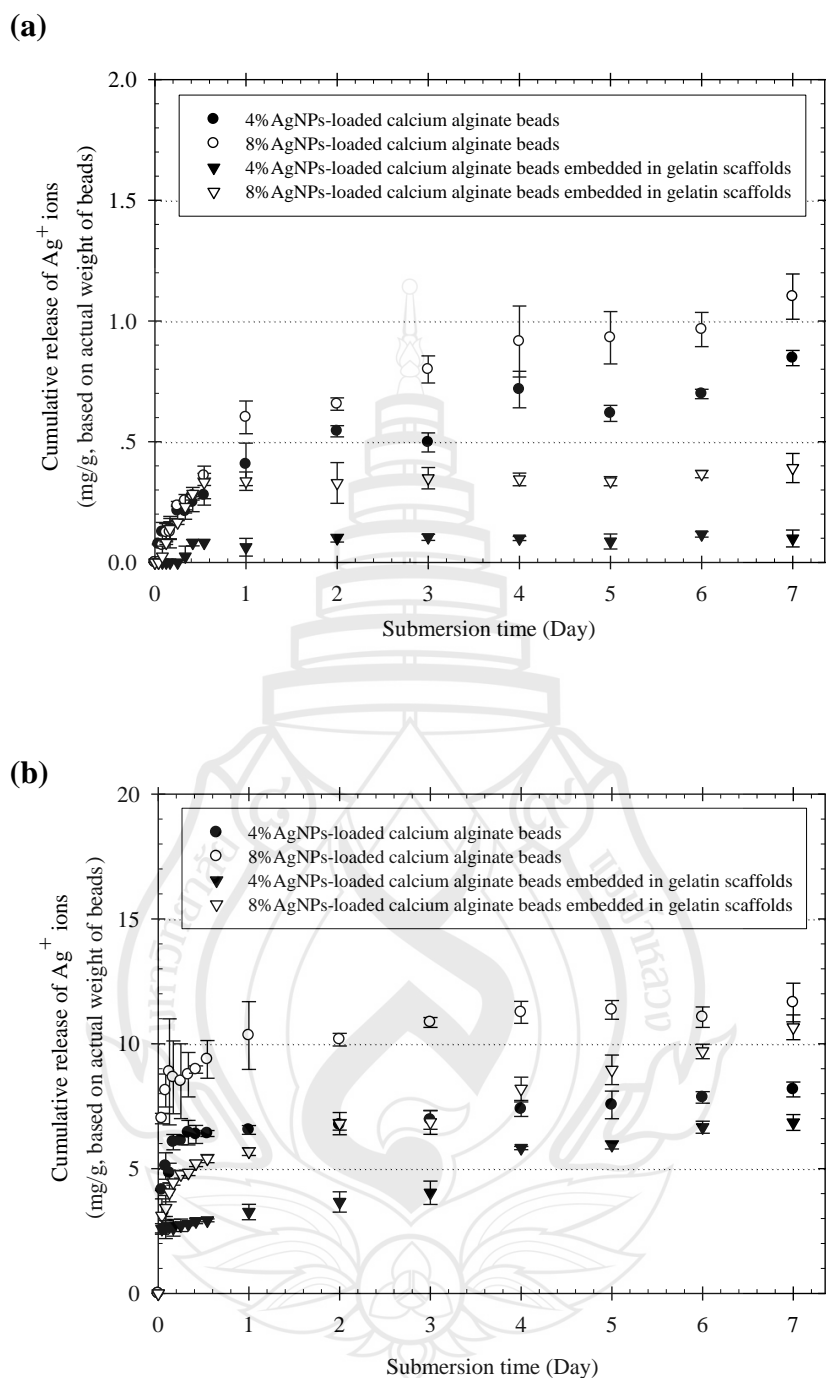


Figure 5.3 Cumulative Release Profiles of Ag^+ Ions from the AgNPs-Loaded Calcium Alginate Beads Embedded in Gelatin Scaffolds, Reported as the Weight of Ag^+ Ions Released Divided by the Actual Weight of the Beads, by Total Immersion Method in (a) DI and (b) PBS at the Physiological Temperature of 37 °C (n = 3)

Table 5.4 Antibacterial Activity of the AgNPs-Loaded Calcium Alginate Beads Embedded in Gelatin Scaffolds (n = 3)

Culture	Sample	Percent reduction (%R)
<i>E. coli</i> TISTR 780	Control	
	4% AgNPs	68.29%
	8% AgNPs	97.76%
<i>S. aureus</i> TISTR 1466	Control	
	4% AgNPs	98.04%
	8% AgNPs	99.97%

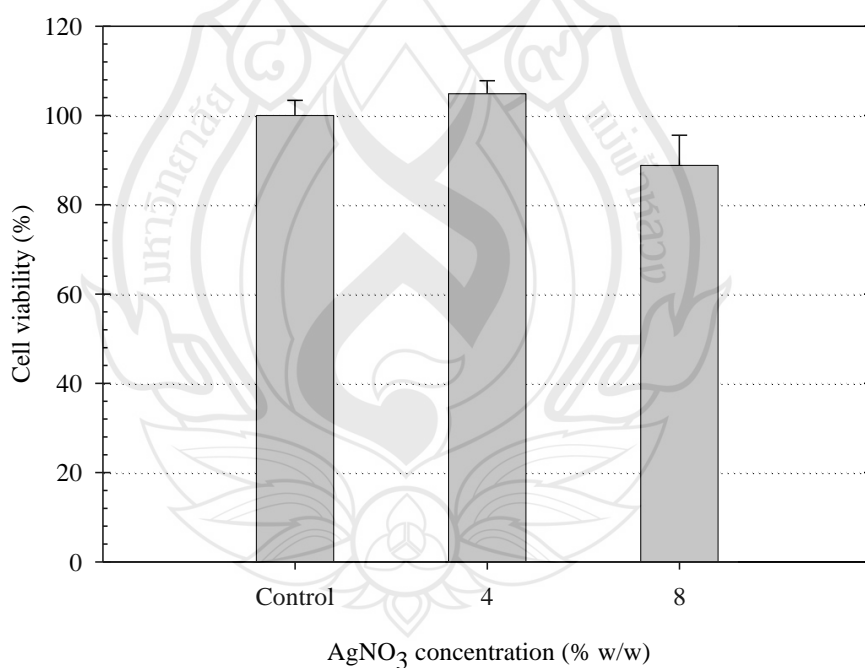


Figure 5.4 Indirect Cytotoxicity Evaluation of the AgNPs-Loaded Calcium Alginate Beads Embedded in Gelatin Scaffolds (n = 3)

CHAPTER 6

SILVER NANOPARTICLES-LOADED CALCIUM ALGINATE BEADS BY EMULSIFICATION/ EXTERNAL GELATION METHOD IN GELATIN SCAFFOLDS FOR USE AS WOUND DRESSINGS

6.1 Abstract

The silver nanoparticles (AgNPs)-loaded calcium alginate beads embedded in gelatin scaffolds were developed to reduce the burst release and sustain the release of silver (Ag^+) ions for long period of time. The AgNPs-loaded calcium alginate beads were prepared by emulsification/external gelation method. The AgNPs-loaded calcium alginate beads were then embedded into gelatin scaffolds and fabricated by freeze-drying method. The water swelling and weight loss behaviors of these scaffolds were investigated in phosphate buffer solution (PBS) at 37 °C for 1, 3, 5, and 7 days. The release characteristics of Ag^+ ions from both the AgNPs-loaded calcium alginate beads and the AgNPs-loaded calcium alginate beads embedded in gelatin scaffolds were carried out in either deionized water (DI) or (PBS) at 37 °C for 7 days. Lastly, the AgNPs-loaded calcium alginate beads embedded in gelatin scaffolds were tested for their antibacterial activity against *Staphylococcus aureus* and *Escherichia coli* and cytotoxicity.

Keywords: Wound dressings/Silver nanoparticles/Alginate beads/ Gelatin scaffolds/
Emulsification method/External gelation method

6.2 Introduction

Porous scaffolds have been commonly used as substrates for wound dressing or skin tissue engineering and drug delivery system applications (Zhong et al., 2010; Tamura, Furuike, Nair & Jayakumar, 2011; Malafaya, Silva & Reis, 2007; Garg, Singh, Arora & Murthy, 2012). One way of sustaining drug delivery system is the use of polymer beads as carriers (Cortesi et al., 1999; Phutane et al., 2010). The polymer beads are used to incorporate drug for protecting the drug from enzymatic degradation, transporting the drug to the targeted site and controlling the drug release (Cortesi et al., 1999; Lee & Yuk, 2007; Gibaud et al., 1996). For this purpose, the polymer beads have been widely employed in as carriers in drug delivery systems (Sinha et al., 2004; Liu, Sun, Wang, Zhang & Wang, 2005). Normally, the polymer beads embedded in scaffolds can be used as polymeric delivery carriers to deliver functional drug/protein over a long period of time (DeFail et al., 2006; Mandal & Kundu, 2009; Santoa, Duarte, Gomes, Mano & Reis, 2010; Yang et al., 2011). Beads embedded in polymeric scaffolds have various advantages such as increasing the local drug/protein concentration, reducing the burst release, and controlling drug/protein release rates when compared to drug/protein-loaded polymeric beads alone (DeFail et al., 2006; Ungaro et al., 2006; Mandal & Kundu, 2009)

Silver nanoparticles (AgNPs) have been widely used in many products because of their antibacterial properties (Sotiriou & Pratsinis, 2010; Sharma et al., 2009). AgNPs may attend as a source of Ag^+ under oxygen conditions through the oxidation of zero-valent Ag (Ag^0) (Lok et al., 2007; Liu & Hurt, 2010). The Ag^+ ions may combine with bacterial proteins in the cell and cell wall, interfere with DNA replication and promote formation of reactive oxygen species inside bacteria cells (Choi & Hu, 2008; Yang et al., 2009; Su et al., 2009). Recent reports, AgNPs dispersed in chitosan solutions were prepared by γ -ray irradiation. They were stable without tendency to precipitate for more than 3 months. AgNPs showed the antibacterial activities against *Staphylococcus aureus* and *Escherichia coli* (Yoksan & Chirachanchai, 2009). Besides, the cumulative amount of silver released from the AgNPs-loaded gelatin hydrogel pads in three types of medium (i.e., acetate buffer,

distilled water, and simulated body fluid buffer) were studied by Rattanuengsrikul et al. The results showed that the cumulative amount of silver released from AgNPs-loaded gelatin hydrogel pads were greatest in the acetate buffer, followed by those in distilled water and the simulated body fluid buffer, respectively. Moreover, these hydrogels exhibited the higher activity against *Staphylococcus aureus* than *Escherichia coli* (Rattanuengsrikul et al., 2009).

An emulsification/external gelation method is a method to produce the polymer beads by dispersing the polymer, drug/protein and divalent cations into an oil phase (such as paraffin oil or organic solvents) in formation of an emulsifier and then the polymer beads are obtained by removing the residual oils or organic solvents (Chan et al., 2006; Liu et al., 2002; Quong et al., 1998). A similar work, the calcium alginate beads with the size less than 150 μm were prepared. The sodium alginate solution was dispersed in oil phase and coagulated to form calcium alginate beads by crosslinking with calcium (Ca^{2+}) ions (Wan et al., 1992). The addition of hydroxypropyl methylcellulose (HPMC) into the sodium alginate improved the shape of the alginate beads to become spherical shape with smooth surface. Moreover, it prevented the aggregation of the alginate beads (Chun et al., 1996). Moreover, an emulsification was used to prepare chitosan microspheres with good morphology. The emulsion system using liquid paraffin oil as a continuous phase and 0.5-4% of Span 80 as a surfactant was used to prepare the microspheres. When the stirring speed was 700 rpm, the average diameter of chitosan microspheres was 297 μm (Al-Helw et al., 1998). Lemoine et al. prepared the alginate beads containing bovine serum albumin (BSA) by emulsification method. The beads showed the spherical and non-aggregated shape with an average diameter of 8 μm . Moreover, high encapsulation efficiency of BSA was obtained (Lemoine et al., 1998). Moreover, Çetin et al. also prepared the alginate beads by an emulsification method. The obtained beads were spherical shape with diameter of 12 μm and non-aggregation. However, the release rate of BSA from the beads was fast (Çetin, Vural, Çapan, & Hincal, 2007).

Alginate is a natural polysaccharide which extracted from marine brown algae or bacteria. It is a linear copolymer composed of 1,4-linked- β -D-mannuronic acid and α -L-guluronic acid residues that can form gels by crosslinking with divalent cations (Martinsen et al., 1989). The alginate beads have been used as a controlled release

matrix materials for use in medical applications (Silva, Ribeiro, Ferreira, & Veiga, 2006; Rastogi et al., 2007; Martins, Sarmento, Souto, & Ferreira, 2007; Zhang et al., 2010) and agricultural applications (Kumar et al., 2014; Riyajan & Sakdapipanich, 2009), due to its good biocompatibility and biodegradability (Lee & Mooney, 2012). Gelatin is a natural biopolymer which is a derivative of collagen by hydrolysis reaction (Bogue, 1923). It has been widely used for drug delivery (Young, Wong, Tabata & Mikos, 2005) and wound dressing applications (Rattanuengsrikul et al., 2009) due to its biocompatibility, biodegradability and high water adsorbing ability (Jopling, 1956; Takahashi et al., 1993; Stevens, Einerson, Burmania & Kao, 2002; Ito et al., 2003). In 2006, the controlled release of doxorubicin from doxorubicin-loaded poly(D,L-lactide-*co*-glycolide) or PLGA microspheres embedded within gelatin scaffolds has been studied. They found that embedding the PLGA microspheres in gelatin scaffolds can be used as a controlled drug delivery system (DeFail et al., 2006).

The aim of this research was to prepare the AgNPs-loaded calcium alginate beads embedded in gelatin scaffolds for reducing the burst release and improving the extended release of Ag⁺ ions. The emulsification/external gelation method was used to prepare the AgNPs-loaded calcium alginate beads. This method was employed to prepare the small diameter alginate beads. Moreover, it is a safe method for mass preparation. The AgNPs-loaded calcium alginate beads embedded in gelatin scaffolds were prepared by freeze-drying method. The AgNPs-loaded calcium alginate beads embedded in gelatin scaffolds were observed for their morphology, compressive modulus, water swelling and weight loss behaviors. Besides, the release characteristics of Ag⁺ ions from these scaffolds were investigated. Lastly, the antibacterial activity against bacteria and the indirect cytotoxicity of these scaffolds were investigated.

6.3 Experimental Details

6.3.1 Materials

Silver nitrate (AgNO_3 ; $\geq 99.9\%$ purity) was purchased from Fisher Scientific (USA). Low-viscosity alginic acid sodium salt and medium-viscosity grade of hydroxypropyl methylcellulose (HPMC) were purchased from Sigma (USA). Gelatin (Type A, porcine skin, ~ 180 Bloom) and Span 80 were purchased from Fluka Analytical (Switzerland). Genipin powder (98% purity) was obtained from Shanghai Angoal Chemical (China). Paraffin oil, calcium chloride (CaCl_2), sodium chloride (NaCl), anhydrous disodium hydrogen orthophosphate (Na_2HPO_4), sodium dihydrogen orthophosphate (NaH_2PO_4), and isopropyl alcohol were purchased from Ajax Chemicals (Australia). Nitric acid (65% w/w) was obtained from Merck (Germany). All chemicals were analytical reagent grade and used without further purification.

6.3.2 Preparation of Neat and AgNPs-Loaded Calcium Alginate Beads

For an aqueous phase of the system, 5% w/v of an aqueous solution containing sodium alginate and hydroxypropyl methylcellulose (HPMC) (9:1) was used to produce the calcium alginate microbeads by emulsification/external gelation method (Wan et al., 1992; Lemoine et al., 1998). An aqueous solution was dispersed into paraffin oil containing 5% v/v of Span 80 with a ratio of 1:4 (i.e., the volume of aqueous phase/the volume of oil phase) by using a magnetic stirrer at 1200 rpm for 30 min. In case of the AgNPs-loaded calcium alginate beads, 2 and 4% w/w AgNO_3 solutions (based on the weight of sodium alginate and HPMC) were added in an aqueous solution containing sodium alginate and HPMC. Then, the Ag^+ ions in an aqueous solution were reduced to AgNPs by UV irradiation at 254 nm for 1 h (Martinez-Gutierrez et al., 2010). After emulsification, 10% w/v CaCl_2 solution was slowly added in the mixture solution and then the mixture solution was continuously mixed for 2 h. 100% isopropyl alcohol was then added to harden the beads. The beads were centrifuged, and washed twice with isopropyl alcohol and water, respectively. Finally, the microbeads were lyophilized for 20 h.

6.3.3 Preparation of Neat Calcium Alginate Beads Embedded in Gelatin Scaffolds and AgNPs-Loaded Calcium Alginate Beads Embedded in Gelatin Scaffolds

First, 10% w/w of dry calcium alginate beads (based on the weight of the gelatin powder) was added into 5% w/v of gelatin solutions. These solutions were then poured into polypropylene (PP) mold and crosslinked with 3% w/w genipin solution at room temperature for 24 h. Finally, the neat calcium alginate beads embedded in gelatin scaffolds were obtained by lyophilization. For the 2% and 4% AgNPs-loaded calcium alginate beads embedded in gelatin scaffolds, 10 %w/w of dry calcium alginate beads (based on the weight of gelatin powder) was added into 5 w/v gelatin solutions. These solutions were then poured into PP mold and crosslinked with 3% w/w genipin solution at room temperature for 24 h. Finally, the AgNPs-loaded calcium alginate beads embedded in gelatin scaffolds were obtained by lyophilization.

6.3.4 Morphological Observation

The size of the neat and the AgNPs-loaded calcium alginate beads and the presence of aggregates were observed by a Motic BA300 optical microscope (OM) equipped with a camera using the magnification of 10x. Prior to observation, the dry bead was suspended in DI and then photographed immediately. The diameters of the beads were measured from OM images using a Motic Images Plus 2.0.

The shape and size of AgNPs in the AgNPs-loaded calcium alginate beads were investigated by a JEOL JEM-2100 transmission electron microscope (TEM). The dispersion of the AgNPs-loaded calcium alginate beads in ethanol solution was placed on carbon-coated copper grid. The sample grid was kept in desiccator cabinet until the solvent was slowly evaporated.

The morphological appearance of the beads and the scaffolds was observed by a LEO 1450 VP scanning electron microscope (SEM). Prior to morphological observation, each sample was coated with a thin layer of gold using a Polaron SC-7620 sputtering device. The diameters of the beads and the pore sizes of the scaffolds were measured from SEM images using a SemAphore 4.0 software.

6.3.5 Mechanical Test

The compressive modulus of both the neat calcium alginate beads embedded in gelatin scaffolds and the AgNPs-loaded calcium alginate beads embedded in gelatin scaffolds was investigated with Instron Machine Model 5566 universal testing machine using a 1 kN load cell at room temperature. The samples were compressed at the crosshead speed of 1.0 mm·min⁻¹ until the samples were about 70% deformed from their original height. The obtained data were modified by connecting with computer for controlling apparatus and analyzing the results.

6.3.6 Thermal Test

The thermal behavior of both the neat calcium alginate beads embedded in gelatin scaffolds and the AgNPs-loaded calcium alginate beads embedded in gelatin scaffolds (3-5 mg) was carried out by a Perkin–Elmer Pyris Diamond Thermogravimetric Analyzer (TGA) under a nitrogen atmosphere, with a heating rate of 10 °C·min⁻¹ from 25-600 °C.

6.3.7 Water Swelling and Weight Loss Behaviors of Neat Calcium Alginate Beads Embedded in Gelatin Scaffolds and AgNPs-Loaded Calcium Alginate Beads Embedded in Gelatin Scaffolds

The water swelling and the weight loss behaviors of both the neat calcium alginate beads embedded in gelatin scaffolds and the AgNPs-loaded calcium alginate beads embedded in gelatin scaffolds were investigated in a phosphate buffer solution (PBS, see below for the preparation of phosphate buffer solution) at 37 °C for 1, 3, 5, and 7 days. The measurements of each sample were calculated according to the following equations:

$$\text{Water swelling (\%)} = \frac{M - M_d}{M_d} \times 100, \quad (6.1)$$

and

$$\text{Weight loss (\%)} = \frac{M_i - M_d}{M_i} \times 100, \quad (6.2)$$

where M is the weight of each sample after submersion in a buffer solution for a certain period of time (1, 3, 5, and 7 days), M_d is the weight of each sample after

submersion in the buffer solution for a certain period of time (1, 3, 5, and 7 days) in its dry state, and M_i is the initial weight of each sample in its dry state.

6.3.8 Release Characteristics of Ag⁺ Ions from AgNPs-Loaded Calcium Alginate Beads and AgNPs-Loaded Calcium Alginate Beads Embedded in Gelatin Scaffolds

6.3.8.1 Preparation of Phosphate Buffer Solution

6.177 g of anhydrous disodium hydrogen orthophosphate and 1.014 g of sodium dihydrogen orthophosphate were dissolved in ~100 mL of distilled water. 8.7 g of sodium chloride was then added into the 20 mL of this solution. Finally, DI was added into the solution to fill the volume up to 1,000 mL and adjust pH to 7.4.

6.3.8.2 Actual Silver Content

The actual amount of silver in both the AgNPs-loaded calcium alginate beads and the AgNPs-loaded calcium alginate beads embedded in gelatin scaffolds was first determined. Each sample was immersed in 10 mL of PBS until the sample was completely dissolved. Prior to determination, the samples were digested with 65% w/w nitric acid at 65 °C for at least 4 h and then allowed to cool down to eliminate the formed AgCl. These solutions were then determined using a Hitachi Z-5000 Atomic Absorption Spectroscope (AAS). The actual amount of silver in the samples was then back-calculated from the resulting data against a predetermined calibration curve.

6.3.8.3 Silver Release Assay

The release characteristics of Ag⁺ ions from both the AgNPs-loaded calcium alginate beads and the AgNPs-loaded calcium alginate beads embedded in gelatin scaffolds were investigated by total immersion method in the PBS (pH 7.4) and DI (pH 7.0) at 37 °C. Each sample was dispersed in PBS-containing dialysis bag with a molecular weight cut-off of 12,000–14,000 Da. The dialysis bag was then immersed in 30 mL PBS. After a specified immersion time ranging between 0 and 7 days, 3 mL of the sample solution was withdrawn and fresh medium was refilled. Prior to determination, the samples were digested with 65% w/w nitric acid for at least 4 h and then allowed to cool down to eliminate the formed AgCl. The amount of

Ag⁺ ions in these sample solutions was determined using AAS. The obtained data were calculated to determine the cumulative amount of Ag⁺ ions released from both the AgNPs-loaded calcium alginate beads and the AgNPs-loaded calcium alginate beads embedded in gelatin scaffolds.

6.3.9 Antibacterial Evaluation of AgNPs-Loaded Calcium Alginate Beads Embedded in Gelatin Scaffolds

The antibacterial activity of the AgNPs-loaded calcium alginate beads embedded in gelatin scaffolds were investigated by the AATCC Test Method 100 (Antibacterial Finishes on Textile Materials: Assessment of The American Association of Textile Chemists and Colorists) or Colonies count. The pathogenic bacteria, *Escherichia coli* TISTR 780 and *Staphylococcus aureus* TISTR 1466, were used to investigate. 1.0 mL of culture medium (10⁵ CFU/mL) was added into each sample and then kept it in incubator at 37 °C for 24 h. The neat calcium alginate beads embedded in gelatin scaffolds were tested as a control. After 24 h incubation, the bacteria were eluted from each sample by adding 5 mL of sterile DI into each sample with vigorously shaking at room temperature for 5 min. Then, the eluted solutions were made a series dilution by using 0.1% peptone. The series diluted solutions were spread (in triplicate) on nutrient agar (NA) plate. These plates were incubated at 37 °C for 24 h. Finally, the colonies on agar plate were photographed and counted (range of 30-300 colonies) to evaluate the antibacterial activity. The number of bacteria presented in the sample was determined (on agar plate) and the percentage of reduction was also calculated.

The percent reduction of bacteria (R, %) was calculated by the following equation:

$$R (\%) = \frac{100 (B - A)}{B} \quad (6.3)$$

where A is the number of bacteria recovered from the treated test sample (AgNPs-loaded calcium alginate beads embedded in gelatin scaffolds) after incubation at 37 °C for 24 h and B is the number of bacteria recovered from the untreated test sample (neat calcium alginate beads embedded in gelatin scaffolds) after incubation at 37 °C for 24 h.

6.3.10 Indirect Cytotoxicity Evaluation of AgNPs-Loaded Calcium Alginate Beads Embedded in Gelatin Scaffolds

The indirect cytotoxicity evaluation of the AgNPs-loaded calcium alginate beads embedded in gelatin scaffolds was investigated in adaptation from the ISO 10993-5 standard test method in a 96-well tissue-culture polystyrene plate (TCPS; Corning Costar®, USA) using normal human dermal fibroblasts (NHDF; 7th passage). The cells were cultured in Dulbecco's modified Eagle's medium (DMEM; Sigma-Aldrich, USA), supplemented by 10% fetal bovine serum (FBS; Invitrogen Corp., USA), 1% L-glutamine (Invitrogen Corp., USA) and 1% antibiotic and antimycotic formulation [containing penicillin G sodium, streptomycin sulfate, and amphotericin B (Invitrogen Corp., USA)]. The 2% and 4% AgNPs-loaded calcium alginate beads embedded in gelatin scaffolds (47 ± 1 mg) were sterilized by UV radiation for ~1 h and then were immersed in 1 mL of serum-free medium (SFM; containing DMEM, 1% L-glutamine, 1% lactalbumin, and 1% antibiotic and antimycotic formulation) for 24 h in incubation to produce extraction media. NHDF cells were separately cultured in wells of TCPS at 10,000 cells/well in serum-containing DMEM for 24 h to allow cell attachment. The cells were then starved with SFM for 24 h. After that, the medium was replaced with an extraction medium and cells were re-incubated for 24 h. The viability of the cells cultured by each of the extraction medium was determined with 3-(4,5-dimethylthiazol-2-yl)-2,5-diphenyltetrazolium bromide (MTT) assay, with the viability of the cells cultured by fresh SFM was used as control.

The MTT assay is based on the reduction of the yellow tetrazolium salt to purple formazan crystals by dehydrogenase enzymes secreted from the mitochondria of metabolically active cells. The amount of purple formazan crystals formed is proportional to the number of viable cells. First, each culture medium was aspirated and replaced with 25 μ L/well of MTT solution at 5 $\text{mg} \cdot \text{mL}^{-1}$ for a 96-well TCPS. The plate was incubated for 2 h at 37 °C. The solution was then aspirated and 100 μ L/well of dimethyl sulfoxide (DMSO) was added to dissolve the formazan crystals. After 3 min of rotary agitation, the absorbance at the wavelength of 570 nm representing the viability of the cells was measured using a SpectraMax M2 Microplate Reader.

6.3.11 Statistical Analysis

The results were represented as means \pm standard errors of means. Statistical analysis was carried out by the one-way analysis of variance (one-way ANOVA) and Scheffe's post hoc test in SPSS (IBM SPSS, USA). The statistical significance was accepted at $p < 0.05$.

6.4 Results and Discussion

6.4.1 AgNPs-loaded Calcium Alginate Beads and AgNPs-Loaded Calcium Alginate Beads Embedded in Gelatin Scaffolds

The neat and the AgNPs-loaded calcium alginate beads were successfully prepared by emulsification/external gelation method. For preparation of the beads, a low viscosity alginic acid sodium salt as a starting material was used to facilitate the diffusion of calcium ions into the gel network during the gelation process (Peters & Van Bommel, 1992). The shapes and diameters of both the wet and dry AgNPs-loaded calcium alginate beads were observed using OM and SEM and the results are shown in Table 6.1. From the OM images, the neat calcium alginate beads, the 2%AgNPs-, and the 4% AgNPs-loaded calcium alginate beads showed spherical shape with a wide size distribution. Moreover, the presence of aggregates was also observed. The average diameters of the wet neat calcium alginate beads, the 2%AgNPs-, and the 4% AgNPs-loaded calcium alginate beads were 12.29 ± 2.93 , 19.25 ± 5.46 , and 22.07 ± 6.24 μm , respectively. While SEM images, the dry beads exhibited a spherical shape with rather smooth surface but the wide size distribution. The average diameters of the dry neat calcium alginate beads, the 2%AgNPs-, and the 4% AgNPs-loaded calcium alginate beads were 1.02 ± 0.71 , 2.11 ± 0.73 , and 2.15 ± 1.05 μm , respectively. However, the incorporation of AgNPs into the calcium alginate beads affected the size of the beads to increase. Moreover, the presence of AgNPs in the calcium alginate beads was observed by TEM as shown in Figure 6.1. This result confirmed that the UV irradiation reduced the Ag^+ ions to AgNPs. Selected SEM images of the 2%AgNPs-loaded calcium alginate beads embedded in gelatin scaffolds are shown in Figure 6.2. The results showed that the interconnected porous structure of the 2%AgNPs-loaded calcium alginate beads embedded in gelatin scaffolds was

obtained. From these results, it confirmed that the embedding of the AgNPs-loaded calcium alginate beads into gelatin scaffolds was successfully prepared as shown in Figure 6.2 (b).

6.4.2 Mechanical Property of Neat Calcium Alginate Beads Embedded in Gelatin Scaffolds and AgNPs-Loaded Calcium Alginate Beads Embedded in Gelatin Scaffolds

The mechanical properties of the materials play an important role *in vivo* application. There are several factors that affect the stability of scaffolds such as strength, elasticity and absorption at the material interface (Nair & Laurencin, 2007). The scaffolds should have suitable mechanical properties for use as wound dressings. Thus, compression test were carried out to evaluate the mechanical strength of scaffolds. For this reason, the compressive modulus of both the neat calcium alginate beads embedded in gelatin scaffolds and the AgNPs-loaded calcium alginate beads embedded in gelatin scaffolds was investigated. The compressive modulus was determined from the slope of stress-strain curves between 2 and 6% strain, due to the first region of compressive deformation was small extent that considered as elastic region (Zhou et al., 2005). The compressive modulus of both the neat calcium alginate beads embedded in gelatin scaffolds and the AgNPs-loaded calcium alginate beads embedded in gelatin scaffolds is shown in Table 6.2. The compressive modulus of the neat calcium alginate beads embedded in gelatin scaffolds, the 4%AgNPs- and the 8%AgNPs-loaded calcium alginate beads embedded in gelatin scaffolds was 11.32 ± 3.58 , 9.47 ± 1.21 , and 7.35 ± 1.75 kPa, respectively. These results showed that the embedding of the AgNPs-loaded calcium alginate beads into gelatin scaffolds decreased the compressive modulus of these scaffolds. From previous study, Pankongadisak et al. prepared the AgNPs-loaded calcium alginate beads with the diameter of ~ 140 μm by electrospraying method. The 4%AgNPs- and the 8%AgNPs-loaded calcium alginate beads embedded in gelatin scaffolds were characterized for their compressive modulus. The results showed that the compressive modulus of these scaffolds was ~ 3 kPa. From these results, the size of the embedded beads can improve the compressive modulus of the scaffolds (Pankongadisak, Ruktanonchai, Supaphol & Suwantong, manuscript under submission).

6.4.3 Thermal Property of Neat Calcium Alginate Beads Embedded in Gelatin Scaffolds and AgNPs-Loaded Calcium Alginate Beads Embedded in Gelatin Scaffolds

Thermal behaviors of both the neat calcium alginate beads embedded in gelatin scaffolds and the AgNPs-loaded calcium alginate beads embedded in gelatin scaffolds were investigated by TGA and the results are shown in Figure 6.3. From Figure 6.3, all scaffolds showed two weight loss processes. The first step was in the temperature range of about 40-200 °C, corresponding to the loss of moisture or water. The second step covered the temperature range of about 250-500 °C, corresponding to the thermal degradation of polymers (i.e., gelatin or alginate). The difference in thermal degradation temperature between the neat calcium alginate beads embedded in gelatin scaffolds and the AgNPs-loaded calcium alginate beads embedded in gelatin scaffolds was found to be ~10%. The presence of AgNPs takes part in degradation of scaffolds, which restricts the percentage of weight loss (Chandra Babu et al., 2013). Moreover, the increase of AgNPs contents embedded in the scaffolds slightly decreased the thermal degradation temperature of the scaffolds. Thus, the thermal stability of the neat calcium alginate beads embedded in gelatin scaffolds was higher than that of the AgNPs-loaded calcium alginate beads embedded in gelatin scaffolds.

6.4.4 Water Swelling and Weight Loss Behaviors of Neat Calcium Alginate Beads Embedded in Gelatin Scaffolds and AgNPs-Loaded Calcium Alginate Beads Embedded in Gelatin Scaffolds

The water swelling and the weight loss behaviors of both the neat calcium alginate beads embedded in gelatin scaffolds and the AgNPs-loaded calcium alginate beads embedded in gelatin scaffolds after submersion in PBS at 37 °C for 1, 3, 5, and 7 day were investigated and the results are shown in Figure 6.4. At 1 day after submersion in PBS, the water swelling of the neat calcium alginate beads embedded in gelatin scaffolds, the 2%AgNPs- and 4%AgNPs-loaded beads embedded in gelatin scaffolds was ~680, ~640, and ~657%, respectively (see Figure 6.4a). At 3 days, the values increased to ~827, ~823, and ~825%, respectively. At 5 days, the values also increased to ~926, ~832, and ~849%, respectively. Moreover, at 7 days, the values

increased to ~965, ~925, and ~965%, respectively. Thus, the water swelling of all scaffolds increased with increasing submersion time. However, the increasing of AgNO₃ content embedded in gelatin scaffolds did not significantly affect the water swelling of these scaffolds.

The weight loss behavior of both the neat calcium alginate beads embedded in gelatin scaffolds and the AgNPs-loaded calcium alginate beads embedded in gelatin scaffolds after submersion in PBS at 37 °C for 1, 3, 5, and 7 day is shown in Figure 6.4b. At 1 day after submersion in PBS, the weight loss of the neat calcium alginate beads embedded in gelatin scaffolds, the 4%AgNPs- and the 8%AgNPs-loaded beads embedded in gelatin scaffolds was ~18, ~17, and ~16%, respectively, while, at 3 days, the values increased to ~16, ~17, and ~18%, respectively. At 5 days, the values increased to ~18, ~21, and ~22%, respectively. At 7 days, the values also increased to ~19, ~22, and ~23%, respectively. Similarly, the weight loss of all scaffolds increased with increasing submersion time. Moreover, the increased AgNO₃ content embedded in gelatin scaffolds did not significantly affect the weight loss of these scaffolds. The AgNPs-loaded calcium alginate beads with the diameter of ~140 µm were prepared by electrospraying method. The water swelling and weight loss behaviors of these beads embedded in gelatin scaffolds after submersion in PBS for 7 days were ~900% and ~20%, respectively which were similar to this research (Pankongadisak, Ruktanonchai, Supaphol & Suwantong, manuscript under submerssion).

6.4.5 Release Characteristics of Ag⁺ ions from AgNPs-loaded Calcium Alginate Beads and AgNPs-Loaded Calcium Alginate Beads Embedded in Gelatin Scaffolds

The actual amounts of silver in both the AgNPs-loaded calcium alginate beads and the AgNPs-loaded calcium alginate beads embedded in gelatin scaffolds were determined prior to investigating the release characteristics of Ag⁺ ions from these samples. The results showed that the actual amounts of silver in the 2%AgNPs- and the 4%AgNPs-loaded calcium alginate beads were 4.99 ± 2.46 and 13.72 ± 1.82 mg/g (based on the actual weight of beads), respectively. While, the actual amounts of silver in the 2%AgNPs- and the 4%AgNPs-loaded calcium alginate beads embedded in gelatin scaffolds were 4.88 ± 0.10 and 13.64 ± 3.48 mg/g, respectively. These

values were later used to calculate the cumulative amounts of Ag^+ ions released from these samples.

The release characteristics of Ag^+ ions from both the AgNPs-loaded calcium alginate beads and the AgNPs-loaded calcium alginate beads embedded in gelatin scaffolds were carried out by the total immersion method over a period of 7 days in either the DI or the PBS medium at 37 °C. The cumulative release profiles of Ag^+ ions from all samples were reported as the percentage of the weight of Ag^+ ions released divided by the actual weight of Ag^+ ions in the samples (see Figure 6.5). The cumulative amounts of Ag^+ ions released from all samples into the DI medium gradually increased within the first submersion time, increased more gradually afterwards, and then reached a plateau value at the longest submersion investigated time. On the other hand, the cumulative amounts of Ag^+ ions released from all samples into the PBS medium rapidly increased within the first submersion time, increased more gradually afterwards, and then reached a plateau value at the early submersion investigated time. Moreover, the cumulative amounts of Ag^+ ions released from all samples in the PBS medium were higher than those in the DI medium. Specifically, the maximum cumulative amounts of Ag^+ ions released from the 2%AgNPs-loaded calcium alginate beads, the 4%AgNPs-loaded calcium alginate beads, the 2%AgNPs-loaded calcium alginate beads embedded gelatin scaffolds, and the 4%AgNPs-loaded calcium alginate beads embedded gelatin scaffolds upon submersion in the DI medium were ~1.6, ~3.2, ~0.36, and ~1.1 mg/g, respectively, on average. On the other hand, the maximum cumulative amounts of Ag^+ ions released from the 2%AgNPs-loaded calcium alginate beads, the 4%AgNPs-loaded calcium alginate beads, the 2%AgNPs-loaded calcium alginate beads embedded gelatin scaffolds, and the 4%AgNPs-loaded calcium alginate beads embedded gelatin scaffolds upon their submersion in the PBS medium were ~3.6, ~4.8, ~2.0, and ~1.2 mg/g, respectively, on average. When calcium alginate gel beads are placed in the PBS of pH 7.4, the Na^+ ions present in the external solution undergo ion-exchange process with Ca^{2+} ions which are binding with COO^- groups mainly in the polymannuronate sequences. Thereby the electrostatic repulsion among negatively charged COO^- groups increases which ultimately causes the chain relaxation and enhances the gel swelling. Therefore, the Ca^{2+} ions present in polymannuronate units

are exchanged with Na^+ ions, causing the beads to swell along with uptake of water. Thus making the bead structure loose, and phosphate ions interact with calcium ions to form calcium phosphate were obtained (Bajpai & Sharma, 2004). The reason might be resulted that the high cumulative amounts of Ag^+ ions released from these samples were obtained in PBS medium as compared with the DI medium, caused by the continued ion-exchange between Ca^{+2} and Na^+ to break the ionic crosslinking between polymer chains.

6.4.6 Antibacterial Evaluation of AgNPs-Loaded Calcium Alginate Beads Embedded in Gelatin Scaffolds

In this research, AgNPs was used as an agent to inhibit Gram-positive and Gram-negative bacteria. *E. coli* TISTR 780 as Gram-negative and *S. aureus* TISTR 1466 as Gram-positive were used to evaluate the antibacterial activity of the AgNPs-loaded calcium alginate beads embedded in gelatin scaffolds. The percentage of inhibition or colony count provides a quantitative procedure for evaluation of the antibacterial activity of the AgNPs-loaded calcium alginate beads embedded in gelatin scaffolds and the results are shown in Table 6.3. From Table 6.3, the neat calcium alginate beads embedded in gelatin scaffolds (i.e., control) showed no activity against the growth of both *E. coli* TISTR 780 and *S. aureus* TISTR 1466. The 2%AgNPs-loaded calcium alginate beads embedded in gelatin scaffolds showed activity against the growth of both *E. coli* TISTR 780 and *S. aureus* TISTR 1466 with percent reduction of 93.18 and 94.19, respectively. However, the 4%AgNPs-loaded calcium alginate beads embedded in gelatin scaffolds showed activity against the growth of both *E. coli* TISTR 780 and *S. aureus* TISTR 1466 with percent reduction of 93.18 and 100.00, respectively. From these results, the increased AgNPs content embedded in gelatin scaffolds increased the activity especially against the growth of *S. aureus* TISTR 1466. However, both the 2%AgNPs- and the 4%AgNPs-loaded calcium alginate beads embedded in gelatin scaffolds showed the higher antibacterial activity against *S. aureus* TISTR 1466 than *E. coli* TISTR 780.

6.4.7 Indirect cytotoxicity evaluation of AgNPs-loaded Calcium Alginate Beads and AgNPs-Loaded Calcium Alginate Beads Embedded in Gelatin Scaffolds

Cell viability was measured by using the MTT assay, which is based on the reduction of the yellow tetrazolium salt to purple formazan crystals by dehydrogenase enzymes secreted from the mitochondria of metabolically active cells. The viability of NHDF cells cultured with the extraction media from these samples in comparison with that of the cells cultured with the fresh culture medium is shown in Figure 6.6. The results showed that the viability of the cells cultured with the extraction media from all samples was lower than that of the cells cultured with the fresh culture medium. The viability of the cells cultured with all the extraction media from the 2%AgNPs-loaded calcium alginate beads, the 4%AgNPs-loaded calcium alginate beads, 2%AgNPs-loaded calcium alginate beads embedded in gelatin scaffolds, and the 4%AgNPs-loaded calcium alginate beads embedded in gelatin scaffolds were ~21, ~23, ~88, and ~84%, respectively, on average. From these results, all the AgNPs-loaded calcium alginate beads were toxic to NHDF cells. On the other hand, all AgNPs-loaded calcium alginate beads embedded in gelatin scaffolds were proven non-toxic to NHDF cells, indicating their potential uses for wound dressings.

6.5 Conclusions

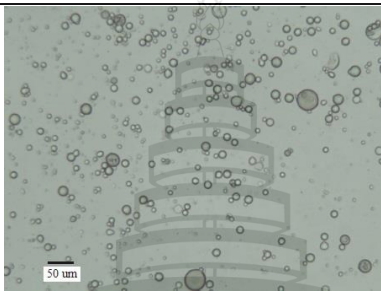
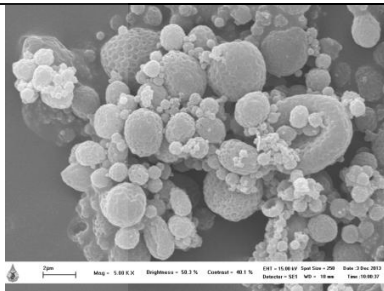
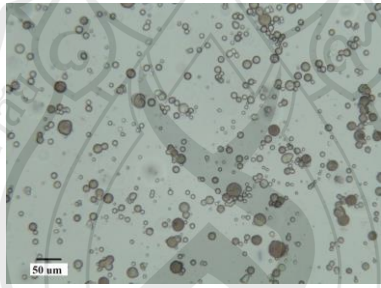
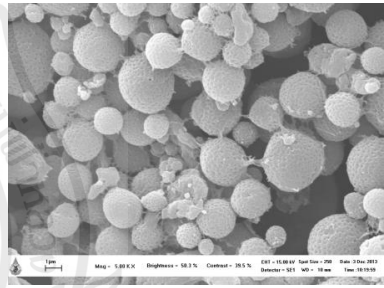
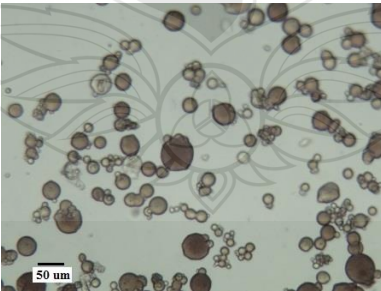
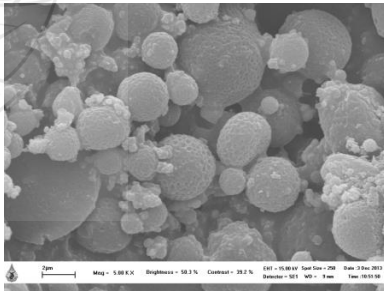
In this study, the neat and the AgNPs-loaded calcium alginate beads with average diameter of 1–2 μm were prepared by emulsification/external gelation method. The spherical shape with rather smooth surface of the both neat and the AgNPs-loaded calcium alginate beads were obtained. The embedding of the AgNPs-loaded calcium alginate beads into gelatin scaffolds was successfully prepared by freeze-drying method. The water swelling and weight loss behaviors of the AgNPs-loaded calcium alginate beads embedded in gelatin scaffolds increased with an increase in the submersion time. The cumulative amounts of Ag^+ ions released from both the AgNPs-loaded calcium alginate beads and the AgNPs-loaded calcium alginate beads embedded in gelatin scaffolds in the PBS medium were higher than

those in the DI medium. Moreover, the cumulative amounts of Ag^+ ions released from the AgNPs-loaded calcium alginate beads in both types of medium were greater than those from the AgNPs-loaded calcium alginate beads embedded in gelatin scaffolds. Thus, the embedding of the AgNPs-loaded calcium alginate beads into gelatin scaffolds reduced the burst release and sustained the release of Ag^+ ions for a long period of time. Moreover, the AgNPs-loaded calcium alginate beads embedded in gelatin scaffolds showed the higher activity with *S. aureus* TISTR 1466 than that with *E. coli* TISTR 780. Lastly, the AgNPs-loaded calcium alginate beads embedded in gelatin scaffolds were non-toxic to the NHDF cells indicating their potential uses for wound dressings.

6.6 Acknowledgements

The authors would like to acknowledge the financial support from the Research, Development and Engineering (RD&E) fund through The National Nanotechnology Center (NANOTEC), The National Science and Technology Development Agency (NSTDA), Thailand (P-11-00986) to Mae Fah Luang University (MFU) and Thailand Graduate Institute of Science and Technology (TGIST) (TG-55-99-55-048M).

Table 6.1 Selected OM and SEM Images of the Neat Calcium Alginate Beads and the AgNPs-Loaded Calcium Alginate Beads at Various Concentrations of AgNO₃ Including Diameters of the Individual Beads (n = 120)

Concentration of AgNO ₃ (% w/w)	Observed by	
	OM	SEM
0		
Bead diameters (μm)	12.29 ± 2.93	1.02 ± 0.71
2		
Bead diameters (μm)	$19.25 \pm 5.46^*$	$2.11 \pm 0.73^*$
4		
Bead diameters (μm)	$22.07 \pm 6.24^*$	$2.15 \pm 1.05^*$

Note. * $p < 0.05$ compared with the neat calcium alginate beads

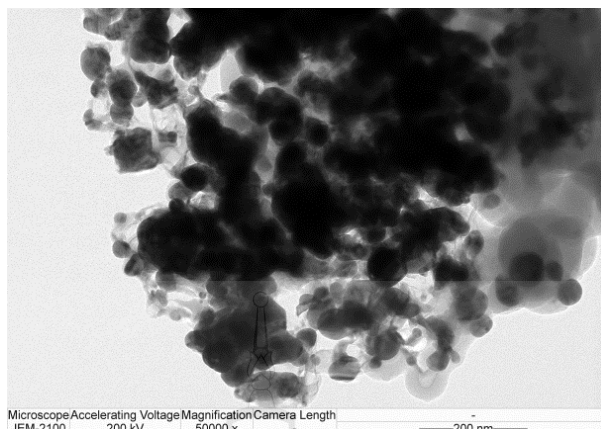


Figure 6.1 Selected TEM Image of the 4% AgNPs-Loaded Calcium Alginate Beads

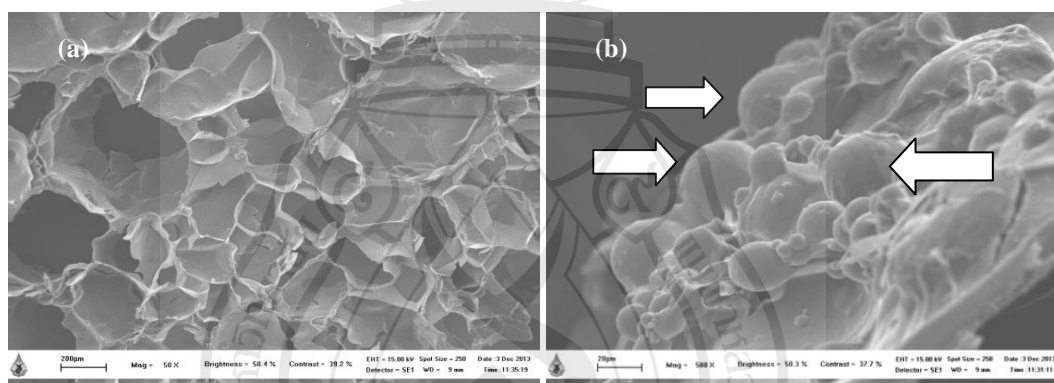


Figure 6.2 Selected SEM Images of the 2% AgNPs-Loaded Calcium Alginate Beads Embedded in Gelatin Scaffolds under Magnification of 50x (a) and Magnification of 500x with the White Arrows Indicating the Embedded Beads in the Scaffolds (b)

Table 6.2 Compressive Modulus of the Neat Calcium Alginate Beads Embedded in Gelatin Scaffolds and the AgNPs-Loaded Calcium Alginate Beads Embedded in Gelatin Scaffolds (n = 6)

Sample	Compressive modulus (kPa)
Neat calcium alginate beads embedded in gelatin scaffolds	11.32 ± 3.58
2% AgNPs-loaded calcium alginate beads embedded in gelatin scaffolds	9.47 ± 1.21
4% AgNPs-loaded calcium alginate beads embedded in gelatin scaffolds	$7.35 \pm 1.75^*$

Note. $*p < 0.05$ compared with the neat calcium alginate beads embedded in gelatin scaffolds

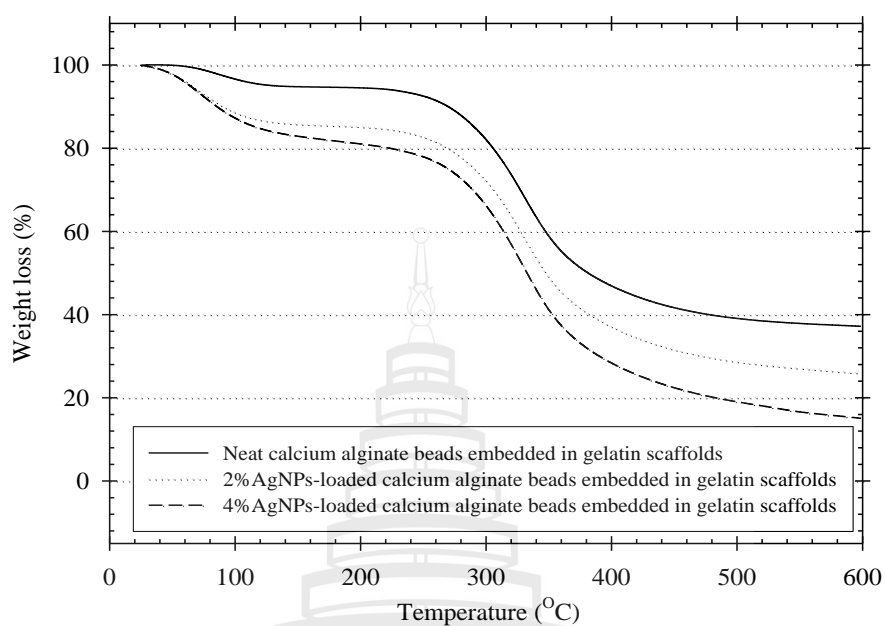


Figure 6.3 Thermogravimetric Analytical Thermograms of the Neat Calcium Alginate Beads Embedded in Gelatin Scaffolds and the AgNPs-Loaded Calcium Alginate Beads Embedded in Gelatin Scaffolds

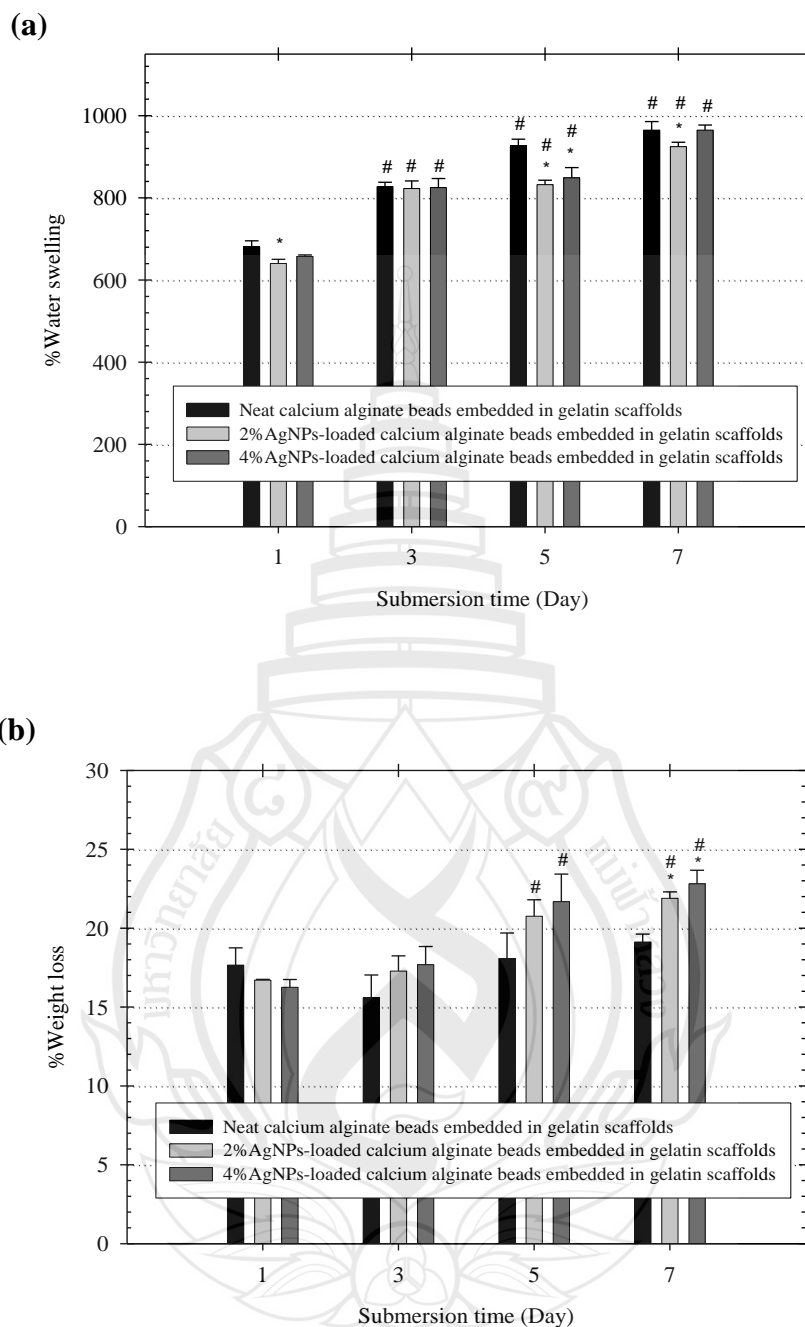


Figure 6.4 (a) Water Swelling and (b) Weight Loss Behaviors of the Neat Calcium Alginate Beads Embedded in Gelatin Scaffolds and the AgNPs-Loaded Calcium Alginate Beads Embedded in Gelatin Scaffolds ($n = 4$). * $p < 0.05$ Compared with the Neat Calcium Alginate Beads Embedded in Gelatin Scaffolds at a Given Time Point and # $p < 0.05$ Compared with 1 Day Submersion Time of a Given Scaffold

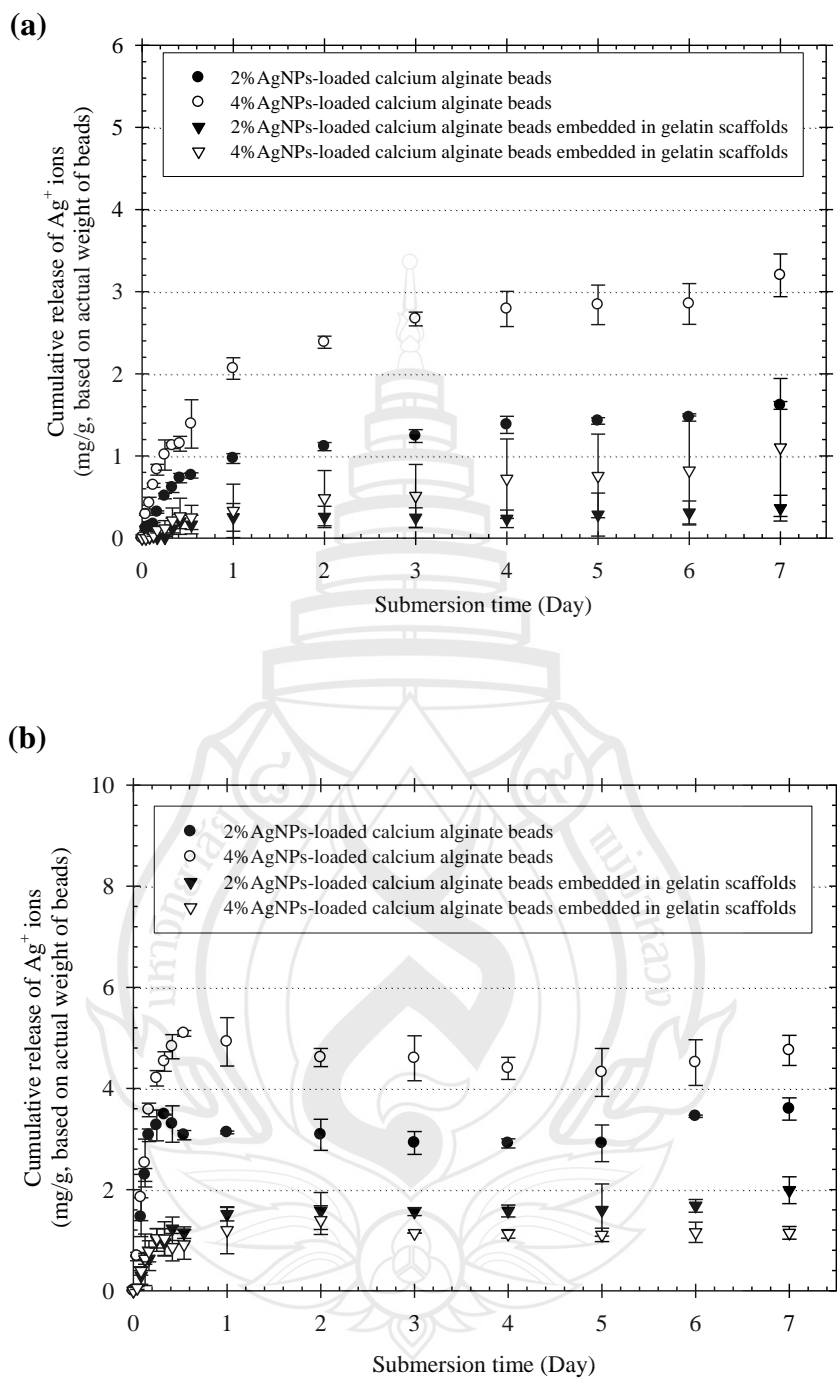


Figure 6.5 Cumulative Release Profiles of Ag^+ Ions from the AgNPs-Loaded Calcium Alginate Beads Embedded in Gelatin Scaffolds, Reported as the Weight of Ag^+ Ions Released Divided by the Actual Weight of the Beads, by Total Immersion Method in (a) DI and (b) PBS at the Physiological Temperature of 37°C ($n = 3$)

Table 6.3 Antibacterial Activity of the AgNPs-Loaded Calcium Alginate Beads Embedded in Gelatin Scaffolds (n = 3)

Culture	Sample	Percent reduction (%R)
<i>E. coli</i> TISTR 780	Control	
	2% AgNPs	93.18%
	4% AgNPs	93.18%
<i>S. aureus</i> TISTR 1466	Control	
	2% AgNPs	94.19%
	4% AgNPs	100.00%

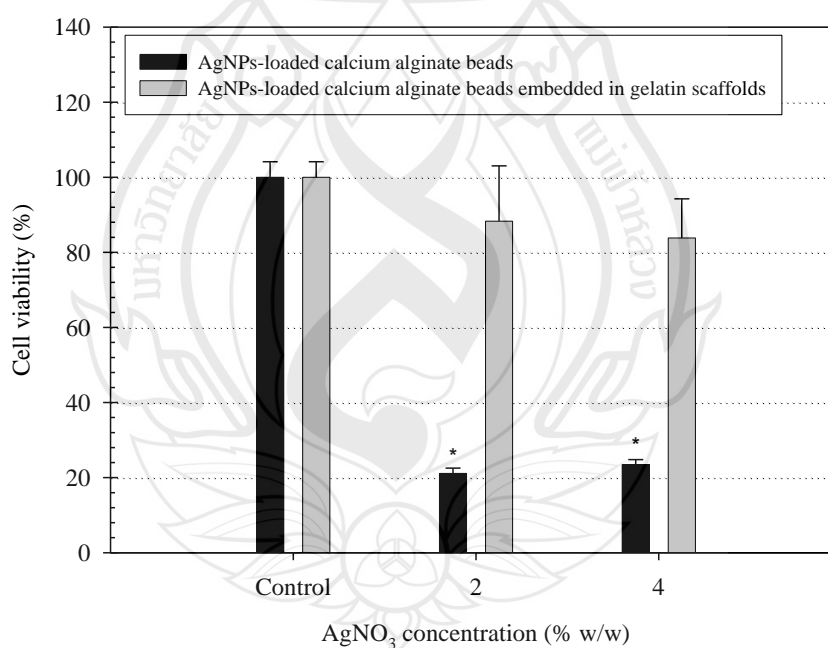


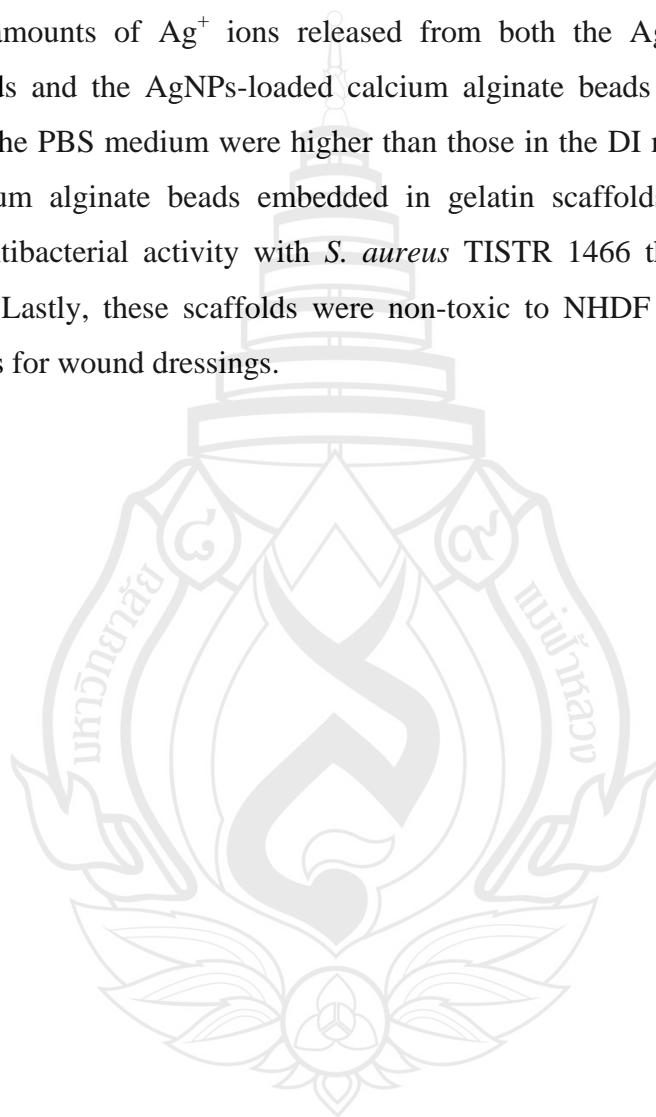
Figure 6.6 Indirect Cytotoxicity Evaluation of the AgNPs-Loaded Calcium Alginate Beads Embedded in Gelatin Scaffolds (n = 3). * $p < 0.05$ Compared with the Viability of NHDF Cells Cultured with the Fresh Culture Medium as Control

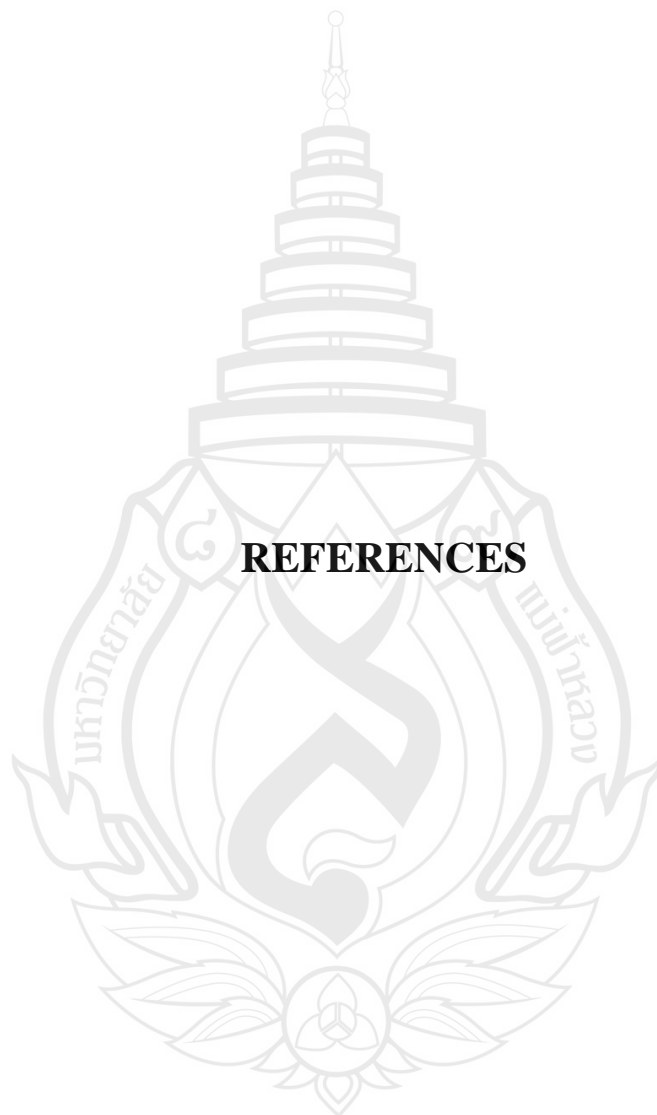
CHAPTER 7

CONCLUSIONS

In this study, the AgNPs-loaded calcium alginate beads embedded in gelatin scaffolds were developed for use in wound dressing and drug delivery applications. This work is divided into two parts for preparing the calcium alginate beads incorporated with AgNPs by; the first part is electrospraying method and the second part is emulsification/external gelation method. UV irradiation technique was used to reduce the Ag^+ ions in alginate solution to AgNPs. For producing the calcium alginate beads by electrospraying; factors affecting the shapes and diameters of the calcium alginate beads were the concentration of alginate solution and applied voltage. Increasing the concentration of alginate solution, the diameters of beads were increased. However, increasing the applied voltage, the diameters of beads were decreased. The incorporation of AgNPs into the calcium alginate beads resulted in a decreased bead diameters. The second, the calcium alginate beads obtained by emulsification/external gelation method exhibited a spherical shape with rather smooth surface but wide size distribution. Furthermore, the incorporation of AgNPs into the calcium alginate beads affected the size of the beads to increase. The increased genipin concentration to crosslink the gelatin scaffolds did not affect the pore size of scaffolds. The embedding of the AgNPS-loaded calcium alginate beads into the gelatin scaffolds did not affect the pore size of scaffolds. The water swelling and weight loss behaviors of the AgNPs-loaded calcium alginate beads embedded in gelatin scaffolds increased with an increase in the submersion time. The cumulative amounts of Ag^+ ions released from both the AgNPs-loaded calcium alginate beads and the AgNPs-loaded calcium alginate beads embedded in gelatin scaffolds in PBS increased rapidly in the first submersion time, increased more gradually afterwards, and then reached a plateau value at the longest submersion investigated time, while those in DI gradually increased in the first submersion time, more increased

afterwards, and then reached a plateau value at the longest submersion investigated time. The cumulative amounts of Ag^+ ions released from the AgNPs-loaded calcium alginate beads in both types of medium were greater than those from the AgNPs-loaded calcium alginate beads embedded in gelatin scaffolds. Moreover, the cumulative amounts of Ag^+ ions released from both the AgNPs-loaded calcium alginate beads and the AgNPs-loaded calcium alginate beads embedded in gelatin scaffolds in the PBS medium were higher than those in the DI medium. The AgNPs-loaded calcium alginate beads embedded in gelatin scaffolds showed the higher efficiency antibacterial activity with *S. aureus* TISTR 1466 than that with *E. coli* TISTR 780. Lastly, these scaffolds were non-toxic to NHDF cells indicating their potential uses for wound dressings.





REFERENCES

- Abbasi, A., Eslamian, M., Heyd, D. & Rousseau, D. (2008). Controlled release of DSBP from genipin-crosslinked gelatin thin films. *Pharmaceutical Development and Technology*, 13, 549-557.
- Abdelgawad, A. M., Hudson, S. M. & Rojas, O. J. (2014). Antimicrobial wound dressing nanofiber mats from multicomponent (chitosan/silver-NPs/polyvinyl alcohol) systems. *Carbohydrate Polymers*, 100, 166-178.
- Adekogbe, I. & Ghanem, A. (2005). Fabrication and characterization of DTBP-crosslinked chitosan scaffolds for skin tissue engineering. *Biomaterials*, 26, 7241–7250.
- Akhavan, O. & Ghaderi, E. (2010). Self-accumulated Ag nanoparticles on mesoporous TiO₂ thin film with high bactericidal activities. *Surface and Coatings Technology*, 204, 3676–3683.
- Al-Helw, A. A., Al-Angary, A. A., Mahrous, G. M. & Al-Dardari, M. M. (1998). Preparation and evaluation of sustained release cross-linked chitosan microspheres containing phenobarbitone. *Journal of Microencapsulation*, 15, 373-382.
- Augst, A. D., Kong, H. J. & Mooney, D. J. (2006). Alginate hydrogels as biomaterials. *Macromolecular Bioscience*, 6, 623-633.
- Bajpai, S. K. & Sharma S. (2004). Investigation of swelling/degradation behaviour of alginate beads crosslinked with Ca²⁺ and Ba²⁺ ions. *Reactive and Functional Polymers*, 59, 129-140.

- Banerjee, I., Mishra, D. & Maiti, T. K. (2009). PLGA microspheres incorporated gelatin scaffold: Microspheres modulate scaffold properties. *International Journal of Biomaterials*, 2009, 1-9.
- Barry, J. J. A., Gidda, H. S., Scotchford, C. A. & Howdle, S. M. (2004). Porous methacrylate scaffolds: Supercritical fluid fabrication and *in vitro* chondrocyte responses. *Biomaterials*, 25, 3559-3568.
- Birdi, G., Bridson, R. H., Smit, A. M., Mohd Bohari, S. P. & Grover, L. M. (2012). Modification of alginate degradation properties using orthosilicic acid. *Journal of the Mechanical Behavior of Biomedical*, 6, 181-187.
- Boateng, J. S., Matthews, K. H., Stevens, H. N. E. & Eccleston, G. M. (2007). Wound healing dressing and drug delivery systems: A review. *Journal of Pharmaceutical Sciences*, 97AUGUST 2008.
- Bogue, R. H. (1923). Conditions affecting the hydrolysis of collagen to gelatin. *Industrial & Engineering Chemistry*, 15, 1154-1159.
- Bryaskova, R., Pencheva, D., Kale, G., Lad, U. & Kantardjiev, T. (2010). Synthesis, characterization and antibacterial activity of PVA/TEOS/Ag-Np hybrid thin films. *Journal of Colloid and Interface Science*, 349, 77-85.
- Burrell, R. E. & Morris, L. R. (1998). Anti-microbial coating for medical devices. US Patent 5770255.
- Çetin, M., Vural, I., Çapan, Y. & Hincal, A. A. (2007). Preparation and characterization of alginate microspheres containing a model antigen. *International Journal of Molecular Sciences*, 32, 103-107.
- Chan, L. W., Lee, H. Y. & Heng, P. W. S. (2006). Mechanisms of external and internal gelation and their impact on the functions of alginate as a coat and delivery system. *Carbohydrate Polymers*, 63, 176-187.

- Chandra Babu, A., Prabhakar, M. N., Suresh Babu, A., Mallikarjuna, B., Subha, M. C. S. & Chowdoji Rao, K. (2013). Development and characterization of semi-IPN silver nanocomposite hydrogels for antibacterial application. *International Journal of Carbohydrate Chemistry*, 243695, 8 page.
- Chang, Y., Tsai, C. C., Liang, H. C. & Sung, H. W. (2001). Reconstruction of the right ventricular outflow tract with a bovine jugular vein graft fixed with a naturally occurring crosslinking agent (genipin) in a canine model. *The Journal of Thoracic and Cardiovascular Surgery*, 122, 1208-1218.
- Chen, G., Ushida, T. & Tateishi, T. (2002). Scaffold design for tissue engineering. *Macromolecular Bioscience*, 2, 67-77.
- Chen, L. & Subirade, M. (2006). Alginate-whey protein granular microspheres as oral delivery vehicles for bioactive compounds. *Biomaterials*, 27, 4646-4654.
- Choi, O. & Hu, Z. (2008). Size dependent and reactive oxygen species related nanosilver toxicity to nitrifying bacteria. *Environmental Science & Technology*, 42, 4583-4588.
- Chourasia, M. K. & Jain, S. K. (2004). Design and development of multiparticulate system for targeted drug delivery to colon. *Journal of Microencapsulation*, 11, 201-207.
- Chun, J., Kang, H., Jeong, L., Kang, Y., Oh, J., Yeo, I., Jung, S., Park, W. & Min, B. (2010). Epidermal cellular response to poly (vinyl alcohol) nanofibers containing silver nanoparticles. *Colloids and Surfaces B: Biointerfaces*, 78, 334-342.
- Chun, K. H., Kwon, I. C., Kim, H. Y., La, S. B., Sohn, Y. T & Jeong, S. Y. (1996). Preparation of sodium alginate microspheres containing hydrophilic β -lactam antibiotics. *Archives of Pharmacal Research*, 19, 106-111.
- Ciach, T. (2006). Microencapsulation of drugs by electro-hydro-dynamic atomization. *International Journal of Pharmaceutics*, 324, 51-55.

- Cleary, G. W. (1984). Transdermal controlled-release systems (Vol. 1). In R. S. Langer & D. L. Wise (Eds.), *Medical Applications of Controlled Release* (pp. 203-251). Florida: Boca Raton.
- Cloupeau, M. & Prunet, B. (1994). Electrohydrodynamic spraying functioning modes: A critical review. *Journal Aerosol Science*, 25, 1021–1036.
- Cloupeau, M. (1994). Recipes for use of EHD spraying in cone-jet mode and notes on corona discharge effects. *Journal of Aerosol Science*, 25, 1143-1157.
- Cortesi, R., Esposito, E., Osti, M., Menegatti, G., Davis, S. S. & Nastruzzi, C. (1999). Dextran cross linked gelatin microspheres as a drug delivery system. *European Journal of Pharmaceutics and Biopharmaceutics*, 47, 153-160.
- Darroudi, M., Ahmad, M. B., Zak, A. K., Zamiri, R. & Hakimi, M. (2011). Fabrication and characterization of gelatin stabilized silver nanoparticles under UV-light. *International Journal of Molecular Sciences*, 12, 6346-6356.
- DeFail, A. J., Edington, H. D., Matthews, S., Lee, W.-C. C. & Marra, K. G. (2006). Controlled release of bioactive doxorubicin from microspheres embedded within gelatin scaffolds. *Journal of Biomedical Materials Research Part A*, 79, 954-962.
- Ding, L., Lee, T. & Wang, C. -H. (2005). Fabrication of monodispersed Taxol-loaded particles using electrohydrodynamic atomization. *Journal of Controlled Release*, 102, 395–413.
- Doshi, J. & Reneker, D. H. (1995). Electrospinning process and applications of electrospun fibers. *Journal of Electrostatics*, 35, 151-160.
- Draget, K. I., Østgaard, K. & Smidsrød, O. (1990). Homogeneous alginate gels: A technical approach. *Carbohydrate Polymers*, 14, 159-178.

- Durán, N., Marcato, P. D., De Souza, G. I. H., Alves, O. L. & Esposito, E. (2007). Antibacterial effect of silver nanoparticles produced by fungal process on textile fabrics and their effluent treatment. *Journal of Biomedical Nanotechnology*, 3, 203-208.
- Eming, S. A., Werner, S., Bugnon, P., Wickenhauser, C., Siewe, L., Utermöhlen, O., Davidson, J. M., Krieg, T. & Roers, A. (2007). Accelerated wound closure in mice deficient for interleukin-10. *The American Journal of Pathology*, 170, 188-202.
- Fonder, M. A., Lazarus, G. S., Cowan, D. A., Aronson-Cook, B., Kohli, A. R. & Mamelak, A. J. (2008). Treating the chronic wound: a practical approach to the care of nonhealing wounds and wound care dressings. *Journal of the American Academy of Dermatology*, 58, 185-206.
- Freed, L. E., Vunjak-Novakovic, G., Biron, R. J., Eaqls, D. B., Lesnoy, D. C., Barlow, S. K. & Langer, R. (1994). Biodegradable polymer scaffolds for tissue engineering. *Biotechnology*, 12, 689-693.
- Frenot, A. & Chronakis, I. (2003). Polymer nanofibers assembled by electrospinning. *Current Opinion in Colloid and Interface Science*, 8, 64-75.
- Garg, T., Singh, O., Arora, S. & Murthy, R. (2012). Scaffold: a novel carrier for cell and drug delivery. *Critical Reviews in Therapeutic Drug Carrier Systems*, 29, 1-63.
- Gautam, S., Dinda, A. K. & Mishra, N. C. (2013). Fabrication and characterization of PCL/gelatin composite nanofibrous scaffold for tissue engineering applications by electrospinning method. *Material Science and Engineering C*, 33, 1228-1235.
- Gibaud, S., Demoy, M., Andreux, J. P., Weingarten, C., Gouritin, B. & Couvreur, P. (1996). Cells involved in the capture of nanoparticles in hematopoietic organs. *Journal of Pharmaceutical Science*, 85, 944-950.

- Gunatillake, P. A. & Adhikari, R. (2003). Biodegradable synthetic polymers for tissue engineering. *European Cells & Materials Journal*, 5, 1–16.
- Guo, S. & DiPietro, L. A. (2010). Factors affecting wound healing. *Journal of Dental Research*, 89, 219-229.
- Habraken, W. J. E. M., Wolke, J. G. C. & Jansen, J. A. (2007). Ceramic composites as matrices and scaffolds for drug delivery in tissue engineering. *Advanced Drug Delivery Reviews*, 59, 234-248.
- Hong, K. H. (2007). Preparation and properties of electrospun poly(vinyl alcohol)/silver fiber web as wound dressings. *Polymer Engineering and Science*, 47, 43-49.
- Hong, S. R., Lee, S. J., Shim, J. W., Choi, Y. S., Lee, Y. M., Song, K. W., Park, M. H., Nam, Y. S. & Lee, S. I. (2001). Study on gelatin-containing artificial skin IV: A comparative study on the effect of antibiotic and EGF on cell proliferation during epidermal healing. *Biomaterials*, 22, 2777-2783.
- Hutmacher, D. W. (2000). Scaffolds in tissue engineering bone and cartilage. *Biomaterials*, 21, 2529–2543.
- Hutmacher, D. W. (2001). Scaffold design and fabrication technologies for engineering tissues -state of the art and future perspectives. *Journal Biomaterials Science Polymer Edition*, 12, 107-124.
- Ikada, Y. (2006). Challenges in tissue engineering. *Journal of the Royal Society Interface*, 3, 589-601.
- Islam, S., Molla, A. I., Sarker, M., Karim, M. M., Masum, S. & Yeum, J. H. (2011). Fabrication of pllulan/silver nanoparticle composite nanospheres using electrospray technique for antibacterial applications. *International Journal of Basic & Applied Sciences*, 11, 36-40.

- ISO 10993-5. (2009). Biological evaluation of medical devices, Part 5: Tests for *in vitro* cytotoxicity. International Organization for Standardization, Geneva, Switzerland.
- Ito, A., Mase, A., Takizawa, Y., Shinkai, M., Honda, H., Hata, K., Ueda, M. & Kobayashi, T. (2003). Transglutaminase-mediated gelatin matrices incorporating cell adhesion factors as a biomaterial for tissue engineering. *Journal of Bioscience and Bioengineering*, 95, 196-199.
- Jaworek, A. & Sobczyk, A. T. (2008) Electrospraying route to nanotechnology: an overview. *Journal of Electrostatics*, 66, 197-219.
- Jaworek, A. (2007). Review: micro- and nanoparticle production by electrospraying. *Powder Technology*, 176, 18-35.
- Jayasuriva, C. A., Assad, M., Jayatissa, A. H. & Ebraheim, N. A. (2006). Dissolution behavior of biomimetic minerals on 3D PLGA scaffold. *Surface and Coatings Technology*, 200, 6336–6339.
- Jin, W., Jeon, H., Kim, J. & Youk, J. (2007). A study on the preparation of poly (vinyl alcohol) nanofibers containing silver nanoparticles. *Synthetic Metals*, 157, 454–459.
- Jopling, D. W. (1956). The swelling of gelatin films. The effects of drying temperature and of conditioning the layers in atmospheres of high relative humidity. *Journal of Applied Chemistry*, 6, 79-84.
- Jung, G. -B., Kim, J. -H., Burm, J. S. & Park, H. -K. (2013). Fabrication of chitosan-silver nanoparticle hybrid 3D porous structure as a SERS substrate for biomedical applications. *Applied Surface Science*, 273, 179-183.
- Kang, H. W., Tabata, Y. & Ikada, Y. (1999). Fabrication of porous gelatin scaffolds for tissue engineering. *Biomaterials*, 20, 1339-1344.

- Kim, J. S., Kuk, E., Yu, K. N., Kim, J. -H., Park, S. J., Lee, H. J., Kim, S. H., Park, Y. K., Park, Y. H., Hwang, C. -Y., Kim, Y. -K., Lee, Y. -S., Jeong, D. H. & Cho, M. -H. (2007). Antimicrobial effects of silver nanopartilces. *Nanomedicine: Nanotechnology, Biology and Medicine*, 3, 95-101.
- Kim, K., Lee, H., Lee, J. & Shin, K. (2010). Poly (ethylenimine)-stabilized silver nanoparticles assembled into 2-dimensional arrays at water-toluene interface. *Journal of Colloid and Interface Science*, 345, 103–108.
- Kim, S. E., Heo, D. N., Lee, J. B., Kim, J. R., Park, S. H., Jeon, S. H. & Kwon, I. K. (2009). Electrospun gelatin/polyurethane blended nanofibers for wound healing. *Biomedical Materials*, 4, 044106.
- Kim, S. -H., Lee, H. -S., Ryu, D. -S., Choi, S. -J. & Lee, D. -S. (2011). Antibacterial activity of silver nanoparticles against *Staphylococcus aureus* and *Escherichia coli*. *Korean Journal of Microbiology and Biotechnology*, 39, 77-85.
- Kumar, S., Bhanjana, G., Sharma, A., Sidhu, M. C. & Dilbaghi, N. (2014). Synthesis, characterization and on field evaluation of pesticide loaded sodium alginate nanoparticles. *Carbohydrate Polymers*, 101, 1061–1067.
- Kumar, M. N. V. R., Muzzarelli, R. A. A., Muzzarelli, C., Sashiwa, H. & Domb, A. J. (2004). Chitosan chemistry and pharmaceutical perspectives. *Chemical Reviews*, 104, 6017–6084
- Langer, R. (1998). Drug delivery and targeting. *Nature*, 392, 5-10.
- Langer, R. (2004). Transdermal drug delivery: Past present, current status and future prospects. *Advance Drug Delivery Review*, 56, 557–558.
- Lee, K. Y. & Mooney, D. J. (2012). Alginate: properties and biomedical applications. *Progress in Polymer Science*, 37, 106-126.
- Lee, K. Y. & Yuk, S. H. (2007). Polymeric protein delivery systems. *Progress in Polymer Science*, 32, 669-697.

- Lee, P. Y., Chesnoy, S. & Huang, L. (2004). Electroporatic delivery of TGF- β 1 gene works synergistically with electric therapy to enhance diabetic wound healing in db/db mice. *Journal of Investigative Dermatology*, 123, 791-798.
- Lee, P. Y., Cobain, E., Huard, J. & Huang, L. (2007). Thermosensitive hydrogel PEG-PLGA-PEG enhances engraftment of muscle-derived stem cells and promotes healing in diabetic wound. *Molecular Therapy*, 15, 1189-1194.
- Lemoine, D., Wauters, F., Bouchend'homme, S. & Pr  at, V. (1998). Preparation and characterization of alginate microspheres containing a model antigen. *International Journal of Pharmaceutics*, 176, 9-19.
- LeRoux, M. A., Guilak, F. & Setton, L. A. (1999). Compressive and shear properties of alginate gel: Effects of sodium ions and alginate concentration. *Journal of Biomedical Materials Research*, 47, 46-53.
- Liapis, A. I., Pikal, M. J. & Bruttini, R. (1996). Research and development needs and opportunities in freeze drying. *Drying Technology*, 14, 1265-1300.
- Lien, S. M., Li, W. T. & Huang, T. J. (2008). Genipin-crosslinked gelatin scaffolds for articular cartilage tissue engineering with a novel crosslinking method. *Materials Science & Engineering C*, 28, 36-43.
- Lim, Y. M., Gwon, H. J., Shin, J., Jeun, J. P. & Nho, Y. C. (2008). Preparation of porous poly(ϵ -caprolactone) scaffolds by gas foaming process and *in vitro/in vivo* degradation behavior using x-ray irradiation. *Journal of Industrial and Engineering Chemistry*, 14, 436-441.
- Lin, H. R., Qu, L. H., Lin, Y. J. & Ling, M. H. (2007). Hollow, pH-sensitive calcium-alginate/poly(acrylic acid) hydrogel beads as drug carries for vancomycin release. *Journal of Applied Polymer Science*, 118, 1878-1886.
- Liu, J. & Hurt, R. H. (2010). Ion release kinetics and particle persistence in aqueous nano-silver colloids. *Environmental Science & Technology*, 44, 2169-2175.

- Liu, X. D., Yu, W. Y., Zhang, Y., Xue, W. M., Yu, W. T., Xiong, Y., Ma, X. J., Chen, Y. & Yuan, Q. (2002). Characterization of structure and diffusion behavior of Ca-alginate beads prepared with external or internal calcium sources. *Journal of Microencapsulation*, 19, 775-782.
- Liu, X., Lee, P. Y., Ho, C. M., Lui, V. C., Chen, Y., Che, C. M., Tam, P. K. & Wong, K. K. (2010). Silver nanoparticles mediate differential responses in keratinocytes and fibroblasts during skin wound healing. *ChemMedChem*, 5, 468-475.
- Liu, X., Sun, Q., Wang, H., Zhang, L. & Wang, J. -Y. (2005). Microspheres of corn protein, zein, for an ivermectin drug delivery system. *Biomaterials*, 26, 109-115.
- Lok, C. N., Ho, C. M., Chen, R., He, Q. Y., Yu, W. Y., Sun, H., Tam, P. K., Chiu, J. F. & Che, C. M. (2007). Silver nanoparticles: partial oxidation and antibacterial activities. *Journal of Biological Inorganic Chemistry*, 12, 527-534.
- Lu, L. & Mikos, A. G. (1996). The importance of new processing techniques in tissue engineering. *MRS Bulletin*, 21, 28-32.
- Luderer, F., Begerow, I., Schmidt, W., Martin, H., Grabow, N., Bünger, C. M., Schareck, W., Schmitz, K. -P. & Sternberg, K. (2012). Enhanced visualization of biodegradable polymeric vascular scaffolds by incorporation of gold, silver and magnetite nanoparticles. *Journal of Biomaterials Applications*, 28, 219-231.
- Ma, P. X. & Choi, J. -W. (2001). Biodegradable polymer scaffolds with well-defined interconnected spherical pore network. *Tissue Engineering*, 7, 23-33.
- Mackay, D. & Miller, A. L. (2003). Nutritional support for wound healing. *Alternative Medicine Review*, 8, 359-377.

- Malafaya, P. B., Silva, G. A. & Reis, R. L. (2007). Natural–origin polymers as carriers and scaffolds for biomolecules and cell delivery in tissue engineering applications. *Advanced Drug Delivery Reviews*, 59, 207–233.
- Mandal, B. B. & Kundu, S. C. (2009). Calcium alginate beads embedded in silk fibroin as 3D dual drug releasing scaffolds. *Biomaterials*, 30, 5170-5177.
- Maneerung, T., Tokura, S. & Rujiravanit, R. (2008). Impregnation of silver nanoparticles into bacterial cellulose for antimicrobial wound dressing. *Carbohydrate Polymers*, 72, 43–51.
- Martinez, C. J., Kim, J. W., Ye, C., Ortiz, I., Rowat, A. C., Marquez, M. & Weitz, D. (2012). A microfluidic approach to encapsulate living cells in uniform alginate hydrogel microparticles. *Macromolecular Bioscience*, 12, 946-951.
- Martinez-Gutierrez, F., Olive, P. L., Banuelos, A., Orrantia, E., Nino, N., Sanchez, E. M., Ruiz, F., Bach, H. & Av-Gay, Y. (2010). Synthesis, characterization, and evaluation of antimicrobial and cytotoxic effect of silver and titanium nanoparticles. *Nanomedicine*, 6, 687-688.
- Martins, S., Sarmento, B., Souto, E. B. & Ferreira, D. C. (2007). Insulin-loaded alginate microspheres for oral delivery—effect of polysaccharide reinforcement on physicochemical properties and release profile. *Carbohydrate Polymers*, 69, 725-731.
- Martinsen, A., Skjåk-Braek, G. & Smidsrød, O. (1989). Alginate as immobilization material: I. Correlation between chemical and physical properties of alginate gel beads. *Biotechnology and Bioengineering*, 33, 79-89.
- Mikos, A. G., Bao, Y., Linda, L. G., Ingber, D. E., Vacanti, J. P. & Langer, R. (1993). Preparation of poly(glycolic acid) bonded fiber structures for cell attachment and transplantation. *Journal Biomedical and Materials Reviews*, 27, 183-189.
- Nair, L. S. & Laurencin, C. T. (2007). Biodegradable polymers as biomaterials. *Progress in Polymer Science*, 32, 762-798.

- Nam, Y. S., Yoon, J. J. & Park, T. G. (2000). A novel fabrication method for macroporous scaffolds using gas foaming salt as porogen additive. *Journal Biomedical Materials Reviews*, 53, 1–7.
- Ouwerx, C., Velings, N., Mestdagh, M. M. & Axelos, M. A. V. (1998). Physico-chemical properties and rheology of alginate gel beads formed with various divalent cations. *Polymer Gels and Networks*, 6, 393-408.
- Pankongadisak, P., Ruktanonchai, U. R., Supaphol, P. & Suwantong, O. Development of silver nanoparticles-loaded calcium alginate beads embedded in gelatin scaffolds for use as wound dressings, manuscript under submission.
- Pankongadisak, P., Ruktanonchai, U. R., Supaphol, P. & Suwantong, O. (2014). Preparation and characterization of silver nanoparticles-loaded calcium alginate beads embedded in gelatin scaffolds. *AAPS PharmSciTech*, DOI: 10.1208/s12249-014-0140-9.
- Parveen, S., Krishnakumar, K. & Sahoo S. K. (2006). New era in health care: tissue engineering. *Journal of Stemcells and Regenerative Medicine*, 1, 8-24.
- Pasparakis, G. & Bouropoulos, N. (2006). Swelling studies and *in vitro* release of verapamil from calcium alginate and calcium alginate-chitosan bead. *International Journal of Pharmaceutics*, 323, 34–42.
- Peters, H. J. W. & Van Bommel, E. M. G. (1992). Effect of alginate properties on the microencapsulation process of oils. *Proceeding of the 6th International Conference Pharmaceutical Technology*, 2, 270-279.
- Pham, Q. P., Sharma, U. & Mikos, A. G. (2006). Electrospinning of polymeric nanofibers for tissue-engineering applications. *Tissue Enginerring*, 12, 1197–1211.

- Phutane, P., Shidhaye, S., Lotlikar, V., Ghule, A., Sutar, S. & Kadam, V. (2010). *In vitro* evaluation of novel sustained release microspheres of glipizide prepared by the emulsion solvent diffusion-evaporation method. *Journal of Young Pharmacists*, 2, 35-41.
- Pitarresi, G., Palumbo, S. F., Fiorica, C., Calascibetta, F. & Giammona, G. (2010). Electrospinning of α,β -poly(N-2-hydroxyethyl)-DL-aspartamide-graft-poly(lactic acid) to produce a fibrillar scaffold. *European Polymer Journal*, 46, 181–184.
- Prabhu, S. & Poullose, E. K. (2012). Silver nanoparticles: mechanism of antimicrobial action, synthesis, medical applications, and toxicity effects. *International Nano Letters*, 2, 1-10.
- Quong, D., Neufeld, R. J., Skjåk-Braek, G. & Poncelet, D. (1998). External versus internal source of calcium during the gelation of alginate beads for DNA encapsulation. *Biotechnology and Bioengineering*, 57, 438-446.
- Rastogi, R., Sultana, Y., Aqil, M., Ali, A., Kumar, S., Chuttani, K. & Mishra, A. K. (2007). Alginate microspheres of isoniazid for oral sustained drug delivery. *International Journal of Pharmaceutics*, 334, 71–77.
- Rattanaaruengsrikul, V., Pimpha, N. & Supaphol, P. (2009). Development of gelatin hydrogel pads as antibacterial wound dressings. *Macromolecular Bioscience*, 9, 1004–1015.
- Rebelatto, M. C., Guimond, P., Bowersock, T. L. & HogenEsch, H. (2011). Induction of systemic and mucosal immune response in cattle by intranasal administration of pig serum albumin in alginate microparticles. *Veterinary Immunology and Immunopathology*, 83, 93-105.
- Riyajan, S. –A. & Sakdapipanich, J. T. (2009). Development of a controlled release neem capsule with a sodium alginate matrix, crosslinked by glutaraldehyde and coated with natural rubber. *Polymer Bulletin*, 63, 609-622.

- Rousseau, I., Le Cerf, D., Picton, L., Argillier, J. F. & Muller, G. (2004). Entrapment and release of sodium polystyrene sulfonate (SPS) from calcium alginate gel beads. *European Polymer Journal*, 40, 2709-2715.
- Rujitanaroj, P.-o., Pimpha, N. & Supaphol, P. (2008). Wound-dressing materials with antibacterial activity from electrospun gelatin fiber mats containing silver nanoparticles. *Polymer*, 49, 4723-4732.
- Sai, K. P. & Babu M. (2000). Collagen based dressings: a review. *Burns*, 26, 54–62.
- Sakchai, W., Churrerat, P. & Srisagul, S. (2006). Development and *in vitro* evaluation of chitosan-eudragit RS 30D composite wound dressings. *American Association of Pharmaceutical Scientists*, 7, E1-E6.
- Sambhy, V. M. (2006). Silver bromide nanoparticle/polymer composites: Dual action tunable antimicrobial materials. *Journal of the American Chemical Society*, 128, 9798-9808.
- Santoa, V. E., Duarte, A. R. C., Gomes, M. E., Mano, J. F. & Reis, R. L. (2010). Hybrid 3D structure of poly(d,l-lactic acid) loaded with chitosan/chondroitin sulfate nanoparticles to be used as carriers for biomacromolecules in tissue engineering. *Journal of Supercritical Fluids*, 54, 320-327.
- Schierholz, J. M., Lucas, L. J., Rump, A. & Pulverer, G. (1998). Efficacy of silver-coated medical devices. *Journal of Hospital Infection*, 40, 257-262
- Sharma, V. K., Yngard, R. A. & Lin, Y. (2009). Silver nanoparticles: Green synthesis and their antimicrobial activities. *Advances in Colloid and Interface Science*, 145, 83-96.
- Shi, P., He, P., Teh, T. K. H., Morsi, Y. S. & Goh, J. C. H. (2011). Parametric analysis of shape changes of alginate beads. *Powder Technology*, 210, 60–66.

- Shi, X., Wang, Y., Rena, L., Zhao, N., Gong, Y. & Wang, D. (2009). Novel mesoporous silica based antibiotic releasing scaffold for bone repair. *Acta Biomaterialia*, 5, 1697-1707.
- Sikareepaisan, P., Ruktanonchai, U. & Supaphol, P. (2011). Preparation and characterization of asiaticoside-loaded alginate films and their potential for use as effectual wound dressings. *Carbohydrate Polymers*, 83, 1457–1469.
- Silva, C. M., Ribeiro, A. J. Ferreira, D. & Veiga, F. (2006). Insulin encapsulation in reinforced alginate microspheres prepared by internal gelation. *European Journal of Pharmaceutical Sciences*, 29, 148-159.
- Sinha, V. R., Singla, A. K., Wadhawan, S., Kaushik, R., Kumria, R., Bansal, K & Dhawan, S. (2004). Chitosan microspheres as a potential carrier for drugs. *International Journal of Pharmaceutics*, 274, 1-33.
- Skjåk-Braek, G., Grasdalen, H. & Smidsrød, O., (1989). Inhomogeneous polysaccharide ionic gels. *Carbohydrate Polymers*, 10, 31-54.
- Son, W. K., Youk, J. H., Lee, T. S. & Park, W. H. (2004). Preparation of antimicrobial ultrafine cellulose acetate fibers with silver nanoparticles. *Macromolecular Rapid Communications*, 25, 1632-1637.
- Sotiriou, G. A. & Pratsinis, S. E. (2010). Antibacterial activity of nanosilver ions and particles. *Environmental Science & Technology*, 44, 5649-5654.
- Srinivasan, S., Jayasree, R., Chennazhi, K. P., Nair, S. V. & Jayakumar, R. (2012). Biocompatible alginate/nano bioactive glass ceramic composite scaffolds for periodontal tissue regeneration. *Carbohydrate Polymers*, 87, 274– 283.
- Stevanović, M., Bračko, I., Milenković, M., Filipović, N., Nunić, J., Filipič, M. & Uskoković, D. P. (2014). Multifunctional PLGA particles containing poly(L-glutamic acid)-capped silver nanoparticles and ascorbic acid with simultaneous antioxidative and prolonged antimicrobial activity. *Acta Biomaterialia*, 10, 151-162.

- Stevens, K. R., Einerson, N. J., Burmania, J. A. & Kao, W. J. (2002). *In vivo* biocompatibility of gelatin-based hydrogels and interpenetrating networks. *Journal Biomaterials Science Polymer Edition*, 13, 1353-1366.
- Su, H. L., Chou, C. C., Hung, D. J., Lin, S. H., Pao, I. C., Lin, J. H., Huang, F. L., Dong, R. X. & Lin, J. J. (2009). The disruption of bacterial membrane integrity through ROS generation induced by nanohybrids of silver and clay. *Biomaterials*, 30, 5979-5987.
- Sudheesh Kumar, P. T., Abhilash, S., Manzoor, K., Nair, S. V., Tamura, H. & Jayakumar, R. (2010). Preparation and characterization of novel β -chitin/nanosilver composite scaffolds for wound dressing applications. *Carbohydrate Polymers*, 80, 761-767.
- Suksamran, T., Opanasopit, P., Rojanarata, T., Ngawhirunpat, T., Ruktanonchai, U. & Supaphol P. (2009). Biodegradable alginate microparticles developed by electrohydrodynamic spraying techniques for oral delivery of protein. *Journal of Microencapsulation*, 26, 563-570.
- Tabata, Y., Hijikata, S. & Ikada, Y. (1994). Enhanced vascularization and tissue granulation by basic fibroblast growth factor impregnated in gelatin hydrogels. *Journal of Controlled Release*, 31, 189-199.
- Takahashi, H., Miyoshi, T. & Boki, K. (1993). Study on hydrophilic properties of gelatin as a clinical wound dressing. I. Hydrophilic properties of gelatin as a wound dressing. *Tokushima Journal of Experimental Medicine*, 40, 159-167.
- Tamura, H., Furuike, T., Nair, S. V. & Jayakumar, R. (2011). Biomedical applications of chitin hydrogel membranes and scaffolds. *Carbohydrate Polymers*, 84, 820-824.
- Thu, H. -E., Zulfakar, M. H. & Ng, S. -F. (2012). Alginate based bilayer hydrocolloid films as potential slow-release modern wound dressing. *International Journal of Pharmaceutics*, 434, 375-383.

- Tonda-Turo, C., Gentile, P., Saracino, S., Chiono, V., Nandagiri, V. K., Muzio, G., Canuto, R. A. & Ciardelli, G. (2011). Comparative analysis of gelatin scaffolds crosslinked by genipin and silane coupling agent. *International Journal of Biological Macromolecules*, 49, 700-706.
- Torres, E., Mata, Y. N., Blazquez, A. L., Munoz, J. A., Gonzalez, F. & Ballester, A. (2005). Gold and silver uptake and nanoprecipitation on calcium alginate beads. *Langmuir*, 21, 7951-7958.
- Tungprapa, S., Puangparn, T., Weerasombut, M., Jangchud, I., Fakum, P., Semongkhon, S., Meechaisue, C. & Supaphol, P. (2007). Electrospun cellulose acetate fibers: effect of solvent system on morphology and fiber diameter. *Cellulose*, 14, 563-575.
- Ungaro, F., Biondi, M., d'Angelo, I., Indolfi, L., Quaglia, F., Netti, P. A. & La Rotonda, M. I. (2006). Microsphere-integrated collagen scaffolds for tissue engineering: Effect of microsphere formulation and scaffold properties on protein release kinetics. *Journal of Controlled Release*, 113, 128-136.
- Wan, L. S. C., Heng, P. W. S. & Chan, L. W. (1992). Drug encapsulation in alginate microspheres by emulsification. *Journal of Microencapsulation*, 9, 309-316.
- Watson, N. F. S. & Hodgkin, W. (2005). Wound dressing. *Surgery*, 23, 53-55.
- Wee, S. & Gombotz, W. R. (1998). Protein release from alginate matrices. *Advanced Drug Delivery Reviews*, 31, 267-285.
- Wei, D., Sun, W., Qian, W., Ye, Y. & Ma, X. (2009). The synthesis of chitosan-based silver nanoparticles and their antibacterial activity. *Carbohydrate Research*, 344, 2375-2382.
- Wells, L. A. & Sheardown, H. (2007). Extended release of high pI protein from alginate microspheres via a novel encapsulation technique. *European Journal of Pharmaceutics and Biopharmaceutics*, 65, 329-335.

- Whang, K., Thomas, H. & Healy, K. E. (1995). A novel method to fabricate bioabsorbable scaffolds. *Polymer*, 36, 837–841.
- Wise, R. A. (1984). Neural mechanisms of the reinforcing action of cocaine. *National Institute on Drug Abuse Research Monograph*, 50, 15-33.
- Woei, K., Hutmacher, D. W., Schantz, J. T., Seng, C., Too, H. P., Chye, T., Phan, T. T. & Teoh, S. H. (2001). Evaluation of ultra-thin poly(epsilon-caprolactone) films for tissue engineered skin. *Tissue Engineering*, 7, 441–455.
- Xie, J., Lim, L. K., Phua, Y., Hua, J. & Wang, C. -H. (2006). Electrohydrodynamic atomization for biodegradable polymeric particle production, *Journal of Colloid and Interface Science*, 302, 103–112.
- Yang, S. F., Leong, K. F., Du, Z. H. & Chua, C. K. (2001). The design of scaffolds for use in tissue engineering: Part 1-traditional factors. *Tissue Engineering*, 7, 89-679.
- Yang, W., Shen, C., Ji, Q., An, H., Wang, J., Liu, Q. & Zhang, Z. (2009). Food storage material silver nanoparticles interfere with DNA replication fidelity and bind with DNA. *Nanotechnology*, 20, 085102.
- Yang, Y., Tang, G., Zhang, H., Zhao, Y., Yuan, X., Fan, Y. & Wang, M. (2011). Controlled release of BSA by microsphere-incorporated PLGA scaffolds under cyclic loading. *Materials Science and Engineering C*, 31, 350–356.
- Yarlagadda, P. K., Chandrasekharan, M. & Shyan, J. Y. (2005). Recent advances and current developments in tissue scaffolding. *Biomedical Materials and Engineering*, 15, 159-177.
- Yerushalmi, N., Arad, A. & Margalit, R. (1994). Molecular and cellular studies of hyaluronic acid-modified liposomes as bioadhesive carriers for topical drug delivery in wound healing. *Archives of Biochemistry and Biophysics*, 313, 267–273.

- Yoksan, R. & Chirachanchai, S. (2009). Silver nanoparticles dispersing in chitosan solution: Preparation by γ -ray irradiation and their antimicrobial activities. *Materials Chemistry and Physics*, 115, 296-302.
- Yoshimoto, H., Shin, Y. M., Terai, H. & Vacanti, J. P. (2003). A biodegradable nanofiber scaffold by electrospinning and its potential for bone tissue engineering. *Biomaterials*, 24, 2077–2082.
- Young, S., Wong, M., Tabata, Y. & Mikos, A. G. (2005). Gelatin as a delivery vehicle for the controlled release of bioactive molecules. *Journal of Controlled Release*, 109, 256–274.
- Zhang, X., Hui, Z., Wan, D., Huang, H., Huang, J., Yuan, H. & Yu, J. (2010). Alginate microsphere filled with carbon nanotube as drug carrier. *International Journal of Biological Macromolecules*, 47, 389–395.
- Zhang, Y. & Zhang, C. (2002). Calcium phosphate/chitosan composite scaffolds for controlled *in vitro* antibiotic drug release. *Journal Biomedical Material Researches*, 62, 378–386.
- Zhong, S. P., Zhang, Y. Z. & Lim, C. T. (2010). Tissue scaffolds for skin wound healing and dermal reconstruction. *Wiley Interdisciplinary Reviews: Nanomedicine and Nanobiotechnology*, 2, 510-525.
- Zhou, Q., Gong, Y. & Gao, C. (2005). Microstructure and mechanical properties of poly(L-lactide) scaffolds fabricated by gelatin particle leaching method. *Journal of Applied Polymer Science*, 98, 1373-1379.
- Zhou, Y., Zhao, Y., Wang, L., Xu, L., Zhai, M. & Wei, S. (2012). Radiation synthesis and characterization of nanosilver/gelatin/carboxymethyl chitosan hydrogel. *Radiation Physics and Chemistry*, 81, 553-560.



APPENDICES

APPENDIX A

DEVELOPMENT OF SILVER NANOPARTICLES- LOADED CALCIUM ALGINATE BEADS EMBEDDED IN GELATIN SCAFFOLDS FOR USE AS WOUND DRESSINGS

Table A1 Compressive Modulus of the Neat Calcium Alginate Beads Embedded in Gelatin Scaffolds and the AgNPs-Loaded Calcium Alginate Beads Embedded in Gelatin Scaffolds

Concentration of AgNO ₃ (% w/w)	Sample	Compressive modulus (kPa)
0	1	1.80
	2	4.00
	3	2.20
	4	1.70
	5	2.70
	6	4.90
	Average	2.88
	SD	1.30
4	1	3.00
	2	3.20
	3	1.60
	4	2.90
	5	1.70
	6	2.60
	Average	2.50
	SD	0.69

Table A1 (continued)

Concentration of AgNO ₃ (% w/w)	Sample	Compressive modulus (kPa)
8	1	1.60
	2	3.10
	3	2.30
	4	3.40
	5	2.50
	6	2.90
Average		2.63
SD		0.64

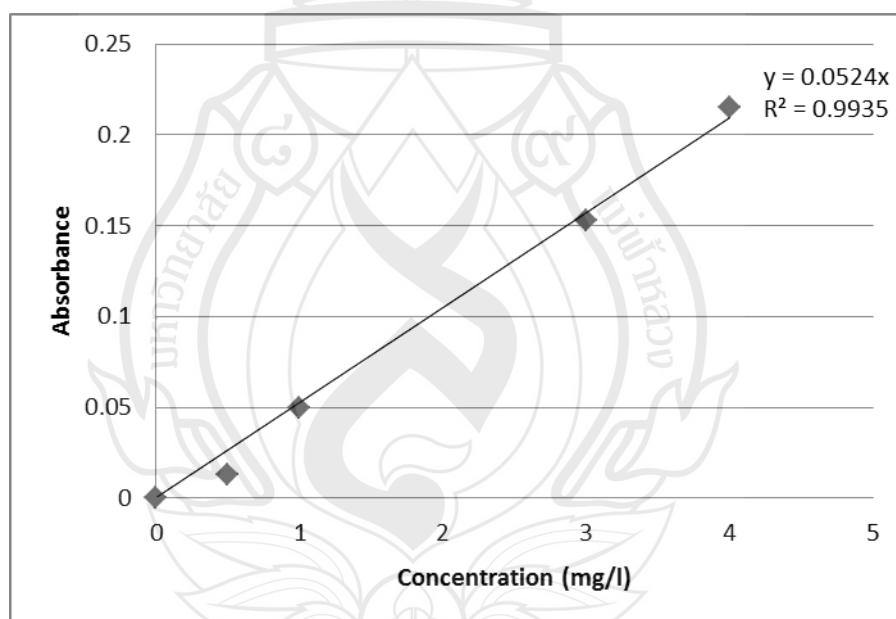
**Figure A1** Standard Curve of AgNO₃ Concentration

Table A2 Antibacterial Activity of the AgNPs-Loaded Calcium Alginate Beads Embedded in Gelatin Scaffolds (n = 3)

Culture	Sample	Rep.	CFU/ml
<i>E. coli</i> TISTR 780	Control	1	2.50×10^8
		2	2.50×10^8
		3	2.60×10^8
	Average		2.53×10^8
	SD		0.06×10^8
	4% AgNPs	1	8.50×10^7
		2	7.50×10^7
		3	8.10×10^7
	Average		8.03×10^7
	SD		0.50×10^7
	8% AgNPs	1	3.00×10^6
		2	1.00×10^7
		3	4.00×10^6
	Average		0.57×10^7
	SD		0.38×10^7
<i>S. aureus</i> TISTR 1466	Control	1	3.54×10^7
		2	3.87×10^7
		3	4.89×10^7
	Average		4.10×10^7
	SD		0.70×10^7
	4% AgNPs	1	1.08×10^6
		2	5.90×10^5
		3	7.40×10^5
	Average		8.03×10^5
	SD		2.51×10^5
	8% AgNPs	1	1.15×10^4
		2	1.38×10^4
		3	1.54×10^4
	Average		1.36×10^4
	SD		0.20×10^4

APPENDIX B

SILVER NANOPARTICLES-LOADED CALCIUM ALGINATE BEADS BY EMULSIFICATION/ EXTERNAL GELATION METHOD IN GELATIN SCAFFOLDS FOR USE AS WOUND DRESSINGS

Table B1 Compressive Modulus of the Neat Calcium Alginate Beads Embedded in Gelatin Scaffolds and the AgNPs-Loaded Calcium Alginate Beads Embedded in Gelatin Scaffolds

Concentration of AgNO ₃ (% w/w)	Sample	Compressive modulus (kPa)
0	1	11.0
	2	10.6
	3	8.3
	4	8.7
	5	18.2
	6	11.1
	Average	11.3
	SD	3.6
2	1	8.7
	2	9.7
	3	8.7
	4	11.7
	5	8.4
	6	9.6
	Average	9.4
	SD	1.2

Table B1 (continued)

Concentration of AgNO ₃ (% w/w)	Sample	Compressive modulus (kPa)
4	1	8.0
	2	8.7
	3	5.9
	4	6.3
	5	5.4
	6	9.8
Average		7.4
SD		1.7

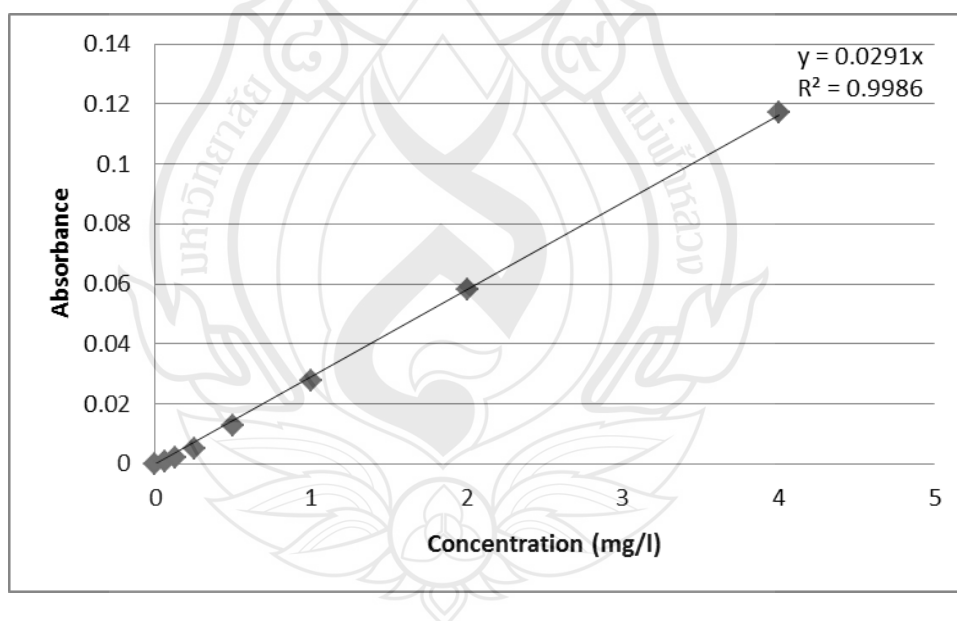
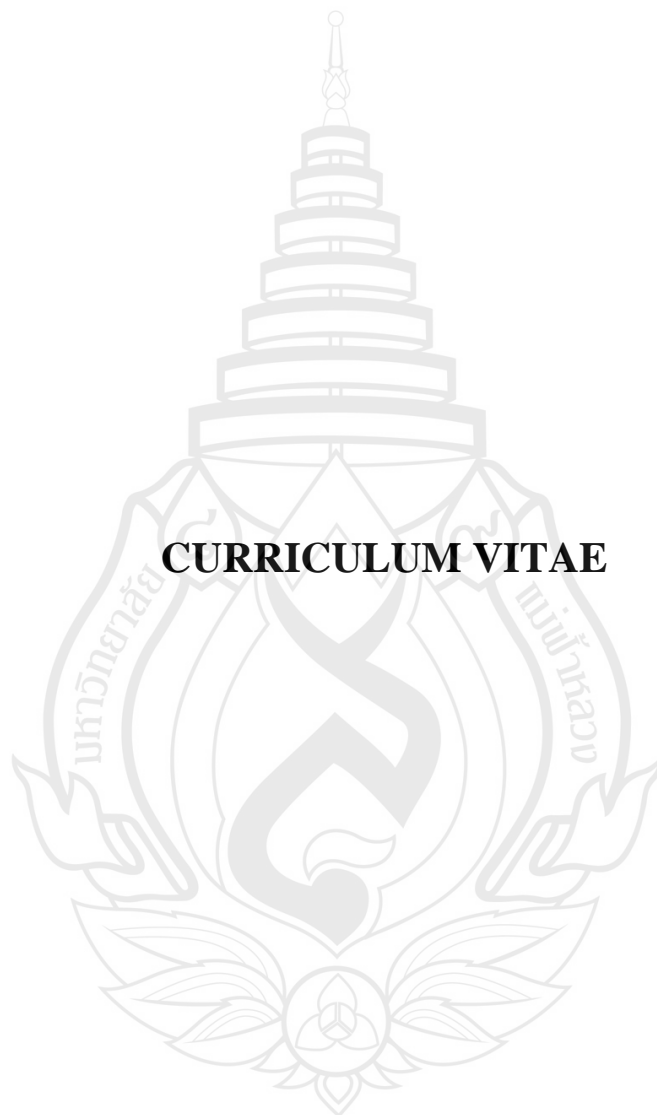
**Figure B1** Standard Curve of AgNO₃ Concentration

Table B2 Antibacterial Activity of the AgNPs-Loaded Calcium Alginate Beads Embedded in Gelatin Scaffolds (n = 3)

Culture	Sample	Rep.	CFU/ml
<i>E. coli</i> TISTR 780	Control	1	3.10×10^7
		2	5.10×10^7
		3	5.00×10^7
	Average		4.40×10^7
	SD		1.13×10^7
	2% AgNPs	1	4.00×10^6
		2	3.00×10^6
		3	2.00×10^6
	Average		3.00×10^6
	SD		1.00×10^6
	4% AgNPs	1	2.00×10^6
		2	6.00×10^6
		3	1.00×10^6
	Average		3.00×10^6
	SD		2.65×10^6
<i>S. aureus</i> TISTR 1466	Control	1	2.20×10^7
		2	2.70×10^7
		3	3.70×10^7
	Average		2.87×10^7
	SD		7.64×10^6
	2% AgNPs	1	0.00×10^0
		2	3.00×10^6
		3	2.00×10^6
	Average		1.67×10^6
	SD		1.53×10^6
	4% AgNPs	1	0.00×10^0
		2	0.00×10^0
		3	0.00×10^0
	Average		0.00×10^0
	SD		0.00×10^0



CURRICULUM VITAE

CURRICULUM VITAE

NAME Miss Porntipa Pankongadisak

DATE OF BIRTH 24 May 1989

ADDRESS 183/49 Moo 2, Sukhumvit Road, Tambon
Nong Mai Daeng, Mueang Chonburi,
Chonburi, Thailand, 20000

EDUCATIONAL BACKGROUND

2011 Bachelor of Science
Applied Chemistry
Mae Fah Luang University

PUBLICATIONS

- Chawgongjakr, T., Pankongadisak, P., Supaphol, P. & Suwantong, O. (2014).
Preparation and characterization of gentamicin sulfate-loaded alginate films.
*The 5th Research Symposium on Petrochemical and Materials Technology and
The 20th PPC Symposium on Petroleum, Petrochemicals, and Polymers*,
657-664. (Proceeding)
- Ngamviriyavong, P., Thananuson, A., Pankongadisak, P., Tanjak, P. & Janvikul, W.
(2010). Antibacterial Hydrogels from chitosan derivatives. *The 6th Thailand
Materials Science and Technology Conference*, 233-235. (Proceeding)
- Pankongadisak, P., Kudithalert, P., Supaphol, P. & Suwantong, O. (2012). Preparation
and characterization of gentamicin sulfate-loaded porous silk fibroin/gelatin
scaffolds. *The 6th Pure and Applied Chemistry International Conference*,
194-198. (Proceeding)

- Pankongadisak, P., Ruktanonchai, U. R., Supaphol, P. & Suwantong, O. (2014).
Study of silver nanoparticles-loaded calcium alginate microbeads embedded in gelatin scaffolds for drug delivery applications. *The 8th Pure and Applied Chemistry International Conference*, 512-515. (Proceeding)
- Pankongadisak, P., Ruktanonchai, U., Supaphol, P. & Suwantong, O. (2013).
Preparation and characterization of alginate microbeads using emulsification and internal gelation. *The 29th National Graduate Research Conference, ST 994-ST1000*. (Proceeding)
- Suwantong, O., Pankongadisak, P., Deachathai, S. & Supaphol, P. (2012).
Electrospun poly(L-lactic acid) fiber mats containing a crude *Garcinia cowa* extract for wound dressing applications. *Journal of Polymer Research*, 19, 9896.
- Suwantong, O., Pankongadisak, P., Deachathai, S. & Supaphol, P. (2013). The potential of electrospun poly(L-lactic acid) fiber mats containing a crude *Garcinia dulcis* extract for use as wound dressings. *Chiang Mai Journal of Science*, 40(3), 517-533.
- Suwantong, O., Pankongadisak, P., Deachathai, S. & Supaphol, P. (2014).
Electrospun poly(L-lactic acid) fiber mats containing crude *Garcinia mangostana* extracts for use as wound dressings. *Polymer Bulletin*, 71, 925-949.

PRESENTATIONS

- Chawgongjakr, T., Pankongadisak, P., Supaphol, P. & Suwantong, O. (2014).
Preparation and characterization of gentamicin sulfate-loaded alginate films. *The 5th Research Symposium on Petrochemical and Materials Technology and The 20th PPC Symposium on Petroleum, Petrochemicals, and Polymers (PETRO-MAT and SYM 2012)*, Queen Sirikit National Convention Center, Bangkok, Thailand. 22 April 2014. (Poster presentation)

- Pankongadisak, P., Ruktanonchai, U. & Suwantong O. (2012). Preparation and Characterization of Silver Nanoparticles-Loaded Calcium Alginate Beads Embedded in Gelatin Scaffolds. *The 1st Mae Fah Luang University International Conference (MFUIC)*, Mae Fah Luang University, Chiang Rai, Thailand. 29-30 Nov and 1 Dec 2012. (Poster presentation)
- Pankongadisak, P., Deachathai, S., Supaphol, P. & Suwantong, O. (2011). Electrospun poly (L-lactic acid) fiber mats containing *Garcinia dulcis* extract and their release characteristics for use as wound dressings. *The 5th Pure and Applied Chemistry International Conference (PACCON 2011)*, Miracle Grand Hotel Bangkok, Thailand. 5-7 January 2011. (Poster presentation)
- Pankongadisak, P., Kudithalert, P., Supaphol, P. & Suwantong, O. (2012). Preparation and characterization of gentamicin sulfate-loaded porous silk fibroin/gelatin scaffolds. *The 6th Pure and Applied Chemistry International Conference (PACCON 2012)*, The Empress Convention Center, Chiang Mai, Thailand. 11 – 13 January 2012. (Poster presentation)
- Pankongadisak, P., Kudithalert, P., Supaphol, P. & Suwantong, O. (2012). Microporous silk fibroin/gelatin blend scaffolds containing gentamicin sulfate for wound dressing applications. *The 38th Congress on Science and Technology of Thailand (STT 38)*, The Empress Convention Center, Chiang Mai, Thailand. 17– 19 October 2012. (Poster presentation)
- Pankongadisak, P., Ruktanonchai, U., Supaphol, P. & Suwantong, O. (2013). Preparation and characterization of alginate microbeads using emulsification and internal gelation. *The 29th National Graduate Research Conference (NGRC29th)*, Mae Fah Luang University, Chiang Rai, Thailand. 24-25 October 2013. (Poster presentation)

- Pankongadisak, P., Ruktanonchai, U., Supaphol, P. & Suwantong, O. (2014). Study of silver nanoparticles-loaded calcium alginate microbeads embedded in gelatin scaffolds for drug delivery applications, *The 8th Pure and Applied Chemistry International Conference (PACCON 2014)*, Centara Hotel and Convention Centre, Khon Kaen, Thailand. 8-10 January 2014. (Poster presentation)
- Pankongadisak, P., Ruktanonchai, U. & Suwantong, O. (2013). Silver nanoparticles-loaded calcium alginate beads embedded in gelatin scaffolds and their release characteristics. *The 7th Pure and Applied Chemistry International Conference (PACCON 2013)*, The Tide Resort, Bangsaen Beach, Chon Buri, Thailand. 23-25 January 2013. (Oral presentation)
- Pankongadisak, P., Warakorn, N., Supaphol, P. & Suwantong, O. (2012). Resveratrol-loaded gelatin films and their release characteristics. *The 38th Congress on Science and Technology of Thailand (STT 38)*, The Empress Convention Center, Chiang Mai, Thailand. 17–19 October 2012. (Poster presentation)
- Pankongadisak, P., Warakorn, N., Supaphol, P. & Suwantong, O. (2012). The potential use of resveratrol-loaded gelatin films for wound dressing applications. *The 3rd Research Symposium on Petrochemical and Materials Technology and The 18th PPC Symposium on Petroleum, Petrochemicals, and Polymers (PETRO-MAT and SYM 2012)*, Queen Sirikit National Convention Center, Bangkok, Thailand. 24 April 2012. (Poster presentation)
- Warakorn, N. Pankongadisak, P., Supaphol, P. & Suwantong, O. (2013). Resveratrol-loaded gelatin films and their potential for use as wound dressings. *The 7th Pure and Applied Chemistry International Conference (PACCON 2013)*, The Tide Resort, Bangsaen Beach, Chon Buri, Thailand. 23-25 January 2013. (Poster presentation)